DEVELOPMENT OF NEW BIOCATALYTIC ROUTES TO PHARMACEUTICAL INTERMEDIATES: A CASE STUDY ON TICAGRELOR

A thesis submitted to The University of Manchester for the degree of Doctor of Philosophy (PhD) in the Faculty of Engineering and Physical Sciences

2014

KATHARINA GLORIA HUGENTOBLER

SCHOOL OF CHEMISTRY

Table of Contents

Word count: 41872

List of figures and tables

Tables

Figures

Abstract

The University of Manchester

Katharina Gloria Hugentobler

A thesis submitted to The University of Manchester for the degree of Doctor of Philosophy (PhD) in the Faculty of Engineering and Physical Sciences

Title: Development of New Biocatalytic Routes to Pharmaceutical Intermediates: A Case Study on Ticagrelor

31 July 2014

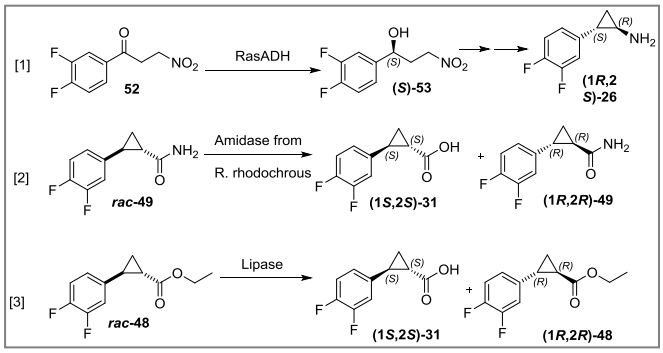

The research carried out within this thesis was aimed at the development and implementation of a biocatalytic route towards Ticagrelor, a platelet-aggregation inhibitor. A bio-retrosynthetic consideration of the target compound yielded different possible strategies, which were analysed in terms of enantioselectivity and efficiency. The ultimate goal was to generate a biocatalyst specifically tailored to the starting material to yield the target compound in high optical purity and conversion. Different approaches to the chemoenzymatic generation of the cyclopropyl subunit (cf figure) in enantiomerically pure form were proposed and tested. The lipase from *Thermomyces lanuginosus* proved to be the most selective and active enzyme tested and was used as a model enzyme, initially yielding an E of 76 at a conversion of 50% after 48h. Through both reaction engineering and rational protein design approaches the time to attain 50% conversion could be reduced to 24 h while the enantioselectivity of the process increased to 100. Moreover, in a rational protein design approach different residues in the lid of the lipase were identified through analysis of the resolved crystal structures and subsequently mutated in order to investigate the influence of these residues on the overall performance of the lipase towards the target biotransformation. Mutations on Asn88 resulted in the inactivation of the enzyme while an Asp57Asn mutation resulted in a more active enzyme. Ultimately, this research has contributed to making the synthetic route towards Ticagrelor more environmentally sustainable, diminishing the need for the use of toxic, unsustainable and sterically demanding auxiliaries, as well as the amount of waste produced. The principles of green chemistry have been applied to the case studied. The synthetic route towards a key fragment of Ticagrelor has been significantly shortened using a biotransformation with an enzyme that can be recycled and employed in catalytic quantities

Declaration

Parts of the work presented in this thesis in § 2.1.3 (amide hydrolysis of compound *rac*-49) have been previously submitted to the University of Manchester, School of Chemistry by Humera Sharif for the Final year project for MChem (Hons) Chemistry (August 2013). Her project was integrated into the work that was performed within this thesis and supervised by Professor Nicholas Turner. Her experiments were planned and discussed with me and performed under my direct supervision. Therefore they are included and discussed within this thesis.

List of Abbreviations

AcOEt	ethyl acetate
AcOH	acetic acid
ADH	alcohol dehydrogenase
ADP	adenosine-5'-diphosphate
API	active pharmaceutical ingredient
ATP	adenosine-5'-triphosphate
AS	asymmetric synthesis
CD	circular dichroism
DCM	dichloromethane
dH_2O	deionised water
DKR	dynamic kinetic resolution
DMF	dimethyl formamide
DMSO	dimethyl sulfoxide
dNTPs	desoxyribonucleotides
EDTA	ethylenediaminetetraacetate
EED	enantioselective enzymatic desymmetrisation
EtOH	ethanol
FDH	format dehydrogenase
GC	gas chromatography
GDH	glucose dehydrogenase
GDP	guanosine-5'-diphosphate
GTP	guanosine-5'-triphosphate

H	hexane
HEPES	4-(2-hydroxyethyl)-1-piperazineethanesulfonic acid
HPLC	high-performance liquid chromatography
IPA	2-propanol
K_M	Michaelis-Menten constant
KR	kinetic resolution
KRED	ketoreductase
MeOH	methanol
mp	melting point
MS	mass spectrometry or spectroscopy
MTBE	methyl *tert*-butyl ether
NAD^+, NADH	nicotinamide-adenine dinucleotide and its oxidized and reduced forms
$NADP^+$, NADPH	nicotinamide-adenine dinucleotide phosphate and its oxidized and reduced forms
NMR	nuclear magnetic resonance
pH	*pondus hydrogenii*, measure for the acidity of a solution
*p*NP	*para*-Nitrophenolate
*p*NPB	*para*-Nitrophenol butyrate
R_f	resolution factor
rpm	revolutions per minute
RT	room temperature
TAE	Tris base, acetic acid and EDTA based buffer
THF	tetrahydrofuran

TLC	thin-layer chromatography
TlL	lipase from *Thermomyces lanuginosus*
TlL_KGH	lipase from *Thermomyces lanuginosus*, own production
TMS	trimethylsilyl
t_R	retention time
Tris	tris(hydroxymethyl)aminomethane
UV	ultraviolet
wt%	weight per cent
w/v	weight per volume
w/w	weight per weight

Acknowledgements

I am grateful to those who supported me in many different ways throughout my PhD and helped me up to this point. It would go beyond the scope of this thesis to name all, thus exemplary for all I want to express my sincere thanks to my supervisors:

To Professor Nicholas Turner, for having granted me the opportunity to work under his direction and for his continued guidance and support.

To Dr. Marcello Rasparini at Chemessentia for his advice and many fruitful discussions.

To Professor John Blacker and group at the University of Leeds for their kind help and support with the flow chemistry experiments.

The experimental work for this thesis could not have been done and the thesis could not have been written without the invaluable help, discussion and support of my friends and colleagues; in particular Dr. Rachel Heath, Dr. Jason Schmidberger, and Nicholas Weise. Thank you!

Funding by CHEMO is gratefully acknowledged.

1 Introduction

1.1 General introduction to Biocatalysis

1.1.1 Green Chemistry

Chemical organic synthesis began with Wöhler's discovery of the synthesis of urea from inorganic starting materials in 1828 (Wöhler, 1828), which marked an end to the *vis vitails* theory, the belief that a substance produced by a living organism cannot be reproduced in a chemical laboratory, and has steadily evolved ever since. The discovery of synthetic dyes and the discovery and extraction of new natural products as therapeutic agents has created a strong chemical industry with ever-growing potential and scope.

In the last decades, awareness has been raised that the chemical synthetic industry puts the environment into pressing danger by using toxic chemicals that can cause damage to nature (e.g. the observed dying of bees), negatively influence the global warming (e.g. production of CO_2 as a side product in manufacture) and affect the ozone layer (e.g. use of halogenated reagents that can radicalise and cause damage to the ozone layer in the stratosphere). The need for environmentally sustainable synthetic processes and the concomitant reduction of waste products has emerged. The E-factor (Sheldon, 2012), has been established as a means to determine the actual waste produced in a synthetic process and equals, in principle, the total mass of raw materials minus the total amount of products. In an ideal process this value is zero. Active research endeavours are currently undertaken to approach the ideal process. It is clearly understandable that the E-value of a reaction increases from bulk chemicals to fine chemicals and finally pharmaceuticals. This is mainly due to the fact that the refined compounds require a higher degree of purity and many more synthetic steps as a result of their higher complexity, which in turn will create more waste products. Classical organic chemistry used stoichiometric amounts of reagents leading to the production of a vast amount of waste (e.g. inorganic salts, metals). This creates the need for the development of scalable, green, catalytic processes that have a broad application spectrum. The United States Environmental Protection Agency (EPA) has defined the Twelve Principles of Green Chemistry (Anastas, 1998) as follows:

1. Waste prevention
2. Atom efficiency
3. Avoidance of hazardous or toxic chemicals

4. Safer products by design
5. Innocuous solvents and auxiliaries
6. Energy efficiency by design
7. Preferably renewable raw materials
8. Shorter syntheses
9. Catalytic rather than stoichiometric reagents
10. Design products for degradation
11. Analytical methodologies for pollution prevention
12. Inherently safer processes

A first step in this direction is the substitution of solvents based on chlorinated or aromatic hydrocarbons with more environmentally friendly alternatives. Exemplary is the synthesis of sertraline (Taber *et al.*, 2004) in which the synthetic route was adjusted to use ethanol as the only solvent (Sheldon, 2012), thereby reducing both the hazards associated with chlorinated or aromatic hydrocarbons as well as the amount of solvent waste created. Various alternative solvents have been studied in recent years, among them water (Kobayashi, 2013), supercritical CO_2 (Licence *et al.*, 2003) and ionic liquids (Pârvulescu and Hardacre, 2007). Water stands out from this list of solvents: it is nontoxic, non-flammable, abundantly available and inexpensive. Small amounts of solvents may still be needed in order to dissolve substrates that are insoluble in water, moreover the recovery of the reaction product will require extraction with an organic solvent. However there is a list of green solvents (Pollet *et al.*, 2014; Prat *et al.*, 2013) to choose from and the total amount of solvent used in this case is less than the amount of solvent needed in a conventional organic reaction.

The application of biocatalysts creates a further improvement of industrial processes. Enzyme catalysed reactions are generally performed in aqueous reaction media under mild reaction conditions, while the catalyst (the enzyme) is environmentally friendly (for a review on general conditions, chiral auxiliaries and chemical catalysts employed in the straightforward chemical synthetic routes towards the target amine (1*R*,2*S*)-**26** please refer to § 1.2.2) and can be reproduced using renewable sources. Moreover, there is potentially no need to purify the catalyst since it can theoretically be employed as a whole cell biocatalyst. Enzymes generally exhibit a high chemo-, regio- and stereoselectivity in their reactions, which avoids the need for protection-deprotection reaction steps otherwise required (examples cf. § 1.2.2). As a result of the above, the overall process becomes more efficient while the E-value is reduced (Yuryev and

Liese, 2010).

One of the first examples of enzyme catalysis in industrial processes was the production of acrylic acid and methacrylic acid for polymer formation using the nitrilase from *Rhodococcus rhodochrous* J1 (Nagasawa et al., 1990). A more recent example is the formation of enantiomerically pure cyanohydrins as intermediates for herbicides and pharmaceuticals. Careful control of the pH and the use of an array of hydroxynitrilases (HnL) in a biphasic system allowed for the preparation of a large library of aromatic and aliphatic (*R*)- and (*S*)-cyanohydrins **4** in a transhydrocyanation reaction (Griengl *et al.*, 2000) with yields of >80%.

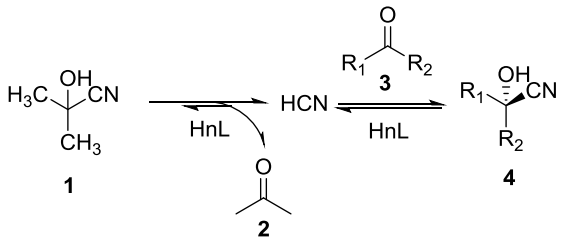

Figure 1.1: HnL mediated formation of cyanohydrins, the hydrocyanic acid is produced *in situ* through an HnL mediated hydrolysis of acetone cyanohydrin **1**.

The list of pharmaceuticals produced with bioorganic reaction process is increasing every day. In the following, a few emblematic examples will be discussed.

The synthesis of Pregabalin (Martinez *et al.*, 2008) features a kinetic resolution of an ester using the lipase from *Thermomyces lanuginosus* (TlL, cf. figure 1.2). The remaining undesired enantiomer is racemised before being hydrolysed in an enantioselective manner again. Subsequent decarboxylation and reduction yields pregabaline **7**.

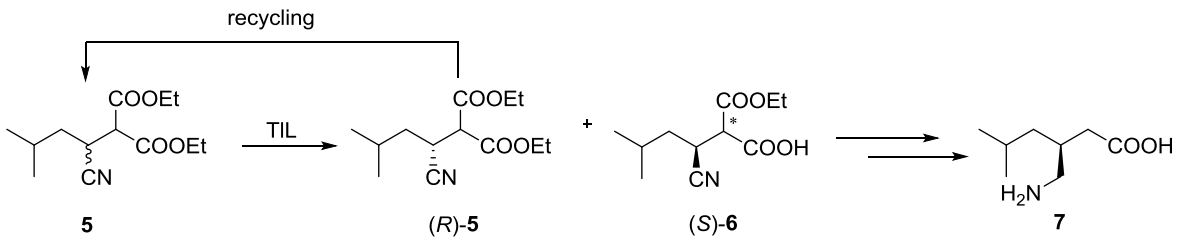

Figure 1.2: TlL mediated kinetic resolution in the synthetic route towards (*S*)-3-(aminomethyl)-5-methylhexanoic acid (Pregabalin, **7**).

Artemisinine, a sesquiterpene lactone endoperoxide **14** (cf. figure 1.3) constitutes the most effective drug against *Plasmodium falciparum*, the malaria pathogen. It can be attained in a semisynthetic synthesis from the precursor dihydro-artemisinic acid **13** (cf. figure 1.3) produced by *Nicotiana benthamiana* (van Herpen et al., 2010).

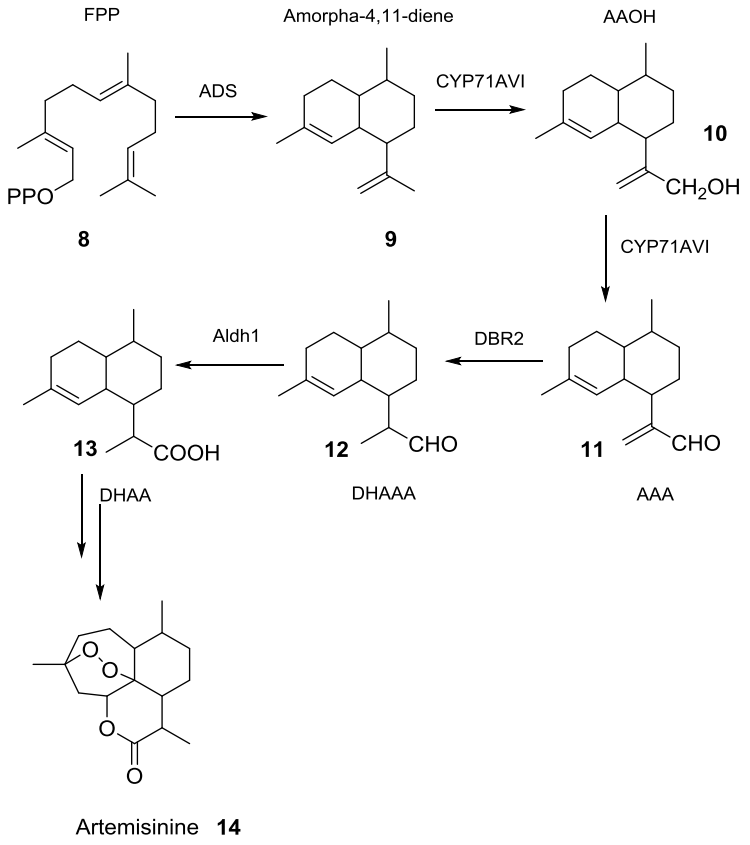

Figure 1.3: Semi-synthetic synthesis towards Artemisine **14**. The synthetic pathway from *Nicotiana benthamiana* was used to attain artemisinic acid, which is converted to Artemisine in a chemical reaction series. The scheme was reproduced from van Herpen *et al*. (2010), intermediates and enzymes from *Nicothiana benthamiana* are abbreviated as follows: amorpha-4,11-diene synthase (ADS), aldehyde dehydrogenase 1 (Aldh1), amorpha-4,11-diene monooxygenase (CYP71AV1), artemisinic aldehyde double bond reductase (DBR2), farnesyl diphosphate (FPP), artemisinic alcohol (AAOH), artemisinic aldehyde (AAA), dihydro-artemisinic aldehyde (DHAAA), dihydroartemisinic acid (DHAA).

Another potent example for the application of enzymes in the synthesis of important pharmaceuticals is the case of Montelukast **16** (cf. figure 1.3), a leukotriene receptor antagonist developed by Merck to control the symptoms of asthma and allergies. A ketoreductase (KRED) has been developed to accept the 'bulky-bulky' Montelukast ketone **15** for the enantioselective

reduction towards Montelukast **16**.

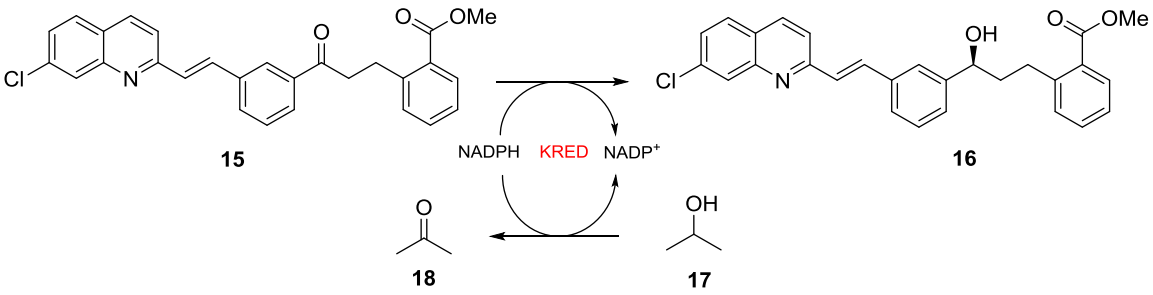

Figure 1.4: KRED-mediated reduction towards Montelukast **16** using a acetone **18** /2-propanol based recycling system to recover the co-factor NADPH

1.1.2 Enzyme Technologies

1.1.2.1 Chirality

The vast majority of biomolecules surrounding us are chiral. Most amino acids, the building blocks of proteins, only occur in the L-series in nature, giving rise to precisely assembled proteins. Taking the different reactivities of enantiomers with other chiral substances into account, it can be concluded that each enantiomer of a racemic molecule very probably shows different energetics in its specific reaction with chiral biomolecules, most importantly with enzymes.

This effect can influence the action of pharmaceutical molecules. The most prominent case that triggered the need for enantioselective synthesis of pharmaceuticals certainly is the case of Thalidomide **19** (cf. figure 1.4), which was used in the 1960s to treat morning sickness in pregnancy. A severe side effect is the inhibition of limb outgrowth which caused mutilations in the unborn child (Mellin and Katzenstein, 1962; Vargesson, 2009). This property of Thalidomide is attributed to the (*S*)- enantiomer, while the (*R*)-enantiomer is reported to be innocuous (Blaschke *et al.*, 1979; Winter and Frankus, 1992). However, it is now known that both enantiomers interconvert rapidly in aqueous systems, which renders the administration of only one enantiomer impossible in that specific case (Eriksson *et al.*, 1995; Teo *et al.*, 2004). Thalidomide is currently explored in anti-cancer treatment (Bennett *et al.*, 2006; D'Amato *et*

al., 1994) as well as in treatment of other diseases (Franks *et al.*, 2004; Villahermosa *et al.*, 2005). Another example of the biological importance of enantiomers is Levofloxacin **20** (cf. figure 1.5), an antibiotic inhibiting the bacterial gyrase which in clinical trials proved to have a highly increased activity (George and Morrissey, 1997) compared to the racemic form Ofloxacin.

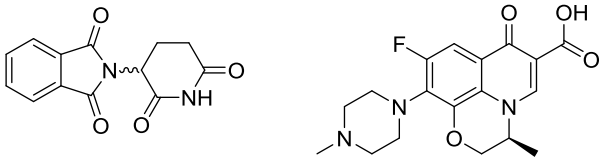

rac-Thalidomide **19** Levofloxacin **20**

Figure 1.5: *rac*-Thalidomide **19** and Levofloxacin **20**, two molecules that exhibit the importance of enantiopure pharmaceuticals

The necessity to be able to produce chiral substances in enantiopure form is therefore evident and the quantity of racemic drugs launched on the market steeply declined during the last two decades while the number of enantiopure compounds strongly increased (Kasprzyk-Hordern, 2010; Sanchez and Demain, 2011).

1.1.2.2 Determination of Enantioselectivity

The enzymatic preparation of optically active substances from a racemic mixture can be achieved due to the difference in reactivity of the enzyme with both enantiomers as a result of the difference in energy of the diastereomeric transition states of the enzyme substrate complex.

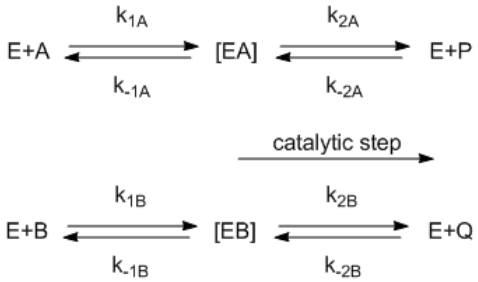

Figure 1.6: Model of enzyme catalysis enzyme (E) and the racemic substrate (A,B) form an enzyme-substrate complex ($EA^{‡}/EB^{‡}$), which upon resolution yields the free enzyme and optically active products (P,Q). the different reactions occur with specific rate constants *k.*

Many enzymes follow Michaelis-Menten kinetics (cf. figure 1.6): when the system is in a steady state the reaction is irreversible (k_{-2} = 0) and the enzyme is not inhibited by the product. Under these conditions, both enantiomers A and B compete for the active centre of the enzyme (E). Energetically different transition states $[EA]^{\ddagger}$ and $[EB]^{\ddagger}$ occur, the collapse (catalytic step) of which gives rise to two enantiomeric products P and Q (cf. figure 1.6 and 1.7). Discrimination between the two enantiomers is determined by the difference in energy between the two transition states (cf. figure 1.7).

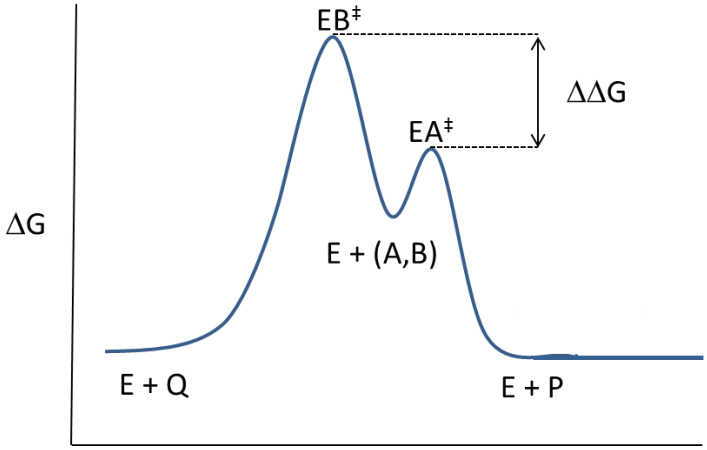

Figure 1.7: Energetics of enzymatic catalysis; enzyme (E) and the racemic substrate (A,B) form an enzyme-substrate complex ($EA^{\ddagger}/EB^{\ddagger}$), which upon resolution yields the free enzyme and optically active products (P,Q). The difference in activation energy between both transition states (ΔΔG) determines the enantioselectivity.

The velocity of the conversion of each enantiomer is determined by the corresponding rate constant k. In the special case of the Michaelis-Menten kinetics (cf. equation 1) these constants are k_{cat} and K_M.

$$v = \frac{v_{max}[S]}{K_M + [S]} \qquad \textbf{Equation 1}$$

k_{cat}, the turnover number, describes the number of substrate molecules each enzyme site converts to product per unit time, while K_M is a measure for the affinity of the enzyme for the particular substrate and the substrate concentration at half maximal reaction velocity. Under the assumption that [S] << K_M the Michaelis-Menten equation is simplified to:

$$v = \frac{v_{max}[S]}{K_M} \qquad \textbf{Equation 2}$$

Under these conditions the enantioselectivity corresponds to the specificity constant defined as the ratio between k_{cat} and K_M (cf. eq. 3 and 4).

$$v_a \approx \frac{-d[A]}{dt} = (\frac{k_{cat}}{K_M})_A[E][A] \qquad \textbf{Equation 3}$$

$$v_b \approx \frac{-d[B]}{dt} = (\frac{k_{cat}}{K_M})_B[E][B] \qquad \textbf{Equation 4}$$

Enantioselectivity, which is defined as the ability of an enzyme to discriminate two enantiomers, is quantified by the enantiomeric ratio *E*. It is an intrinsic property of the enzyme, defined as the ratio of the specificity constants for the reaction with each enantiomer (cf. equation 5, (Chen *et al.*, 1982))

$$E = \frac{(\frac{k_{cat}}{K_M})_A}{(\frac{k_{cat}}{K_M})_B} \qquad \textbf{Equation 5}$$

According to the Arrhenius equation (cf. eq 6), which relates the velocity constants and the energy of the transition state and taking equation 5 into account, it can be deduced that the discrimination between two enantiomers only depends on the temperature and is completely independent of the time of reaction and the substrate concentration (cf. eq. 7). *E* is therefore the most suitable parameter for the comparison of enzymatic kinetic resolutions. However it should be considered, that *E* is dependent on the conditions of reaction, since those may have an influence on k_{cat} and K_M.

$$k = A * e^{-E_a/RT} \qquad \textbf{Equation 6}$$

$$\Delta\Delta G = RTlnE \qquad \textbf{Equation 7}$$

The above shown formulae for *E* are of little practical use as the magnitudes it is related to are difficult to measure. An alternative formulation of *E* in which this parameter is related to the degree of conversion (*c*) and the enantiomeric excesses of the substrate (ee_s) and the product (ee_p; all obtained as experimental data by chiral HPLC or GC) through equation 8 (Chen *et al.*, 1982) is used in practice.

$$E = \frac{\ln[(1-c)(1-ee_s)]}{\ln[(1-c)(1+ee_s)]} = \frac{\ln[1-c(1+ee_p)]}{\ln[1-c(1-ee_p)]}$$ **Equation 8**

The enantiomeric excess (*ee*) of both substrate and product is directly determined from the experimental data as *difference* over *sum* of peak areas in chiral HPLC, while the conversion is determined from the ee of substrate and product as per equation 9.

$$c = \frac{ee_{subst}}{ee_{subst.}+ee_{prod.}}$$ **Equation 9**

The *E* value is indirectly measured. The upper detection limit of the instrument, as well as the experimental error in signal integration needs to be considered when discussing the values obtained. Generally it can be assumed that an *E* below 10 equals a totally unselective enzyme, between 30 and 50 the reaction can be considered to occur with some selectivity. A reaction is considered to occur with good selectivity at E values above 70, while values above 90 are excellent. Being a logarithmic function, the *E* value has no upper limit, however, in practice no further differentiation needs to be made for values > 100 and reactions occurring with an E value of 100 or over are therefore considered to be totally selective.

1.1.2.3 Designing a Biocatalyst

Enzymes in nature are the result of millions of years of evolution, which resulted in their exact and highly specific reactivity. Many enzymes found in nature exhibit a general substrate promiscuity (*vide infra*) acting on substrates that differ from their natural substrates. There is an evolutionary basis for this phenomenon: Modern enzymes are thought to have evolved from primordial, ancient enzymes as a result of promiscuous catalytic behaviour and specialisation in order to adapt to the increasing complexity of life. Even our modern-time (on an evolutionary timeline) enzymes keep evolving according to the same principles and therefore are subject to promiscuity (Babtie *et al.*, 2010; Bornscheuer and Kazlauskas, 2012; Hult and Berglund, 2007). Modern times and the fast development of pharmaceutical industries require this evolutionary process to occur faster than it originally would in nature. The molecular biologist's toolbox of *in vitro* evolutionary techniques allows for the creation of enzymes with new or enhanced properties to occur in a period of weeks or months.

However, it is not obvious that an enzyme is capable of catalysing a desired reaction,

and the substrate scope of an enzyme will always be a limiting factor for the use of enzymes in catalysis. A balance between sufficient specificity and a broad enough substrate spectrum has to be attained. To meet this need, rational protein design approaches aim at creating enzymes that are specifically tailored to perform a certain reaction (Jochens *et al.*, 2010).

The discovery of new enzymes and the understanding of their structure-function relationship furthered not only the application of enzymes as catalysts in highly specific reactions but also the development of technologies to modify enzymes and thus create new, singular catalysts that are bespoke for a particular type of reaction. Bioinformatics, sequence analysis and homology modelling represent an increasingly valuable tool for the prediction of enzyme functions by comparison to similar enzymes. Moreover the simulation of a substrate's interaction with the active site allows the prediction of important residues for the catalysis or enantioselectivity of a particular transformation. Molecular biology techniques in combination with the above mentioned bioinformatics tools allow for the assembly of new enzyme functionalities (Turner, 2009).

After identification of a target site in the enzyme (flexible, near the active site, identified by sequence or structure based modelling) different possibilities for the introduction of the change exist. Random mutagenesis approaches target the enzyme as a whole and aim at creating a new function in an evolution-like approach. This technique creates a large library of variants that require an efficient screening process. Site saturation mutagenesis creates a library of variants with all proteinogenous amino acids at one or a few previously selected sites ('hot spots'). Combinatorial techniques like CASTing (Reetz et al., 2006) and iterative rounds of mutagenesis and analysis aim at a directed evolution of proteins. DNA shuffling approaches create mosaic-like proteins from different starting organisms, while synthetic genes based on homologous enzymes constitute a very rational design-based route towards a target function (Bornscheuer *et al.*, 2012).

The toolkit of (computer aided) molecular biology techniques for the generation of a particular enzyme function is ever increasing and has found broad application in biotechnology research (Kazlauskas and Bornscheuer, 2009). In the following some examples of enzymes that have been tailored to meet a specific need will be reviewed.

An emblematic example was the development of a transaminase specifically tailored

towards the formation of sitagliptin **23**. The application of a transaminase in this process required previous engineering of the binding pockets, which had to be engineered from accepting rather small substituents towards accepting the bulky-bulky prositagilptin ketone **21** (cf. figure 1.8). The creation of this new enzyme using a combined substrate-walking, modelling and mutation approach and subsequent directed evolution to enhance activity towards the target compound **21** allowed for the implementation of a biocatalytic process replacing the rhodium-catalysed asymmetric enamine hydrogenation that was the current state of art at the time (figure 1.8 [A]).

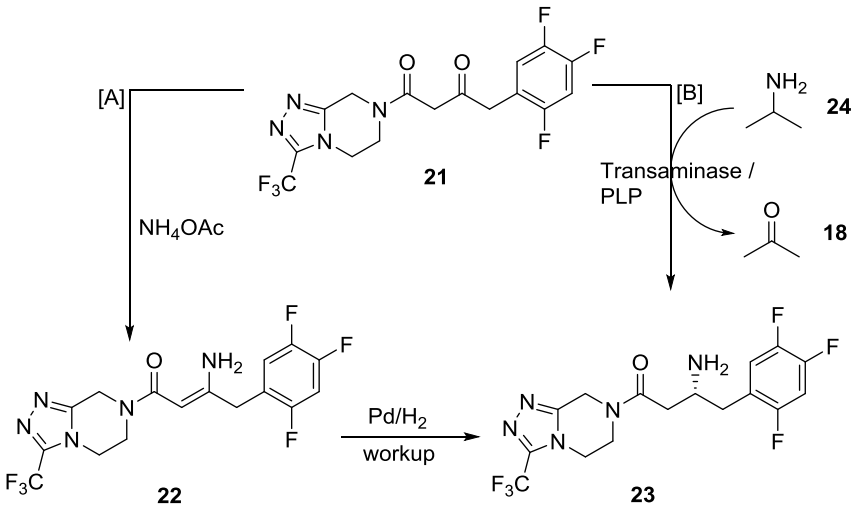

Figure 1.8: Chemocatalytic [A] and enzymatic [B] approach to Sitagliptin

Another example along the same lines is the rational design of a ketoreductase for the enantioselective reduction of Montelukast **16** (cf. § 1.1.1, figure 1.3).

A leading-edge research in terms of enzyme engineering is the work by Svedendahl and co-workers (2010). In a homology modelling/rational design study of the lipase from *Arthrobacter citreum* they discovered the key residue that controlled the activity and enantiomeric preference. A single point mutation of this residue leads to an enzyme variant with inversed enantioselectivity. This study highlights the possibilities that modern informatics techniques provide for tailoring enzyme activities to the target reaction.

Engineering of enzymes is not only limited to increasing or modifying the substrate scope. Research endeavours are made to modify enzymes in terms of stability, solvent tolerance and substrate inhibition, which constitute the main bottlenecks in biotransformations. The research of DeSantis and co-workers explores how gene site saturation mutagenesis (GSSM) can be employed as a tool to create a nitrilase which tolerates substrate concentrations up to 3 M

(DeSantis et al., 2003). A study on a biosynthetic pathway towards Montelukast focussed on enhancing the enantioselectivity of a lipase form *Lactobacillus kefir* towards a key intermediate in the synthetic pathway. The research based on directed evolution yielded a lipase that showed a high enantioselectivity but also featured a tolerance to high substrate loading and retained its activity in 70% organic solvent (Liang *et al.*, 2009).

The above examples serve to indicate the importance of molecular biology techniques in order to create tailored biocatalysts for the enantioselective, green synthesis of target compounds the in pharmaceutical industry (Bornscheuer and Kazlauskas, 2012). Moreover they highlight the scope of biotechnology as a tool for the creation of precise, bespoke catalysts to be employed in organic synthesis (Strohmeier *et al.*, 2011).

` In this sense, the present thesis will focus on the implementation of a biosynthetic route towards Ticagrelor (cf. figure 1.9). In the following, the current state of art of the synthesis of the cyclopropane subunit (cf. figure 1.9, in red) will be introduced, followed by an in depth discussion on the enzymes employed in this research. Results and discussion will follow and are based on the concepts discussed in § 1.2 and 1.3.

1.2 Ticagrelor Synthesis

1.2.1 Introduction

The aim of the present research is to develop and implement a biosynthetic route towards a pharmaceutical intermediate. The cyclopropyl subunit of Ticagrelor **26** (cf. figure 1.9, in red) was chosen as the target compound in the development of a biocatalytic route towards an active pharmaceutical ingredient (API), and the work presented is a case study on the improvement of the existing synthetic routes (cf. § 1.2.2). The aim was to find a 'green chemistry' approach, based on enzymatic synthesis that allowed for both the introduction of the stereocentres and the use of environmentally friendly conditions.

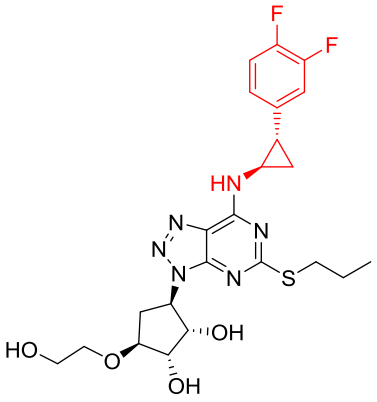

Ticagrelor **25**

Figure 1.9: Ticagrelor **25**, the target cyclopropyl subunit **26** is indicated in red.

Ticagrelor (trade name Brilinta™ in the US, Brilique™ and Possia™ in the EU) is the world's leading drug for the treatment of acute coronary symptom and strokes, developed and marketed by AstraZeneca plc. The drug was approved for use in the European Union by the European Commission in 2010 and by the US Food and Drug Administration in 2011.

As a structural purine analogue, Ticagrelor antagonises adenosine diphosphate (ADP) activation of $P2Y_{12}$ protein on the surface of thrombocytes (Capodanno *et al.*, 2010). $P2Y_{12}$ is a G-protein coupled receptor for ADP which is involved in the aggregation of platelets (simplified mechanism cf. figure 1.10) and is commonly employed to reduce the risk of blood clotting in patients with cardiovascular diseases (Huber *et al.*, 2011).

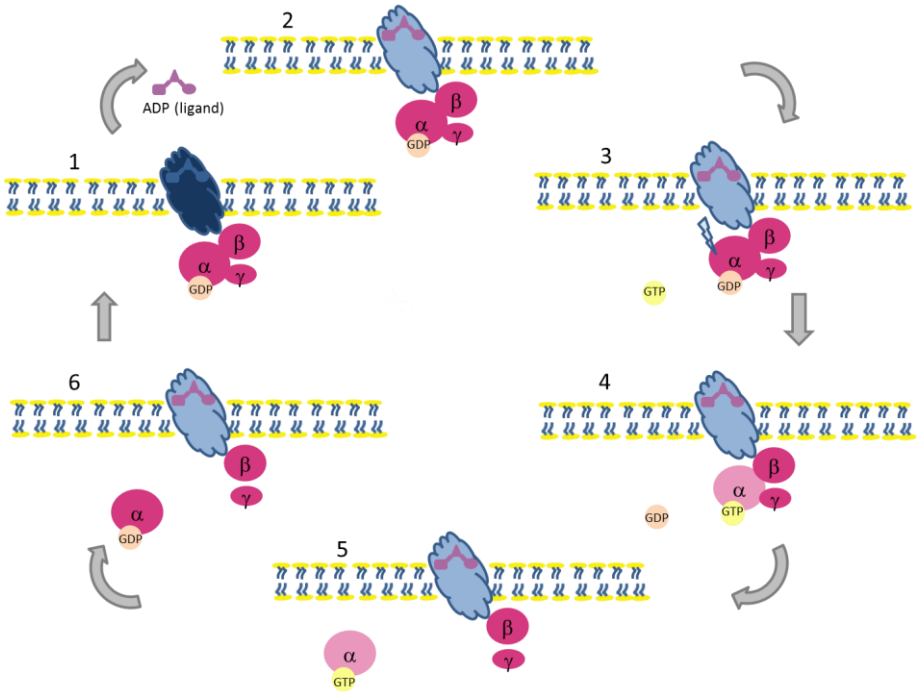

Figure 1.10: Activation of the $P2Y_{12}$ receptor (blue cloud) with a membrane bound G-protein (pink spheres) which is activated by ADP (rosé geometrical shape). The α-subunit of the receptor-associated G-protein (pink circles with αβ and γ subunits) binds guanosine triphospate (GTP, lemon circle, 3) to be activated. Cleavage of GTP to guanosine diphosphate (GDP, apricot circle) renders it inactive and concludes the cycle.

The action of Ticagrelor is illustrated in a simplified manner (adapted from Berg *et al*. (2012)). Under physiologic conditions ADP binds to the receptor and thereby activates it (2). The α-subunit of the receptor-associated G-protein (pink circles with αβ and γ subunits) is triggered to release the bound guanosine diphosphate (GDP, apricot circle) and binds guanosine triphospate (GTP, lemon circle, 3). Binding of GTP activates the α-subunit (4), which dissociates from the receptor and acts as a transmitter that triggers a cascade reaction resulting in reduced blood clotting (5). Then, the α-subunit will eventually hydrolyse the bound GTP to GDP and thereby return to its inactive state (6). Re-association with the β- and γ-subunits at the inactive (no bound ligand) receptor starts a new cycle (1).

Ticagrelor reversibly binds to the $P2Y_{12}$ receptor in proximity to the binding site of ADP, thereby making it inaccessible for any other molecule of ADP (Nawarskas and Clark, 2011; Teng, 2012). Through this mechanism the G-protein cannot be activated and the blood clotting cascade is interrupted (cf. figure 1.11).

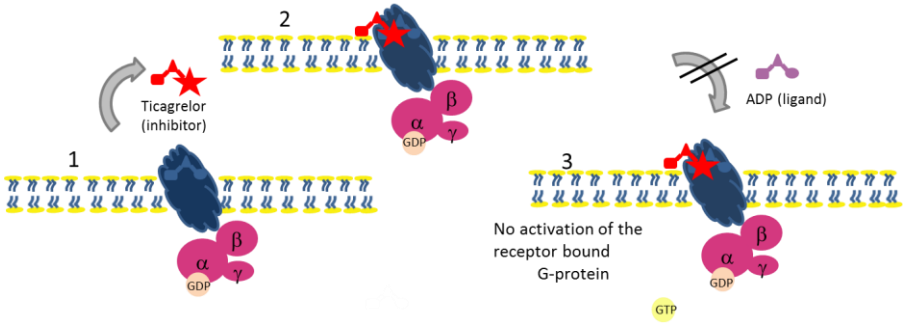

Figure 1.11: Inhibition of the $P2Y_{12}$ receptor (blue cloud) with a membrane bound G-protein (pink spheres) by the allosteric inhibitor Ticagrelor (red geometrical shape). Ticagrelor reversibly binds to the receptor making it inaccessible to any ADP molecule. The G-protein is not activated and no signal is transmitted.

Treatment of acute coronary syndrome with Ticagrelor as compared to Clopidogrel, the previously suggested treatment for acute coronary infarcts (Anderson *et al.*, 2007; Members *et al.*, 2008), significantly reduces the rate of death (Wallentin *et al.*, 2009).

In light of this, Ticagrelor is one of the most potent drugs for the treatment of acute coronary syndrome on the market and was chosen as the target compound in this case study towards the development and introduction of a biocatalytic route to the total synthesis of a pharmaceutical compound. The Ticagrelor cyclopropyl subunit was identified to be a good candidate for this study and was chosen as the target compound. In the following, the existing patent landscape and literature background of synthetic routes towards the target compound **26** will be examined and discussed.

1.2.2 Literature background

In the following, the existing patent landscape towards the Tica amine (1*R*,2*S*)-**26** (cf. figure 1.12) will be described. Special focus will be put on the chiral auxiliaries employed in each step and the required reaction steps in each patent.

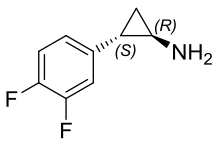

Figure 1.12: Tica amine (1*R*,2*S*)-**26**, the target compound in the present research

The original AstraZeneca product patent (Guile *et al.*, 2000) describes a 7-step route (cf. figure 1.13) towards the amine (1*R*,2*S*)-**26** starting from the commercially available *trans*-3,4-Difluorocinnamic acid **27**. The cyclopropane is made by palladium catalysed cyclopropanation with diazomethane; Oppolzer's chiral camphorsultam **29** is used in this reaction step to control the stereocentres. Subsequent hydrolysis of compound **31**, yields acid **32**, which is transformed into the target amine (1*R*,2*S*)-**26** through a Curtius rearrangement. A final recrystallization with L-tartaric acid yields the desired (1*R*,2*S*)-amine **26**, however in the patent no measure is given of the ratio of the diastereoisomers formed. The main drawback of this route is the need for the use of a chiral auxiliary **29**, which needs to be recovered again after hydrolysis. Moreover the palladium catalysed formation of the cyclopropane using diazomethane is a cost and risk factor. While the use of palladium increases the production cost and creates additional waste to be disposed of (cf. E-factor, § 1.1.1), the use of diazomethane creates a serious hazard, due to it being both highly toxic and explosive.

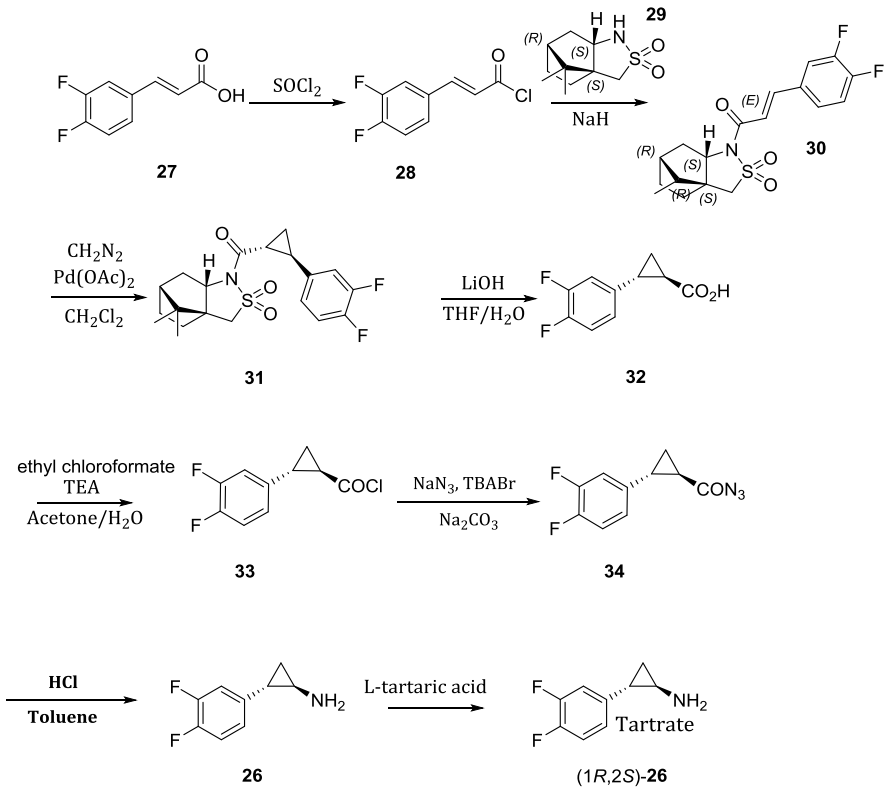

Figure 1.13: Route towards the target Tica amide (1*R*,2*S*)-**26** starting from trans-3,4-difluorocinnamic acid **27** as described in the Astra Zeneca product patent (Guile *et al.*, 2000) using the Oppolzer's chiral camphorsultam **29** for the introduction of the stereocentres (Guile *et al.*, 2000; Springthorpe *et al.*, 2007)

AstraZeneca filed another patent two years later (Clark *et al.*, 2001) in which the stereo-centres are controlled by use of menthol **36** as chiral auxiliary (fig. 1.13)

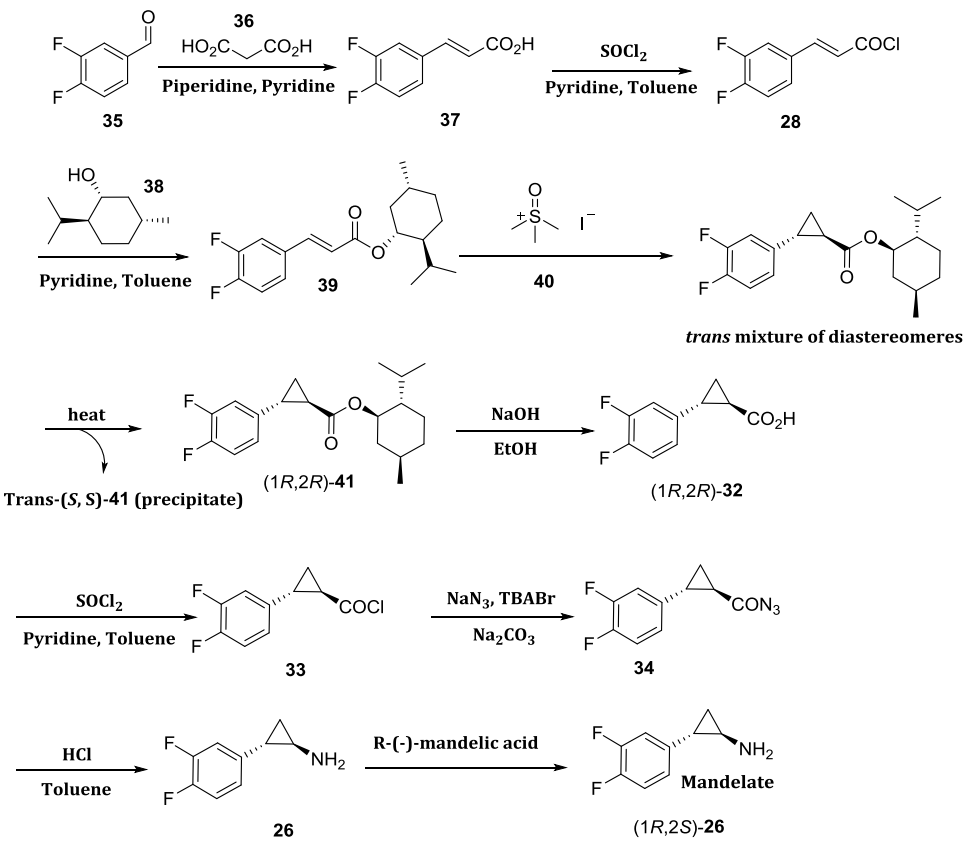

Figure 1.14: Route towards the target Tica amide (1*R*,2*S*)-**26** starting from trans-3,4-difluorobenzaldehyde **35** as described in the Astra Zeneca patent (Clark *et al.*, 2001) using menthol as chiral auxiliary and trimethyl sulfoxonium iodide **40** and base for the formation of the cyclopropane.

In this the use of Oppholzer's auxiliary **28** and the use of diazomethane have been substituted by menthol **36** as chiral auxiliary and trimethyl sulfoxonium iodide **40**/base for the formation of the three membered ring. On the other hand, this synthesis requires many more synthetic steps than the previous route and creates a lot of waste. From the examples the yield and stereoselectivity of the cyclopropanation are low. 14.3 kg of mixture of diastereoisomers of the cyclopropane menthyl ester **41** yield 4.7 kg of the desired isomer (33% yield) mixed with 1.1 kg (8%) of the undesired isomer in a crystallisation step. In order to obtain the pure isomer (1*R*,2*S*)-**26** multiple crystallisations have to be carried out. It seems that no stereocontrol is imparted by menthol in the cyclopropanation step. The menthyl-moiety only serves to yield the *trans* mixture of diastereomers which has to be separated by fractional crystallisation.

In the 2007 Astra Zeneca patents (Dejonghe *et al.*, 2008; Mitsuda *et al.*, 2008) the synthesis starts with a Friedel-Crafts acylation of 1,2-Difluorobenzene **42**. The chiral epoxide **46** derives from an optically pure chlorohydrin **45**, in turn prepared by Corey-Bakshi-Shibata reduction of the corresponding phenacyl chloride **43** using diphenyl prolinol **44** as the ligand. The epoxide is then opened with the anion of triethyl phosphono acetate (TEPA) **47** setting the second stereocentre selectively by induction from the first (cf. figure 1.15). The desired cyclopropyl amine (1*R*,2*S*)-**26** is obtained from tica ester (1*R*,2*R*)-**48** through a Hoffman rearrangement.

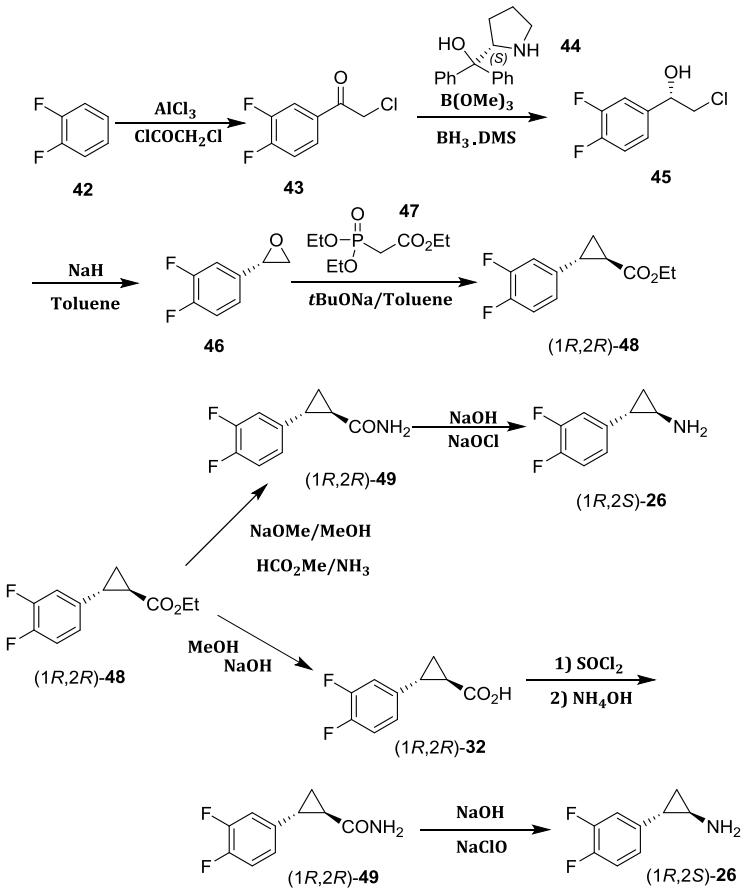

Figure 1.15: Route towards the target Tica amine (1*R*,2*S*)-**26** starting from 1,2-difluorobenzene **42** as described in the AstraZeneca product patents (Dejonghe *et al.*, 2008; Mitsuda *et al.*, 2008). The stereocentres are introduced in a reduction using CBS-borane **44** and a subsequent TEPA **47**-mediated formation of the cyclopropane.

Although borane requires specialized equipment to be used on scale, this method is very neat and requires relatively few synthetic steps. Moreover there is no need for the use of sophisticated chiral auxiliaries. The racemic version of this method (i.e. employing sodium borohydride for the reduction of the chloroketone) is therefore employed (at Chemessentia)

for the synthesis of the tica ester **48** and amide **49**, which is the starting material in most biocatalytic approaches discussed in the following sections. The initial stereoselective reduction of ketone **43** could in principle be achieved using an enzyme as catalyst and would be the best to scale up. However, this is not practical since the patents in question expire later than the original product patent (Guile *et al.*, 2000).

Finally, the desired amine (1*R*,2*S*)-**26** is attained in a different route (cf. figure 1.16) in a patent filed in 2011 by Actavis (Khile *et al.*, 2011).

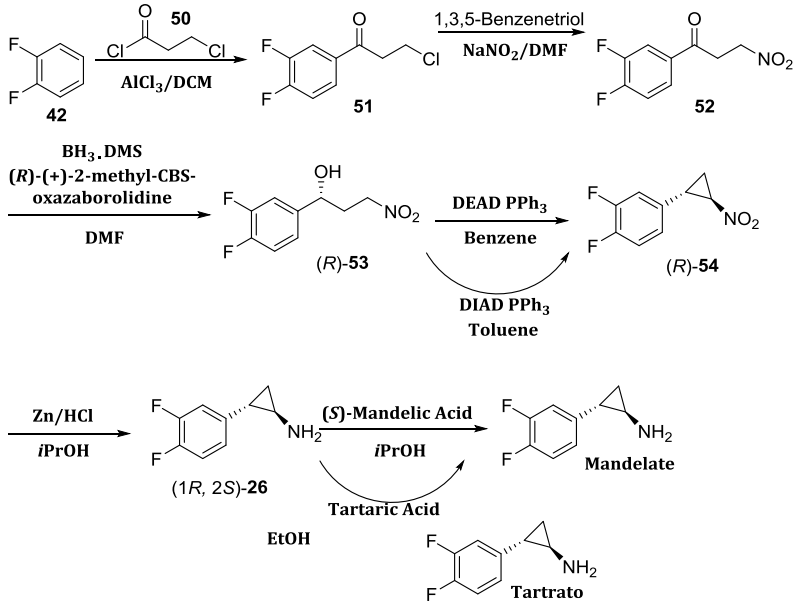

Figure 1.16: Preparation of amine (1*R*,2*S*)-**26** as described in the Actavis patent (Khile *et al.*, 2011) starting from prochiral ketone **52**. The stereocentres are fixed during the closure of the ring in a Mitsunobu type reaction.

1-(3,4-difluorophenyl)-3-nitropropan-1-one **52** is obtained in a two-step synthesis from 1,2-difluorobenzene **42**. Ketone **52** is reduced to alcohol (*R*)-**52** using CBS-borane. A subsequent closure of the ring following a Mitsunobu-mechanism yields the nitrocyclopropane (1*R*,2*S*)-**54** which is then reduced to the desired amine (1*R*,2*S*)-**26**. Both stereocentres are fixed in the cyclopropanation step. The stereoselective reduction of ketone **52** to alcohol (*R*)-**53** determines the first stereocentre. The second stereocentre is introduced during the cyclopropanation reaction. The selective formation of the *trans*-cyclopropane is favoured for steric reasons. Moreover, epimerisation of the plausible *cis*-isomer should occur readily due to the acidic nature of the proton alpha to the nitro group. Recrystallization yields the desired (1*R*,2*S*)-amine **26** in high optical purity.

Early examples (other than those discussed above) of syntheses of cyclopropyl amines of the tica type have been reported by Borne *et al.* (1977). C*is*- and *trans*- 2-phenylcyclopropane carboxylic acids have been prepared by addition of ethyl diazoacetate **56** to styrene **55**. Hydrolysis yielded diastereomerically pure fractions of both compounds, which were then transformed into the respective amines via a Curtius rearrangement (cf. figure 1.17). Although the separation of the diastereomers was achieved, the method does not allow for the separation of enantiomers, the amines **26** and **58** are obtained as a racemate.

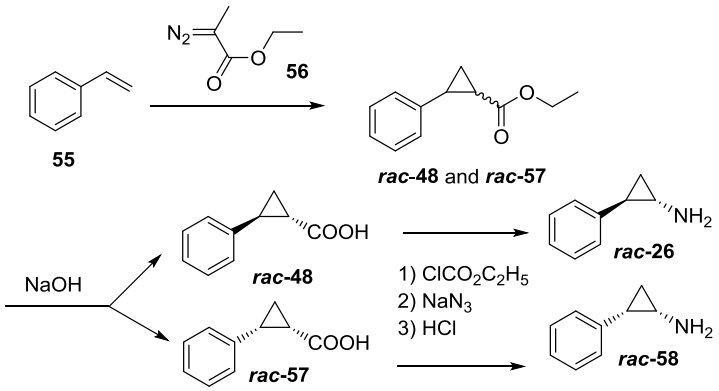

Figure1.17: Preparation of the cyclopropane amine from a reaction between styrene **55** and ethyl diazoacetate **56**.

Finally Nishiyama *et al*. fine-tuned this reaction employing chiral ruthenium complexes in an asymmetric cyclopropanation of olefins and diazoacetates. Employing their catalyst and L-(+)-menthyl diazoacetate they obtained (1*R*,2*R*)-**39** with 97% *ee*. In subsequent studies with catalysts varying in the side chain R as well as different chiral diazoacetates, they were able to direct the stereo- and diastereoselectivity (cf. figure 1.18). Ultimately the use of their catalyst allowed the reaction as done by Borne *et al*. (*vide supra*) to occur with a diastereomeric ratio of 94:6, yielding the desired ester (1*R*,2*R*)-**48** with 91% ee (Nishiyama *et al.*, 1995).

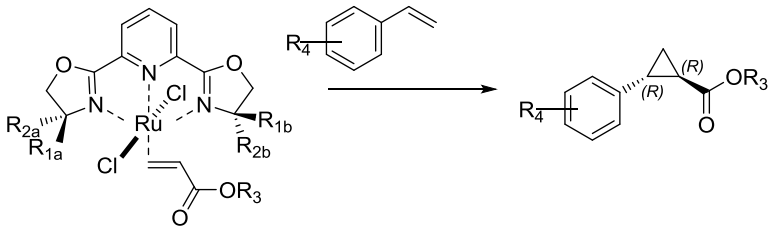

	yield	trans:cis	%*ee* (1*R*,2*R*)
$R_{1a/2b}$ = ^{i}Pr; $R_{1b/2a}$ = H; R_3 = L-(+)-menthol; R_4 = *H*;	83	97:3	96
$R_{1a/2b}$ = ^{i}Pr; $R_{1b/2a}$ = H; R_3 = L-(+)-menthol; R_4 = *p*Cl;	84	96:4	95
$R_{1a/2b}$ = ^{i}Pr; $R_{1b/2a}$ = H; R_3 = L-(+)-menthol; R_4 = *p*MeO;	96	95:5	97
R_1 = *s*-Bu; R_2 = H; R_3 = Et; R_4 = H;	82	94:6	91

Figure 1.18: Asymmetric cyclopropanation of olefins and diazoacetates using a set of differently substituted ruthenium catalysts as described by (Nishiyama *et al.*, 1995). The influence of isopropyl-, menthyl-, and *para*-halide substitution is examined in detail.

Different approaches chosen for the synthesis of amine (1*R*,2*S*)-**26** will be discussed in detail in the following chapter. Since the ultimate goal of the work described herein was the development of a synthetic route based on a biotransformation to be employed in an industrial context two constraints applied simultaneously: scalability of the process and existent patent landscape. Therefore the new routes were designed with these parameters in mind.

1.3 Enzymes used in this thesis

In order to attain target amine (1*R*,2*S*)-**26**, different synthetic routes have been discussed and developed as part of the project in accordance with the state of the art and the patent situation at the time of the experiments (figure 1.19).

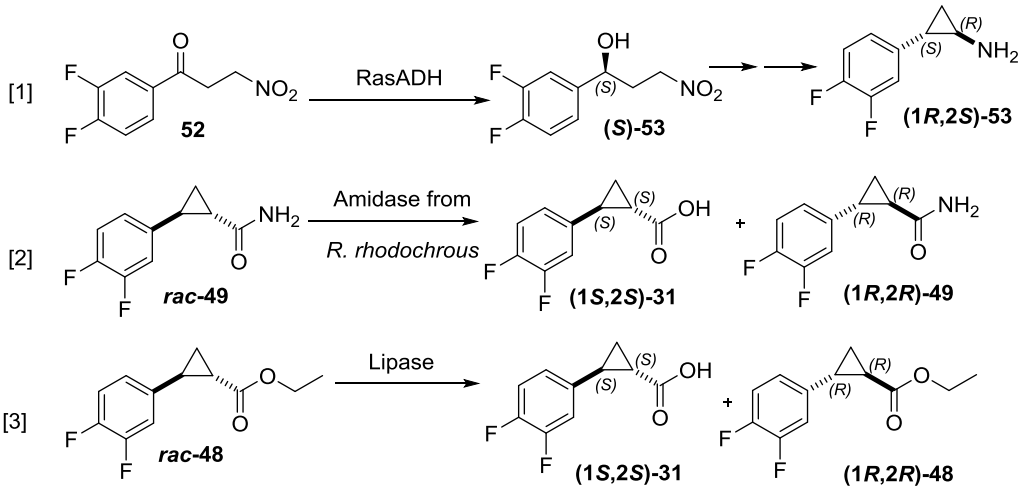

Figure 1.19: Different approaches to the desired amine. [1] highlights a ketoreductase (RasADH) mediated approach towards the alcohol, which will be transformed into the desired cyclopropyl amine in a stereoselective ring closure reaction. [2] and [3] focus on hydrolase mediated kinetic resolution of a racemic trans-cyclopropane precursor which will be subsequently transformed into the desired amine in a Curtius of Hoffman reaction.

The approaches chosen here employ both KREDs and hydrolases. Due to their pronounced importance for this work the hydrolases will be reviewed extensively in the following section. For more information on ketoreductases please refer to § 2.1.2.

1.3.1 Hydrolases (E.C 3) –a general overview

Hydrolytic enzymes (Enzyme class (E.C.) 3) are very common biocatalysts in industrial applications. They act on a broad range of substrates (cf. table 1.1), which makes them a fantastic tool for the chemical industry.

Table 1.1 List of naturally occurring hydrolases and their target bonds

Entry	E.C. number	Acting on	Approximate number[a]
1	3.1	Ester bonds	430
2	3.2	Glycosyl-compounds	220
3	3.3	Ether bonds	13
4	3.4	Peptide bonds	380
5	3.5	C-N bonds other than peptides	209
6	3.6	Acid anhydrides	123
7	3.7	C-C bonds	20
8	3.8	Halide bonds	9
9	3.9	P-N bonds	1
10	3.10	S-N bonds	2
11	3.11	C-P bonds	3
12	3.12	S-S bonds	1
13	3.13	C-S-bonds	2

[a] approximate number taken from ExPASy ENZYME - The Enzyme Data Bank

Of particular interest for the chemical and pharmaceutical industry and also for the scope of the work presented, are those hydrolases that work on ester bonds (E.C. 3.1), peptide bonds (E.C. 3.4) and amide bonds different to peptides (E.C. 3.5). In addition to being the most abundantly occurring enzymes of that class (cf. Table 1.3.1, Entry 1, 4 and 5), they feature some qualities which make them particularly versatile catalysts for industrial applications. Among their most predominant characteristics are a broad substrate specificity and general indifference to harsh reaction conditions (Aouf *et al.*, 2014) all of which make them a versatile catalyst for biotechnological applications (Hernández-Rodríguez *et al.*, 2009).

Hydrolases find applications in various industrial and biotechnological sectors (Bora et al., 2013) -a non-exhaustive list of applications is presented below:

In the food industry, lipases (E.C. 3.1) are used for example to create a monoacylglycerol with palmitic acid at the *sn*-2 position, which represents an important additive in infant milk as well as the production of synthetic low calorie fats (Houde *et al.*, 2004). Moreover they are used to convert fish oils into free eicosapentaenoic acid (Delgado-

García *et al.*, 2012). Xylanases (E.C. 3.2) used in the production of chicken feed to generate cereals that are more easily digestible (Clarkson *et al.*, 1999). Furthermore hydrolases are used as additives in detergents ('bio detergents') for the removal of greasy stains (Hora and Kivits, 1981; Rathi *et al.*, 2001) and the conservation of tissue during washing. In the pulp industry Xylanases and mannanases (E.C. 3.2) find an application in the improvement of paper quality (Dhawan and Kaur, 2007; Juturu and Wu, 2012). Amylases (E.C. 3.2) are moreover used for the production of biofuels (bioethanol) through saccharification of marine microalgae (Karan *et al.*, 2012). Finally, hydrolases are employed in the fine chemical industries. A well-known example is the use of acylases in the synthesis of semi-synthetic antibiotics of the penicillin/cephalosporin type (Buchholz *et al.*, 2012) as well as for the production of amino acids (Baxter *et al.*, 2012).

1.3.2 Structure

Members of this class of enzymes, although they show a difference in their substrate preferences and activation mode (*vide infra*), are unified by their structure. Figure 1.20 shows a condensed representation of the structural elements of the αβ-hydrolase fold. Although variations exist, in particular in the orientation of the last β-strands and the position and amount of α-helices, the αβ-hydrolase fold shown here comprises the structural elements that commonly prevail within most E.C. 3 enzymes.

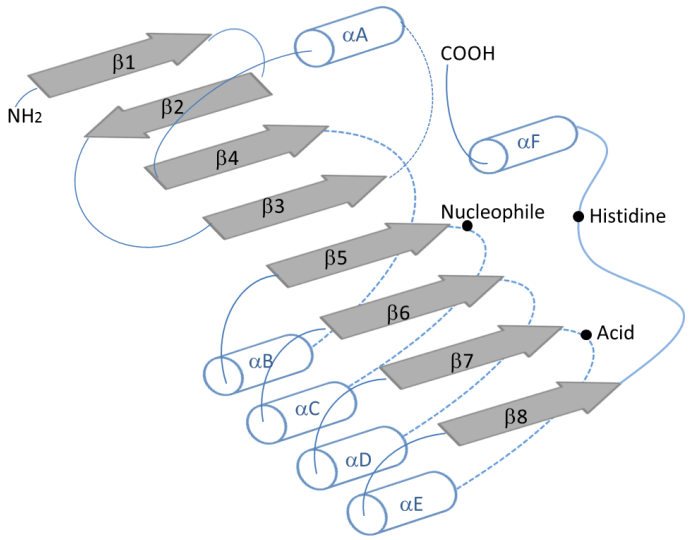

Figure 1.20: A schematic overview of the basic αβ-hydrolase fold. β-sheets are represented as grey arrows, α-helices are shown as white barrels. The catalytic residues are marked as black dots, image adapted from Nardini and Dijkstra (1999).

The common feature of this fold consists of a mostly parallel, eight-stranded β-sheet, which is flanked on both sides by α-helices. The central β-sheet shows a left-handed superhelical twist, generally with the extreme strands crossing each other in space. The α-helices which connect the β-strands of the β-sheet can vary in size and position , however the first helix (counted from the N-terminus) is well conserved throughout the family of the αβ-hydrolases and is believed to play an important role establishing the correct orientation of the catalytic residues in the active site (Holmquist, 2000).

All hydrolases feature some highly conserved amino acids in the catalytic site: an aspartic acid, serine or cysteine acting as a nucleophile is positioned after strand β5, an acidic residue is usually positioned after strand β7 and a highly conserved histidine positioned after the last β strand (Nardini and Dijkstra, 1999). Together these residues form the catalytic triad (cf. figure 1.21).

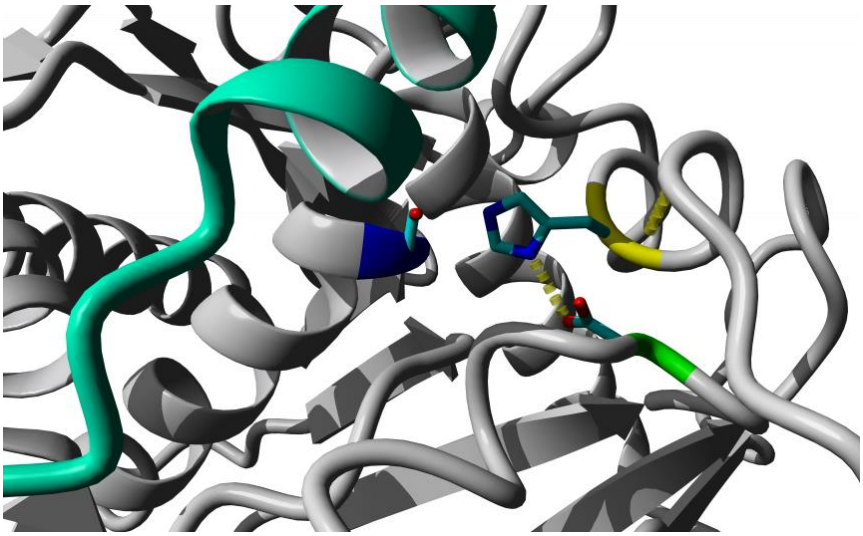

Figure 1.21: Lid closing over the active site of a lipase. The catalytic triad composed of an Aspartat residue (green) and a histidine residue (yellow) act together to deprotonate the Serine (blue) to make it more nucleophilic. The hydrogen bond between asparagine and histidine is indicated as yellow dotted lines.

1.3.3 Mechanism

The mechanism of the hydrolases is that of a base catalysed hydrolysis reaction. The attacking nucleophile is a basic residue (a deprotonated serine or cysteine, generally) in the active site of the enzyme. The reaction occurs according to an addition-elimination mechanism. Figure 1.22 explores the reaction mechanism between a carboxylic acid derivative and a hydrolase by means of a putative catalytic triad composed of the residues aspartate, histidine and serine (cf. also figure 1.20)

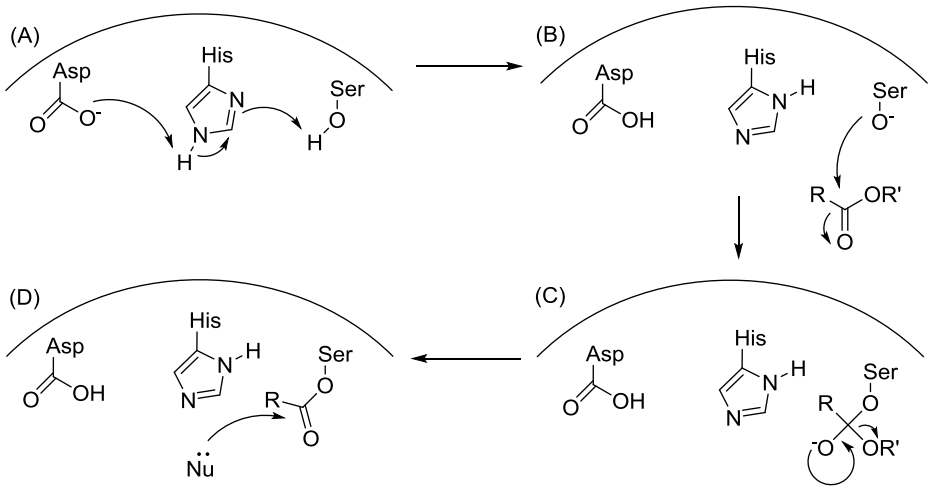

Figure 1.22: Postulated mechanism of the catalytic cycle of hydrolases, explained on the example of an enzyme with a putative catalytic triad composed of the residues aspartate, histidine and serine.

According to the mechanism proposed (Buchholz *et al.*, 2012), the hydroxyl group of the serine is made more nucleophilic by the concerted action of an acidic (*here:* Asp) and a histidine residue in its proximity helping to abstract the hydroxyl proton (figure 1.22, step A). Thereby the attack of the serine to the carbonyl group, in this case an ester, is facilitated. Upon attack of the serine at the carbonyl group (figure 1.22, step B) an addition-elimination reaction takes place. A tetrahedral intermediate is formed (figure 1.22, step C), which upon elimination of the leaving group (OR') turns into the acyl enzyme complex, where the substrate is covalently bound to the active site of the enzyme (figure 1.22, step D). Ensuing attack of a nucleophile (H_2O, an alcohol or an amine) according to the same mechanism releases the new carbonyl compound and regenerates the free enzyme. The tetrahedral transition state is stabilised by the "oxyanion hole" a pocket in the active site of the enzyme that stabilises the deprotonated oxygen through positively charged residues (Berg *et al.*, 2012).

Lipases, a specific class of hydrolases acting on ester bonds (E.C 3.1) have been thoroughly studied in terms of their reaction profile and enantioselectivity. A rule (the Kazlauskas' rule) has been established in an empirical study to determine the enantiopreference of lipases towards secondary alcohols in an esterification. Although this rule has been established based on the comparison of the enantiopreference of cholesterol esterase, the lipase from *Pseudomonas cepacia* and the lipase from *Candida rugosa,* it has been shown to be applicable to nearly all lipases (Kazlauskas *et al.*, 1991). The Kazlauskas' rule establishes that the orientation ((*S*)- or (*R*)- face) in which the compound will bind in the active site depends on the other substituents of the chiral C-atom and their fit into the binding pocket. For esters of secondary alcohols it has been found that enantiomer shown in figure 1.23 reacts faster than its other enantiomer.

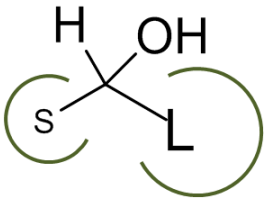

Figure 1.23: The orientation of substrates in the binding pocket (in green) of hydrolases depends on the size of the substituents, (S = smaller substituent; L = larger substituent)

We have already seen that all hydrolytic enzymes share a common fold and highly conserved catalytic residues in the active site. The different subclasses share even more similar structures. In the following, and due to their major importance in industry and for the scope of this work, the E.C. 3.1, 3.4 and 3.5 enzymes will be discussed in more detail with regards to their similarities and differences.

1.3.4 Zooming in on specific hydrolases: Lipases, Esterases, Amidases and Proteases

1.3.4.1 E.C. 3.1: Lipases and Esterases

Our understanding of the structure and properties of lipases and esterases has increased considerably in recent years due to the resolution of their crystal structures and elucidation of their function-structure relationship. The difference between the subclass lipases and the subclass esterases can be distinguished on the basis of their substrate specificity: while esterases primarily act upon water-soluble short acyl chain esters in solution

and are inactive against water-insoluble long chain triacylglycerols, lipases specifically hydrolyse the latter compounds (Chahinian and Sarda, 2009). Both subclasses can be subdivided further by means of individual biological and structural properties

This observed difference in substrate specificity can be traced back to a structural difference, which dramatically changes their catalytic behaviour and substrate specificity: the lid. With a few exceptions (eg. CalB), lipases in contrast to esterases, feature a lid which covers the active site in the inactive conformation. The long-chain substrate esters build a hydrophobic layer onto which the lipases can absorb. The interaction of the lipases with the lipid layer leads to the opening of the lid in a process known as interfacial activation. Many factors play a role for the lid to fully open, among the mode of absorption and the interaction of the hydrophobic residues in the lid with the oily substrate (Hedin *et al.*, 2005; Hernández-Rodríguez *et al.*, 2009; Noinville *et al.*, 2002; Rehm *et al.*, 2010) and will be reviewed for the specific lipase used in section 2.2.1.

1.3.4.2 E.C 3.4 Proteases and E.C. 3.5 Amidases

Another class of hydrolases, present in a wide range of physiological processes present in all kingdoms of life, comprises the enzymes that act on C-N bonds, proteases (E.C 3.4, cleaving peptide bonds) and amidases (E.C. 3.5, cleaving amide bonds other than peptide bonds). Although they rely on the same type of mechanism (Buchholz *et al.*, 2012) as esterases, amidases are capable of cleaving an amide bond. Amides differ from esters in their partial double bond character (due to a resonance effect that is absent in esters) and extra hydrogen at the amide nitrogen that does not occur in esters (cf. figure 1.24, extra hydrogen marked blue). The resonance structure forming partial C-N double bond (cf. figure 1.24 [A]) cannot occur for esters (cf. figure 1.24 [B]), which makes the C-O bond less strong and easier to cleave.

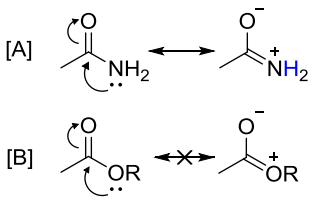

Figure 1.24: Mesomeric effect and partial double bond between in the amide bond, which does not occur in the ester

It has been shown that the energy of the transition state of the scissile C-N bond is

lowered by formation of a hydrogen bond between the N-H (in blue in figure 1.24) and a hydrogen bond acceptor either intramolecular or intermolecular trough interaction with the amino acid side chain (Syrén and Hult, 2011), thereby stabilising the transition state of the tetrahedral intermediate that is formed during hydrolysis. Furthermore, it has been demonstrated that the introduction of a hydrogen bond acceptor into an esterase induces amidase activity, which fully establishes the role of the hydrogen bond in amide hydrolysis (Syrén *et al.*, 2012).

1.3.5 Promiscuity

Another interesting characteristic of hydrolases, in particular lipases, is their extensive promiscuity in terms of conditions, substrates and reactions. Condition promiscuity plays an important role in process development, when enzymes are employed under conditions different to their physiological ones. An example is the use of organic co-solvents or the change of pH and temperature from the natural conditions to the conditions that are required for the process. Substrate promiscuity occurs when the enzyme is able to perform the reaction on substrates of the same chemical group but different to its natural substrates. This has been wildly demonstrated and practically applied. An example is the use of lipases and esterases to catalyse the kinetic resolution of a series of esters and amides that do not occur in nature (García-Urdiales *et al.*, 2000). Finally the most striking type of promiscuity, and the most powerful tool for biotechnologists, is the promiscuity in terms of the reaction catalysed. Among the most studied enzymes are the hydrolases, which have been shown to catalyse an astonishing range of reactions from Markownikow additions (Wu *et al.*, 2005a; Wu *et al.*, 2005b; Wu *et al.*, 2006), Aldol additions (Branneby *et al.*, 2002), Michael additions (Kitazume *et al.*, 1986; Svedendahl *et al.*, 2005), as well as Knoevenagel condensations (Hu *et al.*, 2012) and a Mannich reaction (Xue *et al.*, 2012). The capacity of an enzyme to catalyse a reaction relies on the stabilisation of the transition state. Therefore the ability to accommodate a substrate in its active site that attains the same transition state (in terms of spacial orientation, conformation and electron distribution) is essential for catalytic promiscuity. This can occur naturally or can be induced by lowering the rigidity of the enzyme by means of temperature or the addition of a co-solvent

In this sense the ability of hydrolases to catalyse many different types of reaction

together with their ease of application (*vide supra*) and their versatility makes them a very attractive tool for biocatalytic applications and molecular biological 'tailoring'. Hydrolases were therefore chosen as the target enzymes for protein engineering experiments in this research.

2.0 Results and Discussion

2.1 Synthesis of (1*R*,2*S*)-26 using commercial enzymes:

2.1.1 Introduction

A bio-retrosynthetic consideration, as proposed by Turner and O'Reilly (2013), of the target compound yielded different possible strategies towards the cyclopropyl subunit (1*R*,2*S*)-**26** (§ 1.5) starting from low value precursors that are either commercially available or can be easily synthesised by the industrial partners on a large (kg) scale. Three approaches were chosen (cf. figure 2.1a) for examination and are discussed below.

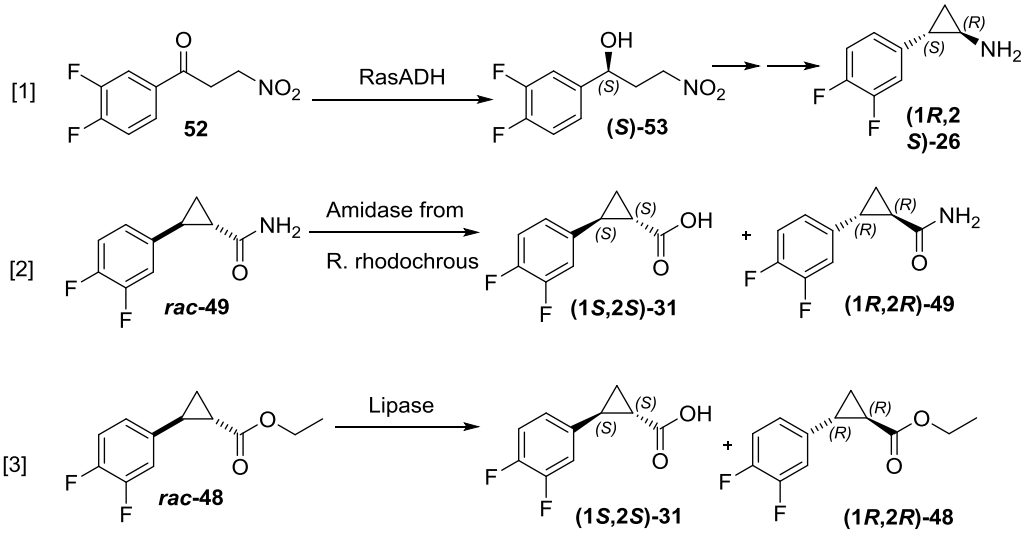

Figure 2.1: Different approaches towards the Tica amine (1*R*,2*S*)-**26**, [1] KRED approach towards the (*S*)-alcohol (*S*)-**53**, which can be transformed into the desired compound (1*R*,2*S*)-**26** in subsequent reaction steps; [2] Amidase mediated hydrolysis of the amide *rac*-**49** towards the acid (1*S*,2*S*)-**31**; [3] lipase-mediated hydrolysis of a Tica ester and *rac*-**48** towards the acid (1*S*,2*S*)-**31**.

The possibilities that synthetic chemistry allows in order to obtain the desired compound (1*R*,2*S*)-**26** were explored in this range of reactions using both cyclic and acyclic precursors as substrates for the biotransformations. An acyclic precursor was employed (cf. Figure 2.1 [1]; § 2.1.1) in one of the syntheses studied. In this case, the stereocentres were introduced into the molecule through a combined chemoenzymatic route. In other cases the cyclopropyl moiety was already present in the precursors used (§ 2.1.3. and 2.1.4) and the stereocentres were attained through kinetic resolution of the racemate. While the first route allows for a theoretical 100% yield only a maximum 50% yield can be attained in the second

route. In the following, the three approaches will be discussed and evaluated individually in terms of their feasibility and industrial applicability.

2.1.2 Ketoreduction

The oxidation of alcohols via hydrogen transfer represents an environmentally sustainable 'green' redox protocol. In this context, the first approach to be tested was an enzyme-mediated ketoreduction (cf. Figure 2.1a, [1]). The oxidation of *sec*-alcohols to the corresponding ketones and *vice versa* has been amply discussed and reviewed (Hollmann *et al.*, 2011a; Hollmann *et al.*, 2011b). Evidence in literature suggests this to be a viable route towards the desired tica alcohol (*S*)-**53**. Many different ketoreductases seem to accept bulky-bulky ketones as their substrate (Cuetos *et al.*, 2012; Lavandera *et al.*, 2008b). The envisaged route starts from the prochiral ketone **52** which is structurally similar to the substrate used by Yang and co-workers (2009). If the ketoreductase exhibits high enantioselectivity towards the tica ketone **52** the (*S*)-configuration of the chiral centre will be introduced into the molecule. The introduction of the configuration at the second chiral centre occurs spontaneously during a 1,8-diazabicyclo[5.4.0]undec-7-ene (DBU) mediated cyclisation reaction owing to the steric impediments imposed by the substituents (Yu *et al.*, 1992; Zindel and de Meijere, 1995). Finally the reduction of the nitro-substituent yields the desired (1*R*, 2*S*)-tica amine **26** in a combined chemo-enzymatic route (cf. figure 2.2).

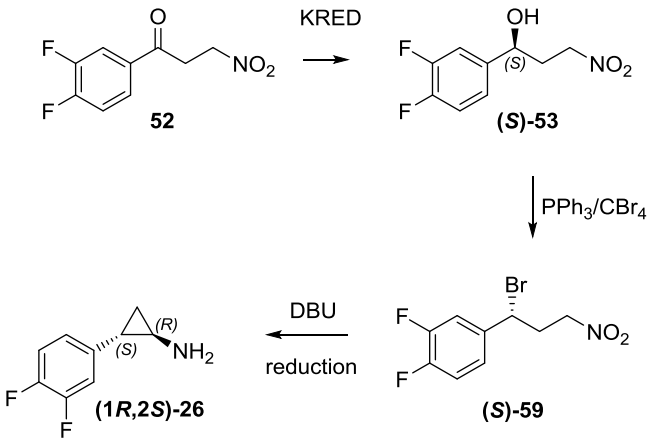

Figure 2.2: Chemo-enzymatic approach towards the tica amine (1*R*,2*S*)-**26.**

In order to generate the alcohol via an enzymatic ketoreduction a recycling system had to be established that allowed for the regeneration of the co-factor nicotinamide adenine

dinucleotide phosphate (NAD(P)H) without causing a bottleneck in the biotransformation (Buchholz *et al.*, 2012). Whole-cell, enzyme-based and substrate-based recycling systems (cf. figure 2.3) are discussed in literature (Edegger *et al.*, 2006; Hartog *et al.*, 2011). A whole cell system has the advantage of supplying the recycling system and providing reduction equivalents through the cell's metabolism and does not require purification of the enzyme. On the other hand, this system is unfavourable since side-reactions from the cell's own dehydrogenases cannot be excluded. Therefore, the enzyme- or substrate-based recycling system marks the preferred approach. If acetone/isopropanol is accepted as a co-solvent and substrate by the dehydrogenase, a substrate-based system (cf. figure 2.3 [1]) can be used, where the oxidation of isopropanol to acetone by the same dehydrogenase regenerates the co-factor. While this system does not require additional components to be added to the reaction mixture, care needs to be taken to ensure that the K_M of the dehydrogenase for 2-propanol is below the Michaelis-Menten constant (K_M) for the actual substrate. This is to ensure the transformation of the substrate ketone into the desired alcohol and the recycling of the co-factor occur via the acetone/2-propanol system. The enzyme-based system on the other hand, relies on an additional enzyme and substrate (usually glucose and glucose dehydrogenase, GDH cf. figure 2.3 [2]) to be added to the reaction mixture. Again, the recycling step needs to proceed at a higher rate than the ketoreduction reaction, which can be attained by using a very efficient dehydrogenase like the GDH (250 U/mg (Chenault *et al.*, 1988)) for the recycling. Moreover, the coupled assay using formate dehydrogenase (FDH cf. figure 2.3 [3]) is of special interest, since it irreversibly oxidises the formate to CO_2 thereby helping to shift the equilibrium towards product formation (Hummel *et al.*, 2003).

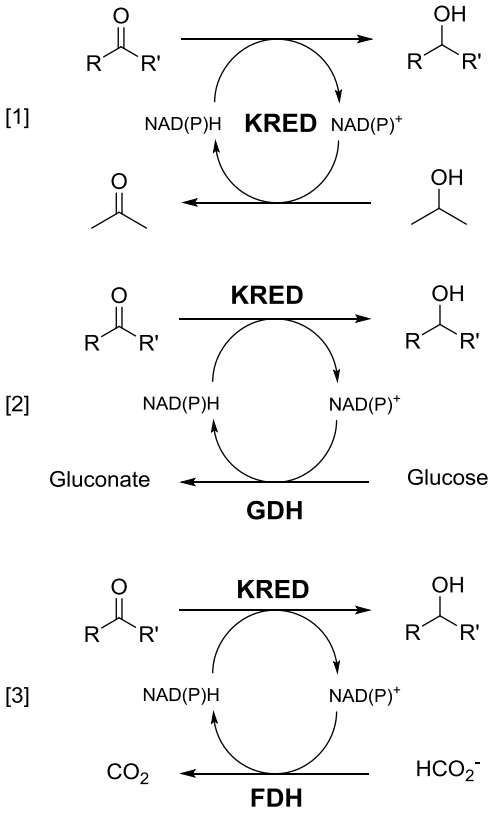

Figure 2.3: Different types of co-factor recycling: KRED is used to distinguish the biocatalyst from the recycling enzyme (glucose dehydrogenase, GDH; formate dehydrogenase, FDH). [1] substrate-based recycling, [2] enzyme-based recycling using GDH, [3] enzyme-based recycling using FDH to pull the equilibrium towards product formation.

In order to find a ketoreductase that would transform ketone **52** to the corresponding (*S*)-alcohol (*S*)-**53**, with high enantioselectivity, different panels of commercially available ketoreductases were screened. Very few of the enzymes tested showed activity towards the target compound. The KRED-130 and KRED(NADH)-110, both from Codexis, transformed the tica ketone **52** with 71.6 ee_p (KRED(NADH)-110) and ee_p 99.9 (KRED-130). KRED-130 proved to be particularly active, 100% conversion was attained after 48 h of reaction (results collected in table 2.1a) Conversions had to be determined by NMR analysis of the reaction crude mixture due to the low UV absorption of the ketone in chiral HPLC, which interfered with its accurate quantification (for an exemplary NMR cf. figure 2.4).

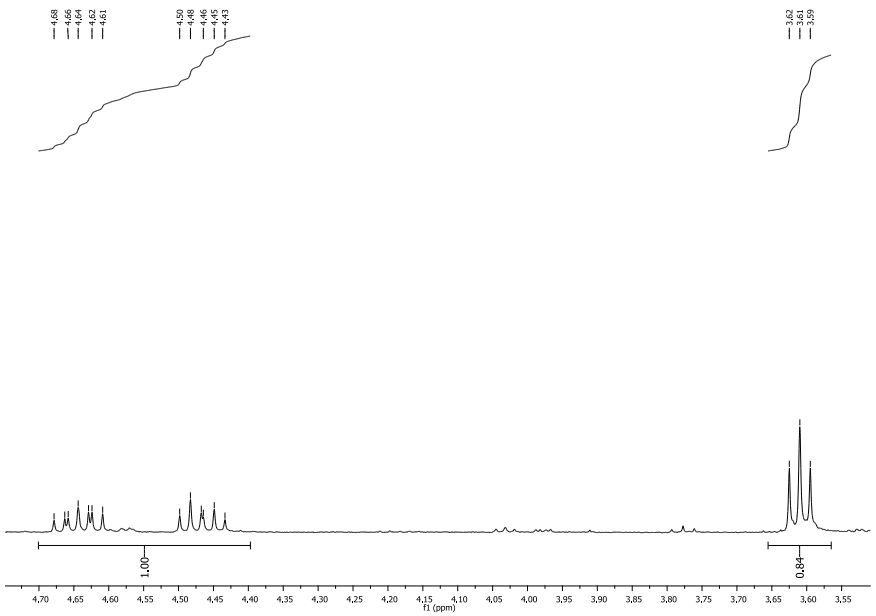

Figure 2.4: Exemplary NMR-analysis (crude of the reaction mixture) of conversion rates. The region shown is the region of the CH_2 adjacent to the nitrogroup in the alcohol (4.4 – 4.7 ppm) and the α -CH_2 in the ketone (3.55-3.65 ppm) which were chosen for comparison because there is no overlapping of the integrals of alcohol and ketone and allow for a clear determination of 55% conversion.

The focus was then shifted towards non-commercially available enzymes (cf. table 2.1) known to work on bulky-bulky ketones (Bisogno *et al.*, 2009; Lavandera *et al.*, 2008a; Lavandera *et al.*, 2008b).

Table 2.1: Hits in the ketoreduction approach using KREDs (COdexis) and non-commercial alcohol dehydrogenases for the reduction of ketone **52** towards alcohol **53**

Entry	Enzyme[a]	t [h]	*c*	*ee*[b]	Enantiopreference
1	KRED-130	48	100	99.9	S
2	KRED(NADH)-110	48	23	71.6	R
3	RasADH	48	34	91.6	S

[a] conditions applied: 100mM potassium phosphate buffer (pH 7), 5 g/L ketone **52** in 10% DMSO, 5 g/L ketoreductase, 1 g/L GDH, 1 g/L NAD(P)H, 1.25 molar equivalents of glucose.
for RasADH: Tris HCl buffer (pH 7.5) 50 mM, 8 g/L ketone **52**, 37 g/L ketoreductase, 0.7 g/L cofactor, 1 g/L, 2 molar equivalents of glucose.

[b] enantiomeric excess of the product, determined by chiral HPLC.

The Ras-ADH, kindly provided by Dr. Iván Lavandera, (Bioorganic group, University of Oviedo, Spain) is known to be *S*-selective (Barcellos *et al.*, 2011), and as expected, transformed the ketone **52** in favour of the desired (*S*)-enantiomer. The reaction occurred with 91.6% *ee* and a corresponding *E* of 23 (cf. table 2.1 entry 3).

All systems were tested in combination with both enzyme- and substrate-based recycling systems. However the addition of 2-propanol seemed to have a detrimental effect on the process (data not shown). The conversion attained in the reaction was 10 % in 48 h. Therefore the enzyme-based recycling system was chosen in order to provide the required reduction equivalents (cf. figure 2.5).

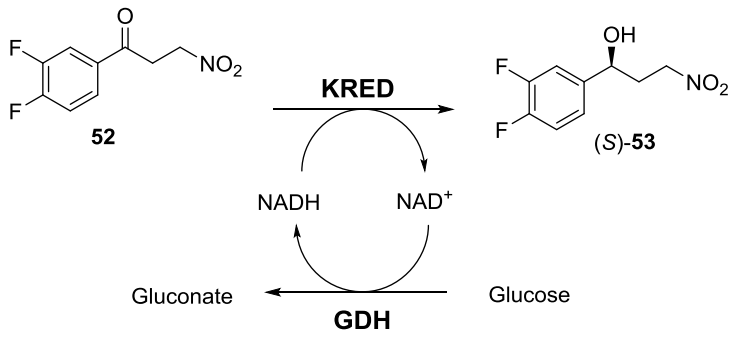

Figure 2.5: Enzyme mediated reduction of ketone **52** towards the alcohol precursor of the cyclopropylamine, GDH was used following the standard protocol in the group.

Concurrent to the discovery of this route the ketone **52** and alcohol (*S*)-**53** intermediates have been claimed in a patent (Khile *et al.*, 2011) and therefore the KRED approach was abandoned in favour of different, unpublished approaches as discussed below cf. figure 2.1 [2] and [3]).

2.1.3 Amide hydrolysis of compound *rac*-**49**

The kinetic enzymatic resolution of carboxylic acid derivatives of homo- and heterocyclic compounds is an active field of research. The resolution of homo and heterocyclopropane compounds with amidases from *Rhodococcus* sp. has been thoroughly studied. Among the first results is the enantioselective hydrolysis of an *O*-benzoylated β-hydroxy amides through biotransformation with *Rh. rhodochrous* IFO 15564 (cf. Figure 2.6), which was reported twenty years ago (Yokoyama *et al.*, 1996). The results obtained show that

the reaction occurs not only with excellent enantioselectivity but also with high chemoselectivity, since the benzoate group was barely transformed.

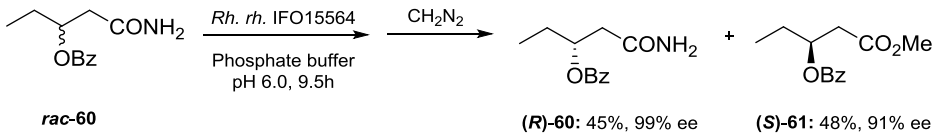

Figure 2.6: Bacterial catalysed resolution of (±)-3-benzoyloxypentanamide followed by chemical conversion of the acid to its methyl ester

Due to its relevancy to the present work the bacterial resolutions of cyclopropyl amides performed by M.-X. Wang *et al.* will be reviewed briefly. The authors use the commercially unavailable *Rhodococcus* sp. AJ270, which has the activity of a nitrile hydratase and amidase to examine the kinetic resolution of *cis*- and *trans*- 2- and 2,2,3-substituted derivatives of the cyclopropane carboxamide (cf. Fig 2.7).

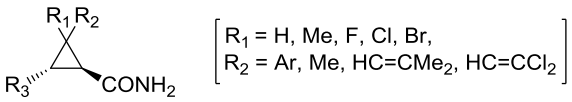

Figure 2.7: Different 2- and 2,2,3-substituted trans-cyclopropane carboxamides acids used for biotransformations with *Rhodococcus* sp. AJ270 in the Wang group

It is noteworthy that the enzyme discriminates strongly between the two diastereomers. Generally, it was found that the *cis*-compounds reacted at a significantly slower rate compared to the *trans*-compounds (Wang and Feng, 2002a; Wang and Feng, 2002b). However, comparison of the *cis*- and *trans*-diastereomers shows that the enantioselectivity for the *trans*-diastereomers is higher. This relationship is maintained within each family of compounds (Wang and Feng, 2002a). Moreover, it was found that the introduction of substituents played an important role concerning both the enantio- as well as the stereoselectivity. Enantioselectivities significantly decreased with the increase in size of the substituent at the 3-position of, 2,2-dimethyl-3-arylcyclopropane-1-carboxamide (cf. figure 2.8 (Wang and Feng, 2002b).

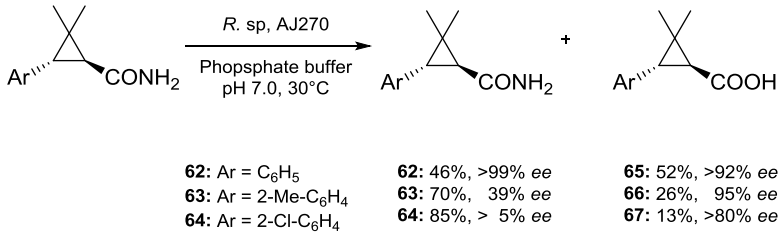

Figure 2.8: The influence of the residue in 3-position on the enantioselectivity of the amidase catalysed hydrolysis of amines **62-64**

Furthermore, substitution at the 2-position interferes strongly with the enantioselectivity of the process, again influenced by an increase in the size of the substituent. Although it has not yet been proven by crystallization of the enzyme, these findings suggest that the active site of the enzyme would be narrow and located relatively deep within the enzyme (Wang and Feng, 2002c). Drastic changes in both positions described above is therefore likely to dramatically affect the binding of the substrate to the enzyme, thereby altering the reaction rate as well as the chiral recognition process.

The genomic sequence for the amidase from *Rhodococcus rhodochrous* IFO 15564 enzyme has not been identified and the enzyme has never been purified. Biotransformations using this amidase therefore have to be performed as whole cell reactions employing resting cells. The expression of the amidase is induced in the bacteria during the cultivation by addition of β–caprolactam to the medium (Yokoyama *et al.*, 1996). Very similar results were attained in a *Rhodococcus rhodochrous* IFO15564 mediated hydrolysis of azaridines (cf. figure .2.9 (Morán-Ramallal *et al.*, 2007; Morán-Ramallal *et al.*, 2010)).

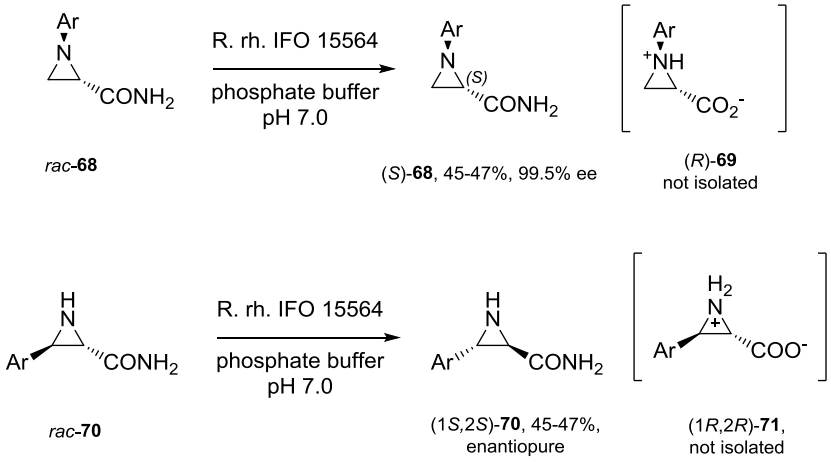

Figure 2.9: *Rhodococcus rhodochrous* mediated biotransformations of racemic 3- and *N*-substituted aziridine-2-carboxamides

The acids resulting from this biotransformation could not be isolated from the reaction medium. However, the remaining amides were obtained with almost 50% yield (upper limit for kinetic resolutions) and were enantiopure (cf. figure 2.9). When different aryl groups were employed as substituents an effect of the substituent on the time of reaction could be observed while the enantioselectivity of the process was scarcely altered.

These results were taken as the basis for further trials in a *Rhodococcus rhodochrous* IFO15564 mediated hydrolysis of a range of cyclopropane carboxamides (Hugentobler and Rebolledo, 2014). In these trials it was found that both the O-benzyl and N-benzyl amides were transformed with very good enantioselectivity (cf. figure 2.10).

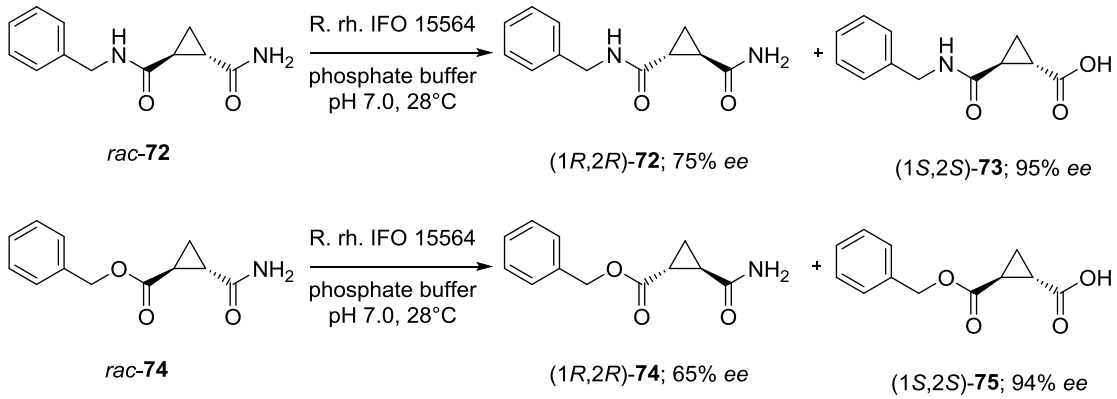

Figure 2.10: *Rhodococcus rhodochrous* mediated biotransformations of racemic 2-*O*-benzyl and 2-*N*-benzyl cyclopropane carboxamides.

Taking the findings reviewed above into account it is very likely that the amidase from *Rhodococcus rhodochrous* will accept the tica amide **49** as a substrate to attain the desired (1*R*, 2*R*)-amide (cf. figure 2.1 [2]) which can be transformed into the desired (1*R*,2*S*)-amine **26** through a Hoffman rearrangement. The optimal conditions tested for a similar biotransformation (Hugentobler, 2011) have been taken as a starting point for the trial.

Given that the *E* of a reaction is related to the reaction temperature through the Ahrrenius equation (cf. equation 5, § 1.1.2.2), a change in the temperature of the reaction should be reflected in the enantioselectivity of the process. Moreover, other parameters like the use of co-solvents should have a direct or indirect influence on the outcome of the reaction, caused primarily by solvation effects and denaturing of the enzyme (Carrea, 1984). In an ideal system the amount of catalyst should not influence the enantioselectivity with which the reaction occurs (cf. eq. 1.1.2.2.f, § 1.1.2.2). However, in this specific case the ratio of

substrate to catalyst (cells) could have an indirect influence the outcome of the reaction, which is caused for example by secondary effects like the substrates' cytotoxicity or interference with the cell metabolism.

Experiments were performed to explore the influence of cell density, temperature and cosolvent on this biotransformation[1]. The effect of the cell density was tested on small scale with cell densities (OD_{600}) of 1.5 to 0.25 employed (results collected in table 2.2). It is illustrated through this experiments that in this special case the enantioselectivity of the process is influenced by the concentration of the catalyst. At high optical densities (OD_{600}) the enantioselectivity of the process is poor and conversion rates exceed 50% in order to attain a 98% enantiomeric excess in the desired (*R*)-amide (cf. entry 1-3). Lowering the OD_{600} to 0.25, however, significantly increases the enantioselectivity of the process to an *E* of 46 (cf. entry 4). These findings are in good accordance with previous results (Hugentobler, 2011). If care is taken to fully dissolve the amide in the buffer prior to the addition of the cells the enantioselectivity of the process increases significantly (cf. table 2.2, entry 5).

Table 2.2: Influence of the optical density on the enantioselectivity of the whole-cell biotransformation of compound *rac*-**49**

Entry	OD 600	T [C]	t [h]	ee_s [a]	ee_p [b]	c [c]	E [d]
1	1.5	26	23	97.8	43.2	69.4	10
2	1	26	23	96.8	60.2	61.7	16
3	0.5	26	23	98.0	60.0	62.0	17
4	0.25	26	20	92.5	86.6	51.6	46
5[e]	1	26	24	99.9	64.4	60.8	66

Conditions: 25 mg substrate in 10% EtOH in 25 ml bacterial suspension of different OD_{600}s, shaken at 26°C, 200 rpm

[a] enantiomeric excess of the substrate, determined by chiral HPLC

[b] enantiomeric excess of the product, determined by chiral HPLC

[c] determined as $c = \frac{ee_s}{ee_s + ee_p}$

[d] determined from ee_s and ee_p as in equation 8, § 1.1.2.2

[e] the substrate was dissolved in EtOH (in 1% v/v), after addition of the phosphate buffer the mixture was treated in the ultrasonic bath until the substrate was dissolved almost to homogeneity, subsequent addition of a concentrated cell suspension yielded the reaction mixture at $OD_{600} = 1$

[1] These experiments were performed in collaboration with Humera Sharif as part of her Master thesis (Sharif, 2013)

Therefore, reactions were performed to compare the effect of temperatures and co-solvents (results collected in table 2.3). Although examples in the literature suggest an improvement of the enantioselectivity at reduced temperature (Hugentobler and Rebolledo, 2014) data obtained from these experiments show that the reduction of temperature and the change of the co-solvent did not have any significant influence on the enantioselectivity of the process (cf. table 2.3, entry 1-3). Methanol and ethanol were tested and compared as co-solvents, while DMSO was known to have an adverse effect on amidase activity (Kashiwagi et al., 2004) and therefore it was not tried. Interestingly, the absence of the co-solvent reduced the enantioselectivity to an E of 19 (cf. table 2.3, entry 4) equalling the *E* obtained in reactions at higher cell density (cf. table 2.2, entry 1-3).

Table 2.3: Comparison of different conditions (co-solvent and temperature) on the enantioselectivity of the amidase in the biotransformation of *rac*-**49**.

Entry	cosolvent	T [C]	ee_s [a]	ee_p [b]	C [c]	E [d]
1	EtOH	4	32.0	94.9	25.2	°
2	EtOH	26	16.7	95.3	14.9	49
3	MeOH	26	92.5	86.6	51.6	46
4	none	26	11.8	88.7	11.7	19

Conditions: 25 mg substrate *rac*-**49** in 25 ml bacterial suspension of an OD_{600} = 0.25, shaken at 200 rpm for 20h (24h, entry 5); 10% (v/v) co-solvent

[a] determined by chiral HPLC

[b] determined by chiral HPLC

[c] determined as $c = \frac{ee_s}{ee_s + ee_p}$

[d] determined from ee_s and ee_p as in equation 8, § 1.1.2.2

Amide *rac*-**49** dissolved readily in methanol and ethanol when slightly heated, but partially precipitated after coming into contact with the aqueous reaction medium. The precipitate disappeared over the course of reaction as the amide was slowly hydrolysed by the amidase. In the case of the solvent free trial, the reaction medium formed a suspension between the cell suspension and the hydrophobic amide. Only small amounts will have dissolved, thereby creating a substrate/catalyst ratio similar to that attained in the reaction performed at high cell density.

The data show an inverse proportional behaviour of the enantioselectivity to the cell loading. This result is contrary to the theoretical independence of the enantioselectivity and the concentration of catalyst, thereby strongly suggesting the impact of the cells on the biotransformation. A possible explanation for this phenomenon could be found in the uptake of the substrate. Resting cells are employed in these experiments, therefore the observed amidase activity has to be due to an intracellular enzyme (extracellular enzymes are removed through several washing steps). In order for the substrate to be converted by the specific amidase it has to be taken up by the cells. A dual mechanism for the uptake and conversion of the substrate amide is proposed (cf. figure 2.11).

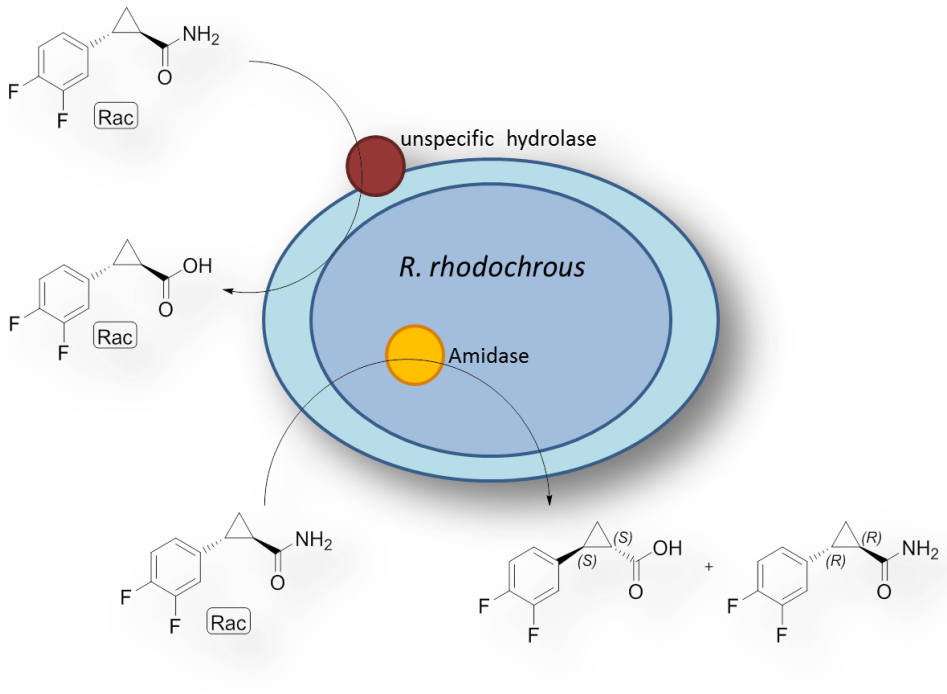

Figure 2.11: Possible dual mechanism of amide hydrolysis; the yellow circle represents the induced specific amidase whereas the burgundy circle represents a possible unspecific hydrolase

A quick, unspecific reaction, possibly mediated by unspecific hydrolases present in the periplasm or peptidoglycan cell wall (cf. fig 2.8, burgundy circle), takes place at the outer cell wall when the precipitated amide is in direct contact with the cells. On the other hand, the dissolved amide can permeate the periplasm and is slowly transformed by the specific amidase (cf. fig 2.8, yellow circle). A reduced cell density will result in a reduced unspecific contact between the amide and the cells, thereby allowing the slower, specific hydrolysis reaction to take place. This hypothesis is sustained by the fact that the use of co-solvent, which will

diminish the contact between the precipitated amide *rac*-**49** and the cells, increases the enantioselectivity (cf. table 2.3). Full solvation of the amide in the co-solvent and the buffer prior to addition of the cells to avoid precipitation of the substrate enhances the enantioselectivity of the process 1000 fold (cf. table 2.2, entry 2 and entry 5) which further supports this hypothesis.

Due to an infringement with a patent from AstraZeneca (Dejonghe, 2006) which claims the cyclopropane carboxamide **49** as an intermediate this process could not be chosen for further development either. The focus was therefore shifted to the ester hydrolysis (cf. figure 2.1 [3]) discussed below.

2.1.4 Lipase mediated hydrolysis of the tica esters

2.1.4.1 Study and screen of commercial lipases

Both lipases and esterases (cf. § 1.3.1) have been shown to catalyse the formation as well as the hydrolysis of many different esters (Buchholz *et al.*, 2005) and are widely used as synthetic tools for the enantioselective preparation of different carboxylic acids, esters and amides in fine chemical industries(Straathof *et al.*, 2002).

The Lipase-Kit™ from Almac combines a large amount of lipases, esterases and proteases from different sources and taxonomy (fungi, bacteria, plants; cf. table 2.4). Due to this broad variety of enzymes the likelihood of finding an enzyme that would transform the target ester **48** is high. At first, the different lipases were screened for hydrolytic activity towards tica ester **48** in small scale, TLC-controlled reactions in water saturated MTBE. Positive candidates were identified through appearance of a new UV-active spot with an R_f-value of 0.1 on a TLC plate eluted with H:EtOAc 4:1 (results collected in table 2.4).

Table 2.4: TLC activity in ester hydrolysis of the tica ester **48** observed in the enzymes from the Almac Kit; y stands for a UV-active stain in the TLC assay

Entry	Enzyme	kingdom	TLC[a]
1	Lipase A *Alcaligenes sp*	bacteria	n
2	Lipase B *Alcaligenes sp*	bacteria	n
3	Lipase C *Alcaligenes sp*	bacteria	n
4	Lipase *P. stutzeri*	bacteria	y
5	Lipase *P. cepacia*	bacteria	y
6	Lipase A *Candida rugosa*	fungi	n
7	Lipase D *Alcaligenes sp*	bacteria	y
8	Lipase E *Alcaligenes sp*	bacteria	y
9	Lipase B *Candida rugosa*	fungi	y
10	Lipase F *Alcaligenes sp*	bacteria	n
11	Lipase (fungal source)	fungi	n
12	Protease A *B. subtilis*	bacteria	n
13	Phytase	plant	n
14	Alkaline protease A	bacteria	n
15	Alkaline lipase A	bacteria	n
16	Lipase *Bromeliacea sp.*	plant	n
17	Lipase *Carica papaya*	plant	n
18	Neutral protease A	bacteria	y
19	Alkaline Protease B	bacteria	n
20	Acidic protease A	bacteriae	y
21	Protease A *A. oryzae*	fungi	n
22	Protease B *B. subtilis*	bacteriae	n
23	Acylase *Aspergillus sp.*	fungi	n
24	Lipase B *Candida rugosa*	fungi	n
25	Lipase *Rhizopus niveus*	fungi	n
26	Protease *B. stearothermophilus*	bacteriae	n
27	Lipase *A. niger*	fungi	y
28	Lipase *Penicillium roquefort*	fungi	n
29	Protease *A. niger*	fungi	n
30	Lipase *A. oryzae*	fungi	n
31	Protease *A. melleus*	fungi	n
32	Lipase *Penicillium camembertii*	fungi	n
33	Protease C *B. subtilis*	bacteria	n
34	Protease B *A. oryzae*	bacteria	n
35	Lipase *P. fluorescens*	bacteria	n
36	Lipase A *Burkholderia cepacia*	bacteria	y
37	Lipase B *Burkholderia cepacia*	bacteria	n
38	Lipase A *Rhizomucor mihei*	fungi	y
39	Lipase *C. antarctica*	fungi	y
40	Lipase *T. lanuginosus*	fungi	y

41	Protease A *Bacillus sp.*	bacteria	y
42	Lipase B *C. antarctica (liq)*	fungi	n
43	Lipase A *C. antarctica*	fungi	n
44	Protease B *Bacillus sp.*	bacteria	n
45	Lipase *T. lanuginosus*	fungi	y
46	Lipase C *Rhizomucor mihei*	fungi	y
47	Lipase Porcine Pancrease Type II	animalia	n
48	Ficin	planta	n

[a] initial screenings were performed in water-saturated MTBE

It is noteworthy that in this broad variety in enzymes from many different sources 30% showed any activity towards the target compound **48**. The hits were evenly distributed between enzymes from a bacterial and a fungal source. Interestingly, the hits comprised the majority of enzymes that have been known in literature for a long time (Ansorge-Schumacher and Thum, 2013; Houde *et al.*, 2004; Schmid and Verger, 1998) as a versatile catalyst for a broad range of different substrates. Enzymes showing activity in the TLC based assay were tested in terms of conversion rate and enantioselectivity.

Although most of the TLC-active enzymes were not enantioselective towards the target compound in a HPLC-monitored reaction, a few select enzymes exhibited an acceptable enantioselectivity in the hydrolysis reaction of ester *rac*-**48** (exemplary data shown in table 2.5).

Table 2.5: Results of example biotransformations employing selected enzymes form the ALMAC kit.

Entry	Enzyme	$\%\ ee_s$ [a]	$\%\ ee_p$ [b]	% c [c]	E [d]	Enantiopreference
1	Lipase E *Alcaligenes sp*	16.0	84.4	16.0	14	S
2	Lipase *T. lanuginosus* (immob.)	36.5	84.5	30.2	17	S
3	Lipase *T. lanuginosus* (liq.)	14.7	100.0	12.8	>200	S

Conditions: 5 mg ester *rac*-**48**, 5 wt% lipase in 1 mL MTBE, 48h at 30C

[a] determined by chiral HPLC

[b] determined by chiral HPLC

[c] determined as c = $\frac{ee_s}{ee_s + ee_p}$

[d] determined from ee_s and ee_p as in equation 8, § 1.1.2.2

Interestingly, all enzymes showed (*S*)-selectivity. Although in principle, an (*R*)-selective enzyme would be the preferable outcome from this screening, the main attention was laid on high enantioselectivity in the reaction, since the (*R*)-ester **48** can easily be transformed into the desired (*R*)-acid **32** via a hydrolysis step (cf. figure 2.12).

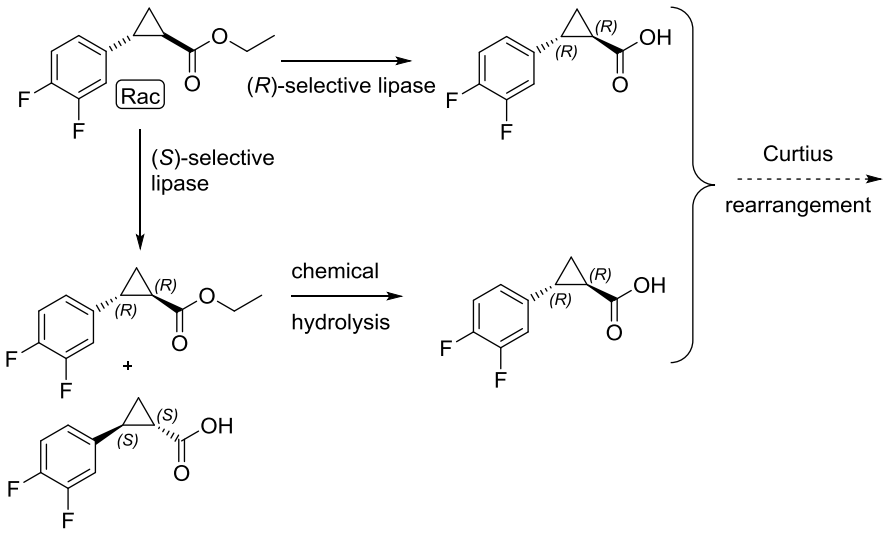

Figure 2.12: Possible lipase-mediated routes towards the (1*R*,2*R*)-tica acid **32**

The lipase from *Thermomyces lanuginosus* was the most promising candidate among the screened enzymes because it transformed the ester *rac*-**48** with a very high enantioselectivity. The absolute value of >200 (cf. Table 2.5, entry 3) should be taken cautiously however, since the conversion is too low to allow for accurate measurements. Intriguingly, the conversion seemed to be higher and the enantioselectivity significantly lower when the immobilised lipase (cf. table 2.12) was employed instead of the liquid preparation (cf. table 2.5, entry 2 and 3). Encouraged by these first results obtained with the lipase from *Thermomyces lanuginosus* (TlL), these results were taken as a starting point for the development of a biocatalytic process towards ticagrelor.

Different preparations of the TlL were compared with the results obtained in the first trial (table 2.5), however, none of the tested enzymes showed an enhanced enantioselectivity but all enantioselectivities were more or less of the same order of magnitude (results collected in table 2.6).

Table 2.6: Biotransformation of compound *rac*-**48** with different preparations of the lipases from *Thermomyces lanuginosus.*

Entry	Enzyme	% ee_s [a]	%ee_p [b]	% c [c]	E [d]	Enantiopreference
1	Lipozyme TL 100	9.1	85.7	9.6	14	S
2	Lipozyme TL IM	40.1	85.7	31.9	19	S
3	Lipex 100L	6.1	68.3	8.3	6	S
4	AH40	37.1	88.0	29.7	23	S

Conditions: 5 mg ester *rac*-**48**, 5 wt% lipase in 1 mL MTBE, 48h at 30C

[a] determined by chiral HPLC

[b] determined by chiral HPLC

[c] determined as c = $\frac{ee_s}{ee_s + ee_p}$

[d] determined from ee_s and ee_p as in equation 8, § 1.1.2.2

As a conclusion it can be said that good enantioselectivities are obtained in the TlL mediated hydrolysis of compound *rac*-**48**. The *ee* of the substrate (ee_s) is within limits of acceptance (cf. table 2.6 entry 1-3). The required enantiomeric excess of 99.5% will be attained in downstream processing of the intermediate ester (1*R*,2*R*)-**48**. The conversion levels, however, were low and the enzyme loading were too high for industrial application. Therefore, the following research endeavour was undertaken to enhance the conversion rates obtained with TlL in the hydrolysis of ester **48**. Firstly, the reaction conditions were changed and the effect of engineering the reaction medium on the overall process was studied (cf.§ 2.1.4.2 and 2.1.4.3). Concurrently a rational protein design approach was chosen to study the influence of several residues in the lid (cf. § 2.2) on the conversion rate and this is explored in chapter 2.2. The rest of this chapter describes the reaction conditions that were explored in order to optimise the conversion.

2.1.4.2 Solvent:

The first parameter tested was the influence of the co-solvent. Although lipases have been amply reported to be stable and work in neat organic solvents (Hernández-Rodríguez *et al.*, 2009; Zaks and Klibanov, 1985) in this particular case it has to be taken into account that the organic solvents cannot be used dry but need to contain at least one equivalent of water.

When performing the reaction in MTBE a fluctuation in ee of the substrate and consequently the E (fluctuation of the E between >200 and 35, data not shown) of the reaction has been observed in several repeats of the reaction. This may be due to uncontrolled amounts of water in the reaction medium. Furthermore, the water activity has proven to play an important role (Valivety et al., 1994). Although there is general acceptance of the fact that enzymes are stable in dry aprotic organic solvents, and therefore should remain catalytically active for long periods, recent studies on a variety of enzymes opposes these findings and instead reports a strongly reduced activity after exposure to organic solvents for several hours (Castillo et al., 2006).

Taking the above into account and assuming that the quantity of water in MTBE is changing from reaction to reaction and is the critical parameter to attain conversion (since it is the attacking nucleophile in ester hydrolysis), and ultimately enantioselectivity, a more conventional approach was undertaken: the enzymatic resolution was performed in purely aqueous buffered medium in order to obtain more stable *ee* and *E* values. Phosphate buffers (pKa 7.0) in different concentrations were employed and the pH was monitored (pH paper) throughout the reaction and remained neutral the whole time (results collected in table 2.7)

Table 2.7: *Thermomyces lanuginosus* (Lipolase 100 TL – liquid preparation entry 1 and 3 / Lipozyme TL IM – immobilised enzyme, entry 2 and 4) mediated hydrolysis of the ethyl ester *rac*-**48** in aqueous medium; effect of buffer strength and immobilisation.

Entry	time [h:min]	Buffer [M]	% ee_s [a]	%ee_p [b]	% c [c]	E [d]
1	18:40	0.1	97.5	70.8	57.9	25
2	18:40	0.1	99.8	77.2	56.4	51
3	18:40	1	93.9	72.5	56.4	22
4	18:40	1	87.2	79.2	52.4	24

Conditions: 5 mg ester *rac*-**48**, 5 wt% lipase in 0.5 ml phosphate buffer at 30C

[a] determined by chiral HPLC

[b] determined by chiral HPLC

[c] determined as c = $\frac{ee_s}{ee_s + ee_p}$

[d] determined from ee_s and ee_p as in equation 8, § 1.1.2.2

From the data it can be seen that a 0.1 M phosphate is strong enough to buffer the reaction. The pH remains stable throughout the time of reaction (tested with pH paper, data not shown). The *E* value of the reaction performed with the liquid preparation of the enzyme remains the same at both buffer concentrations (cf. table 2.7 entry 1 and 3), while a drop in selectivity is noted when the immobilised enzymes is employed (cf. table 2.7 entry 2 and 4). This latter finding is most likely due to the higher ionic strength of the solution, which feasibly can have an influence on the immobilised enzyme through interaction with the immobilisation agent and the bound enzyme. Overall, the enantioselectivity did not vary much from those values generally obtained in small reactions and usually was above those obtained in reactions performed in neat MTBE (cf. table 2.6). Although the *E* attained in buffered reaction was significantly below those obtained in MTBE (cf. table 2.5, entry 3 and table 2.7, entry 1) the result was stable and reproducible and therefore a value more likely to represent the reality in the test tube. Due to the heterogeneous nature of the reaction (the substrate is an emulsion in the buffer), the reactions performed on a screening scale (5 mg, reactions performed in Eppendorf tubes with orbital shaking) were found to yield irreproducible results. The observed difference in *E* values between both reactions performed at 5 mg (cf. table 2.5) and 50 mg (cf. table 2.6) scale can be attributed to the inhomogeneity within the reaction mixture. Therefore a medium sized reaction scale, large enough to ensure reproducible values and small enough to allow for many reactions to be run and worked up simultaneously (50 mg of ester *rac*-**48** in 5 ml of buffer) was adopted for further determination of several critical parameters for the enantioselectivity (*vide infra*).

It is known that lipases act at a water-lipid interface (Buchholz *et al.*, 2012). An interface can been artificially created (Laane *et al.*, 1987) by adding a water-immiscible organic solvents to create a bi-phasic system. Addition of organic solvents in general for enzyme catalysed reactions has been reported to have a beneficial influence on the catalytic activity of the enzyme in some cases. Low substrate and/or product solubility can be overcome by the use of a water-miscible co-solvent, while enzyme deactivation at higher levels of organic solvent and product inhibition have to be considered as a possible challenge. With water immiscible organic solvents on the other hand, the situation changes dramatically; the created biphasic system can help to mitigate effects of product inhibition (Carrea, 1984). Good results have been reported in literature in the enantioselective lipase catalysed reactions at an organic-inorganic interface (Csuk *et al.*, 1996; O'Neill *et al.*, 2012). Therefore, experiments were performed using the liquid preparation of TlL in a reaction medium containing 10% (v/v) of

different water immiscible co-solvents. However, contrary to the expectation, the addition of co-solvents did not have a beneficial influence in most cases (results collected in table 2.8).

Table 2.8: Effect of the addition (10% v/v) of different water immiscible organic co-solvents on the biotransformation of *rac*-**48**.

Entry	cosolvent	% ee_s [a]	%ee_p [b]	% c [c]	E [d]
1	DCM	0	0	0	0
2	AcOEt	0	0	0	0
3	MTBE	3.1	76.5	3.9	8
4	Cyclohexane	46.3	96.9	32.3	101
5	buffer	18.4	99.1	15.6	> 200

Conditions: 50 mg ester *rac*-**48**, 2 wt% lipase (liquid preparation) in 5 ml phosphate buffer, magnetic stirring for 48h at 20C

[a] determined by chiral HPLC

[b] determined by chiral HPLC

[c] determined as c = $\frac{ee_s}{ee_s + ee_p}$

[d] determined from ee_s and ee_p as in equation 8, § 1.1.2.2

There is –to the best of my knowledge- no evidence in literature using or stating that dichloromethane (DCM) has a beneficial influence on enantioselective enzyme catalysed processes. Therefore it is not surprising to find no catalytic turnover in a biotransformation with 10% DCM (cf. table 2.8 entry 1). The results obtained in the biotransformation of *rac*-**48** with 10% EtOAc were surprising. It was shown that EtOAc had the same effect as DCM, no transformation was observed after 48h (cf. table 2.8, entry 2). It is likely that the TlL hydrolysed the EtOAc easier than the tica ester *rac*-**48**. If TlL showed a preference for AcOEt over tica ester *rac*-**48**, the decrease in activity can be explained due to a change in medium composition (decrease in pH upon hydrolysis) or saturation of the enzyme with the co-solvent/alternative substrate. Moreover, a substrate or product inhibition could have occurred. It was shown that even the addition of 10% (v/v) methyl tert-butyl ether (MTBE) had a negative influence on the biotransformation compared to a biotransformation performed only in buffer (cf. table 2.8, entry 3 and 5). Finally, addition of hexane seemed to have a beneficial influence on the conversion of the biotransformation. The conversion was double compared to the conversion obtained in a buffered system without co-solvent (cf. table 2.8, entry 5). Conversion in the buffered system without co-solvent was too low (15%) to attain reliable values of enantiomeric

excesses, therefore the *E* obtained (>200, cf. table 2.8, entry 5) is not considered accurate and it is assumed that both reactions occur with an *E* ~ 100, which is an optimal result for a biotransformation.

2.1.4.3 pH effects

Generally, enzymes are known to work in aqueous, buffered systems at pH 7, since this represents the physiological properties of most living organisms. However extracellular enzymes or enzymes present in organelles may have a different pH optimum since the pH in the surrounding medium or in the organelles may differ significantly from pH 7 (Demaurex, 2002). Thus, the influence of the pH was investigated.

The biotransformation was performed in standard conditions (50 mg ester, enzyme (2% w/v), 5 mL reaction volume, magnetic stirring at room temperature) over a pH range from pH 6 to pH 10. The enzyme used was the wild type (WT) enzyme that was expressed in house (cf. chapter 2.2.3). In order to rule out any mechanical errors in setup and analysis leading to a false positive or negative, reactions were performed in triplicate.

Since different buffer systems had to be used to span the desired pH range the buffers were chosen to overlap with each other, lest the observed changes were due to the buffer composition and not to the pH. A 0.1 M potassium phosphate buffer was used for pH 6 to pH 8, and a 0.1M glycine / NaOH buffer was used to span pH 8 to pH 10. Negative controls were performed at pH 6 and pH 10 to exclude autohydrolysis (results collected in table 2.9). The enzyme used here was prepared in house following an established protocol (Naik *et al.*, 2010). In order to avoid a bias of the obtained data due to stabilisators added to the commercial enzyme. Moreover further mutation studies were performed (§ 2.2) to elucidate the influence of several residues on the overall performance of the enzyme. For comparison reasons the pH profile was therefore taken using the enzyme produced in-house.

Table 2.9: pH dependency of the conversion and resulting enantioselectivity of TlL (wild type enzyme, for preparation cf. § 2.2.3) catalysed hydrolysis of compound *rac*-**48** observed over a pH range from 6-8; the buffer used in entry 1-3 and 7 was a potassium phosphate buffer (0.1 M), the buffer system was switched to Glycine-NaOH (0.1 M) for entires 4-6 and 8.

Entry	pH	% ee_s [a]	%ee_p [b]	% c [c]	E [d]	Enantiopreference
1	6.0	37.8	96.2	26.9	77	(*S*)
2	7.0	31.7	97.0	24.6	90	(*S*)
3	8.0	26.4	97.0	20.8	95	(*S*)
4	8.0	87.5	92.3	48.7	72	(*S*)
5	9.0	92.8	90.9	50.5	76	(*S*)
6	10.0	83.5	96.6	46.2	136	(*S*)
7 [e]	6.0 (-)	0	0	0	0	n/a
8 [e]	10.0 (-)	0	0	0	0	n/a

Conditions: 50 mg ester *rac*-**48**, 2 wt% lipase (WT) in 5 ml phosphate buffer, magnetic stirring for 48h at 20C

[a] determined by chiral HPLC

[b] determined by chiral HPLC

[c] determined as c = $\frac{ee_s}{ee_s + ee_p}$

[d] determined from ee_s and ee_p as in equation 8, § 1.1.2.2

[e] negative control, no enzyme was added to the reaction mixture

It can be seen from table 2.9 that no auto hydrolysis takes place under these conditions (entries 7 and 8). This is most likely attributed to the biphasic system; the substrate ester is not miscible in water and therefore autohydrolysis cannot take place over the time of reaction. The enantioselectivity did not change significantly in function of the pH, as expected. Enantioselectivities meandered around a value of 80, the enantioselectivity of >100 attained at pH 10 is an artefact caused by the mode of its determination (cf. § 1.1.2.2) and are not considered to be significant. Concerning the enzyme catalysed reactions it can be seen that the change from a phosphate buffered system to a glycine buffered system had a beneficial influence on the overall activity of the lipase. (cf. table 2.9 entries 1-3 and entries 4-6). At pH 9 and 10 the highest conversion (50 at pH 9 and 46 at pH 10) were attained (cf. table 2.9, entries 5 and 6). The enantioselectivity was acceptable in both cases. This result is in accordance with evidence in literature stating a pH optimum of 8 to 12 or higher (Neves Petersen *et al.*, 2001). Several residues on the surface of the lipase might be susceptible to changes in the pH and

become de-protonated thereby changing the activity of the lipase. This effect and application will be thoroughly studied in chapter 2.2.4.4. The temperature has a direct influence on enantioselectivity and also on the conversion levels through the Ahrrenius equation (cf. equation 1.1.14). However, since the setup of this reaction (magnetic stirring required for a homogeneous reaction mixture) does not allow for temperature control, the influence will be discussed more thoroughly in chapter 2.3.

2.1.4.4 Conclusion

As conclusion it can be said that the optimal conditions for laboratory scale reactions were established and are summarised in figure 2.13. The glycine-NaOH buffer at pH 9 has been found to be most beneficial in terms of enantioselectivity and conversion (cf. table 2.9), a buffered reaction without the addition of co-solvents gave the best enantioselectivity (cf. table 2.8). The reaction needs to be magnetically stirred since orbital shaking does not allow for sufficient mixing between the substrate and the enzyme in buffer (results not shown). These findings are graphically illustrated in figure 2.13. The conversion rate needs to be further enhanced. This will be discussed in detail in the following chapters.

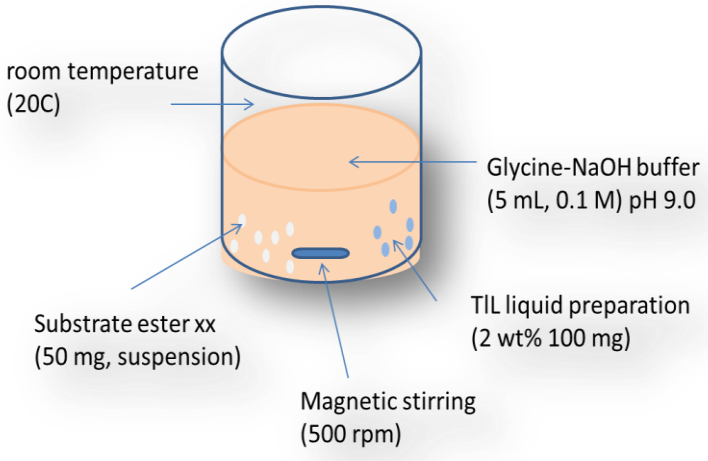

Figure 2.13: Reaction conditions at laboratory scale for the TIL mediated hydrolysis of ester *rac*-**48**.

2.2 Improving the activity of TlL following a rational protein design strategy

2.2.1 Introduction

In the previous chapter the conditions for a TlL mediated kinetic resolution of ester *rac*-**48** have been optimised. The activity of TlL has proven to be a potential bottleneck in the process, leading to prolonged reaction times and/or the need for high catalyst loading (cf. figure 2.2 and § 2.1.4).

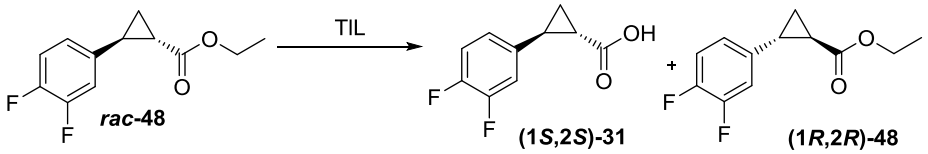

Figure 2.14: TlL mediated hydrolysis of ester *rac*-**48**, the process occurs with good enantioselectivity (E > 50). The conversion reaches 50% in the best case after 48h.

Low activity against the target substrates leads to prolonged reaction times in which the lipase might degrade or denature partially, which can compromise the enantioselectivity of the enzyme. Moreover, addition of large amounts of enzyme to the reaction might generate problems in the workup and is not optimal for scale up to industrial levels. The activity of an enzyme can be enhanced by engineering the conditions of the reaction to attain the optimal conditions for the enzyme (cf. § 2.1.4). Another possibility to modulate activity is to engineer the enzyme in order stabilise the active or destabilise the inactive conformation of the enzyme. This chapter discusses the design, expression and characterisation of TlL mutants with the aim of improving the conversion of the enzyme towards target ester *rac*-**48**.

The crystal structure of TlL has been solved several times and theoretical as well as experimental studies on the activation of the lipase have been performed (Brzozowski *et al.*, 2000; Holmquist *et al.*, 1993a; Holmquist *et al.*, 1994; Martinelle *et al.*, 1996). These publications were taken as a starting point for the rational protein design approach.

2.2.2 Literature background

Lipases, as opposed to esterases, typically have a lid-structure that regulates access to

a predominantly hydrophobic active site (cf. § 1.3.2). In order for the enzyme to bind substrate molecules, the lid has to open. Generally, lid opening will occur at a lipid-water interface (cf. figure 2.15), in a process known as interfacial activation. The catalytic cycle includes the adsorption of the lipase on the oil-water interface and the subsequent induced opening of the lid. Only then will the substrate enter the active site to form the substrate-enzyme complex, which upon attack of the nucleophilic serine (cf. §§ 1.2.3a and 1.21) is transformed to an enzyme-acyl intermediate complex. A second nucleophilic attack, normally by a water molecule, cleaves the ester bond linking the acyl group to the active site serine, and yields the free product and free enzyme which can undergo a new catalytic cycle. The influence of the lid on substrate/product trafficking to the active site (allosteric activation), is the basis for the reason that lipase-catalysed reactions of water insoluble substrates do not follow Michaelis-Menten kinetics (Derewenda *et al.*, 1994; Ricard and Cornish-Bowden, 1987).

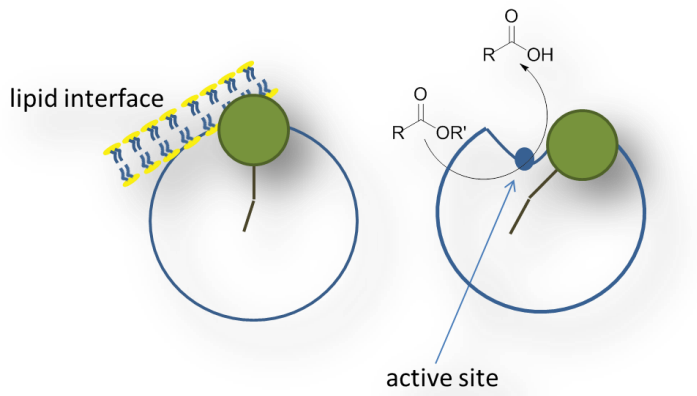

Figure 2.15: Allosteric activation; upon adsorption of the lipase to the lipid-water interface the lid slides open and the reaction can take place in the buried active site.

A model for lid-activation of the lipase has been proposed (Brzozowski *et al.*, 2000; Derewenda *et al.*, 1994) and shall be discussed in depth in the following paragraphs. A comparative study of different lipase homologs of TlL strongly suggests that specific molecular interactions between enzyme and hydrophobic molecules in the reaction medium have a stabilising effect on the open conformation of the lipase (Derewenda *et al.*, 1994). The lid in the TlL lipase is characterised as a 6 amino acid long amphipathic helix, showing high mobility in aqueous medium, moving as a rigid body. The authors come to the conclusion that the reality is most likely in the middle of both theories whereby interfacial activation shows both substrate and enzyme components (Derewenda *et al.*, 1994).

A more recent publication (Brzozowski *et al.*, 2000) focusses on the activation state of TlL. Special focus is given to several residues and their role in promoting the open conformation is explored. Principally, lipases have been discovered to crystallise into three different states, the low (LA) active and active (A) forms (both with the lid in the closed position) and the fully active (FA) form with the lid in an open position (cf. figure 2.14b).

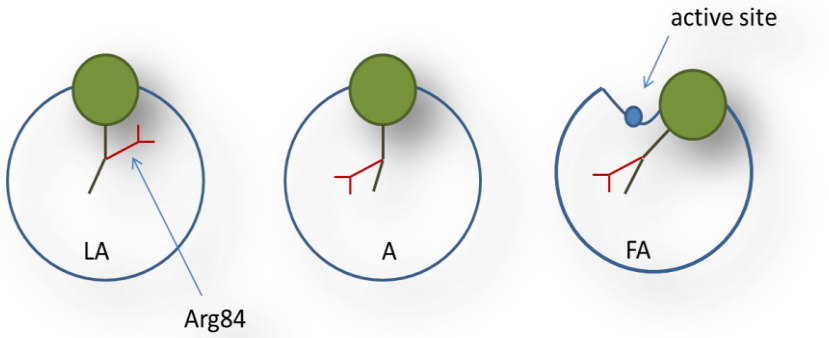

Figure 2.16: Schematic model of the activation modes of TlL (abbreviated model taken from (Brzozowski *et al.*, 2000)): the low activity (LA), active (A) and fully active (FA) states are described by the movement of the lid (green circle) to reveal the active site and the special rearrangements of several amino acid residues of which the Arg84 (red) shows the most dramatic changes.

The amino acids that were identified (Brzozowski et al., 2000) to play an important role in interfacial activation were Arg84 in the hinge of the lid, Asp57 in the body of the lipase and Ser85 as well as Asn88 both within the lid of the lipase. Interactions of these residues with the body of the lipase seem to stabilise the two conformational changes of the lid of TlL.

In a low activity (LA) form, the lid is still closed and the enzyme would have no catalytic activity owing to an inaccessible active site. Figure 2.17 depicts TlL in the open and closed conformation. The role of the lid (blue/cyan) to shield the active site from the surrounding medium in the inactive conformation can be appreciated.

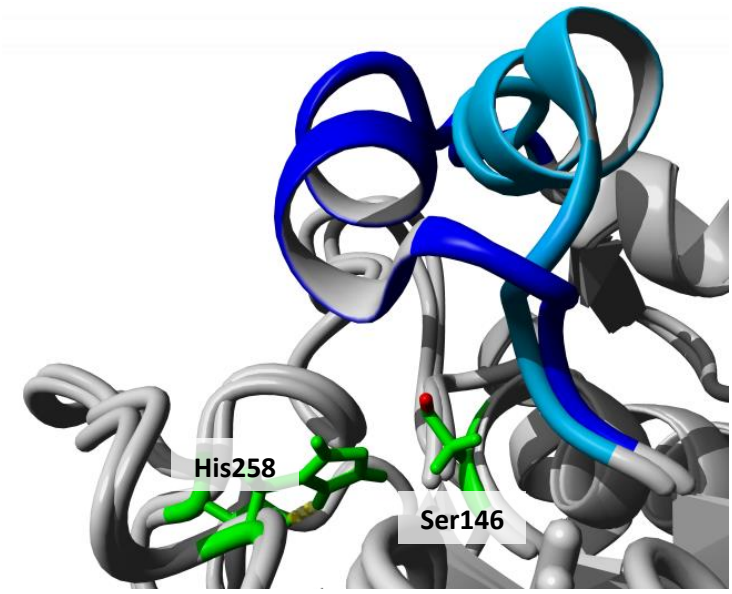

Figure 2.17: Lid closing over the active site of TlL. The lid covers (dark blue helix) the entrance to the active site (in green: catalytic triade; the nucleophilic OH of Ser146 is marked in red). Upon activation a conformational change takes place and the lid slides open (cyan helix) making the active site accessible to substrate molecules.

In the closed conformation the Arg84 at the hinge of the lid forms a salt bridge with Asp57 in the body of the lipase and Ser85 is engaged in a hydrogen bond with Asn88 (cf. figure 2.18). A disulfide bond between the residues Cys22 and Cys268 exists in the left-handed form (cf. figure 2.18, green). In the activated (A) state the lid of the lipase is still closed, albeit a little disordered, however more dramatic conformational changes have taken place within the enzyme. The Cys22-Cys246 disulfide bridge has changed its orientation. Isomerisation of the disulfide bridge between Cys22 and Cys268 is triggered by spatial reorganisations within the enzyme. The disulphide bridge now adopts a right handed form (cf. figure 2.18, yellow) and can establish hydrogen bonds between the Arg84 and the carbonyl oxygen of Cys268, which stabilise the open conformation. The most dramatic change occurs for Arg84 that has shifted in its spacial orientation (cf. figures 2.16, A and 2.18 in red and orange) facing in the opposite direction and allowing it to engage in hydrogen bonds with the backbone of Cys268. Moreover, the Ser85-Asn88 hydrogen bonds are fully disrupted (cf. figure 2.18)

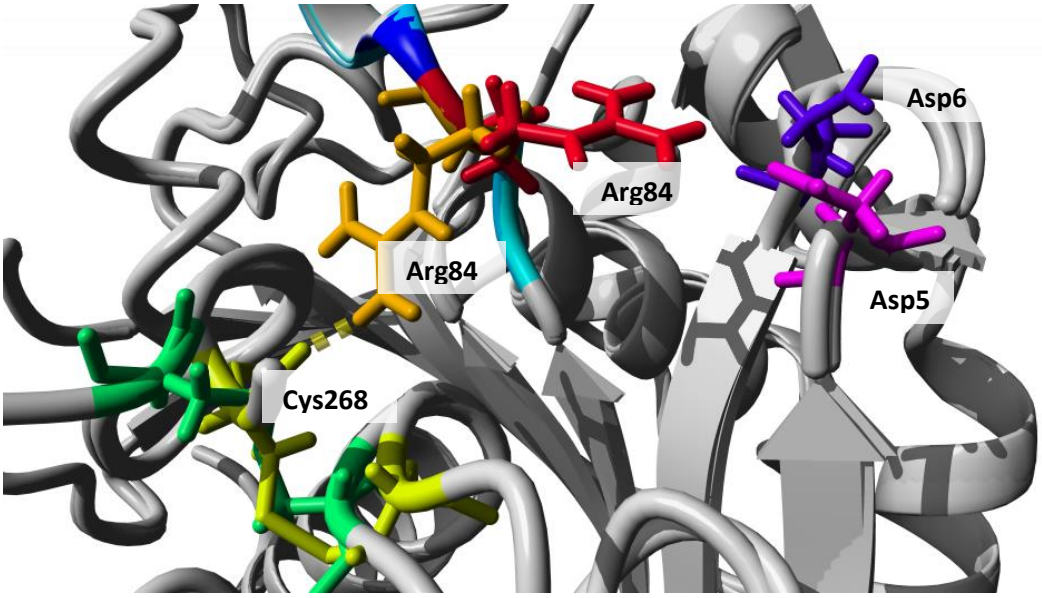

Figure 2.18: TlL with closed lid (blue structure). In the LA state the internal hinge-lid interaction is intact and Arg84 (red) is held back by a salt bridge with Asp57 (pink). An additional interaction with Asp62 (purple) is feasible. In the active state (A) the lid is still closed, but the Arg84-Asp57 interaction has been disjointed. Arg84 (orange) is engaged in a hydrogen bond (dotted yellow) with the main-chain carbonyl of Cys268 (yellow). The change of the orientation of the disulphide bridge is shown in green (left handed) and yellow (right handed).

Finally, the fully active (FA) state is characterised by a repositioning of the lid to a maximal open position (cf. figure 2.16). This configuration is stabilised by hydrogen bonds between Asn88 and Asp62 in the body of the lipase, Asn88 is engaged in hydrogen bonds with the carbonyl backbone of Gly61. A Ser85-Asp62 hydrogen bond further stabilises the lid in the open position.

From these published (Brzozowski *et al.*, 2000) results we learn that the internal lid hinge (Ser85-Asn88) has to be broken in order for both amino acid residues to form hydrogen bonds to amino acids in the body of the enzyme to stabilise the open conformation. Secondly the Asp57-Arg84 salt bridge needs to be broken for the Arg84 to flip and engage in stabilising interactions with the carbonyl oxygen of Cys268 (cf. figure 2.18). Mutating the Arg84 to a glycine results in a drastically reduced activity of the lipase (Brzozowski *et al.*, 2000). Based on these results the Asp57-Arg84 and Ser85-Asn88 interactions were chosen as targets for the rational protein design approach. The activated state (A) with the lid closed can to some extent be considered the transition state between open and closed conformation. Breaking the

interactions that foment the closed state should make the open state thermodynamically more favourable and thereby encourage the transition of the lipase into the open conformation.

2.2.3 Choosing the mutations

Evidence in literature suggests that the lid is very susceptible to changes in its amino acid composition. Martinelle and co-workers as well as Holmquist and co-workers have studied the role of Glu87 and Trp89 in interfacial activation of TlL. Trp89 was found to modulate activity and specificity towards the alcohol moiety of the substrate with respect to chain length. A mutation to uncharged amino acids (Trp89Phe/Leu/Gly) has influenced the substrate specificity but has also led to a decrease in activity. (Martinelle *et al.*, 1996) A Glu87Ala mutation of the lid was shown to alter the enantioselectivity of the TlL (Holmquist *et al.*, 1993a). Finally modifications in the lid of the *Rhizomucor mihei* lipase (Derewenda *et al.*, 1994), were found to increase activity in some cases (Holmquist *et al.*, 1993b). Taking these findings into account a range of enzyme variants targeting two residues located in the lid domain were designed and created in the laboratory (§ 2.2.4). As explained in detail below the residues chosen were Asp57 and Asn88 (also cf. figure 2.19).

Figure 2.19: Important residues and structural elements in the vicinity of the lid (green sphere) of Tl Lipase that were subject to on within this thesis. The active site (blue ellipsoid) is situated directly underneath the lid.

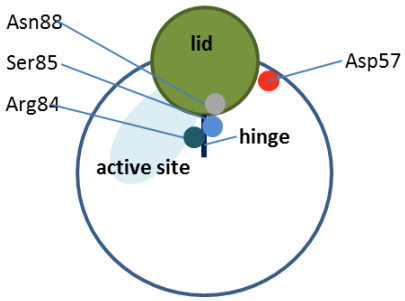

Knowing that Arg84 plays a key role in stabilising the open confirmation the Asp57 was chosen as the first target amino acid, in order to interrupt the salt bridge formed between these residues (cf. figure 2.18). The idea was to create a repelling force that destabilises the closed conformation and drives the lipase to adopt the active state. For this purpose histidine, asparagine and arginine were introduced. The varying size of these residues and the resulting

spatial requirements may also have a de-stabilising influence on the closed state and encourage the conformational changes necessary to attain the activated state (A). Finally, as a proof-of-concept, the hydrogen bonding between Asp57 and Arg84 was completely removed by means of the introduction of an isoleucine residue. This change should be quite conservative in terms of the spatial requirements but since isoleucine is an aliphatic amino acid the hydrogen bond in the Asp57Ile mutant will be broken which should trigger the Arg84 to switch and therefore should allow the TlL to enter the active (A) state.

Next the interaction between Ser85 and Asn88 was examined. Ser85 is located adjacent to Arg84, on the edge of the first of the two lid hinge regions (residues 82-85; (Brzozowski *et al.*, 2000)) that are involved in the mobility of the lid domain. A hydrogen bond links Asn88 to Ser85 in the LA conformational mode. This interaction in the LA form is not thought to be of great importance to lid movement itself as it is observed to be interrupted in the A conformational mode with little change to the main-chain of Ser85. However, in the open (FA) mode, Ser85 and Asn88 are both involved in important hydrogen bonds between the lid and the enzyme body. In particular, Asn88 is reported to form key interactions with the main-chain carbonyl oxygens of Gly61 and Asp62.

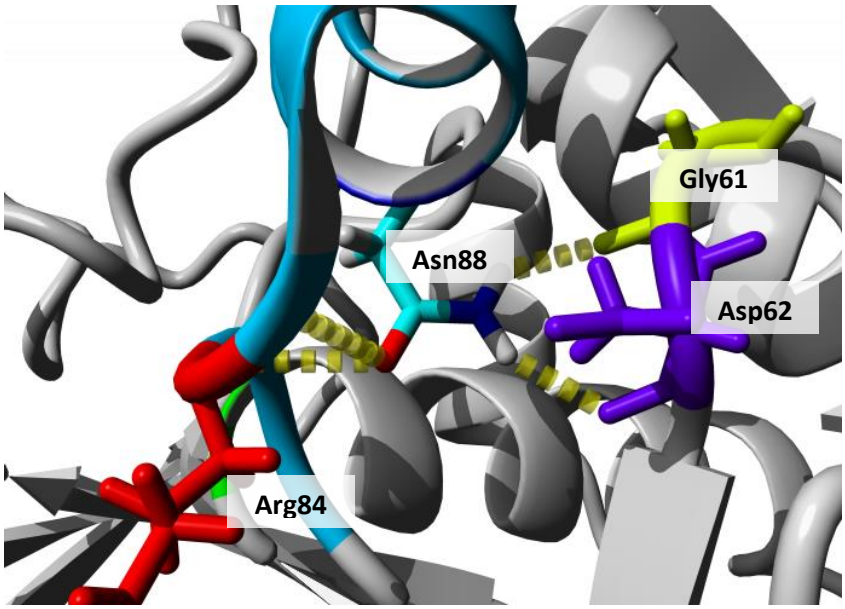

Figure2.20: Interactions of Asn88 (centre) with the residues in its proximity. The open conformation of the lid (cyan) is stabilised through interactions of Asn88 (cyan, centre) with the main chain carbonyls of Gly61 (lemon) and Asp62 (purple). Arg84 (red) has switched its orientation towards its stabilising hydrogen bond with the mainchain carbonyl of Cys 268.

A mutational strategy to modulate this interaction would therefore only be feasible by focusing on Asn88 that participates through its side chain rather than main chain. As such Asn88 was chosen and mutated to a series of different amino acids. An Asn88Ile mutation was chosen for the same reasons as the Asp57Ile mutation. Additionally, since Asn88 is moderately buried in the open conformation, it was worth investigating if a buried hydrophobic residue would stabilise the open state through interactions with a proximal hydrophobic patch consisting of Val63, Leu147, and Leu151. An Asn88Pro mutant was attempted in order to disrupt the lid helix and thereby distort the lid itself, artificially exposing the active site and effecting a more active enzyme. Finally an Asn88His mutation was chosen in order to explore the steric context of the buried Asn88 while preserving a hydrogen-bonding candidate.

Table 2.10: Position and exchange of amino acids introduced into the lipase from *Thermomyces lanuginosus* to establish the importance of these positions in determining lipase activity.

Entry	Residue	Exchange for
1	Asp57	His
2	Asp57	Ile
3	Asp57	Asn
4	Asp57	Arg
5	Asn88	His
6	Asn88	Ile
7	Asn88	Pro

2.2.4 Creation of the variants

2.2.4.1 Choice of the expression strain

The choice of the host organism for heterologous expression of proteins is crucial in many ways. Considering that TlL is a lipase from a fungal source several parameters have to be respected. Proteins from eukaryotic sources are more often than not glycosylated. Moreover the eukaryotic translation apparatus includes the Golgi apparatus and endoplasmatic

reticulum where translated proteins are subjected to posttranslational modifications like for example the formation of disulphide bonds (Berg *et al.*, 2012). These post-translational modifications do not occur in bacterial cells to that extent; expression strains generally need to be carefully engineered to be capable of implementing these modifications.

Published results (cf. §2.2.2) show that the correct formation of disulphide bonds is crucial for the activity of this lipase. Moreover it is known that the lipase is a glycoprotein (Boel and Huge-Jensen, 1995; Naik *et al.*, 2010)). Glycosylation in a protein is postulated to play a role in attaining the correct folding and may help to gain enhanced stability in secreted proteins. *Escherichia coli* strains designed to facilitate the formation of disulphide bonds and enhance the correct folding of proteins exist. For example, the *Escherichia coli* Origami strain (Novagen) shows a mutation in both the thioredoxin reductase (trxB) and glutathione reductase (gor) genes and thereby enable the strain to form disulfide bonds in the cytoplasm leading in the best case to soluble, correctly folded proteins. Moreover plasmids like pET22b(+) (Novagen) adds the pelB leader sequence to the target protein, which leads to the secretion of the protein into the periplasm, where the more oxidative environment will enhance the possibility of disulphide bond formations.

An alternative, versatile system is the expression in yeast cells like *Pichia pastoris* (Cregg *et al.*, 1993; Macauley-Patrick *et al.*, 2005). *Pichia pastoris* fermentation has been used both for industrial and academic application. This expression system is uniquely suited for the expression of foreign, eukaryotic proteins due to its relative ease of manipulation compared to other eukaryotic expression systems and the ability of *Pichia pastoris* to perform many protein modifications, including glycosylation, disulfide-bond formation, and proteolytic processing (Cereghino and Cregg, 2000). Moreover, high cell-density fermentation and the possibility to secrete the protein into the expression medium allows for a high protein yield. *Pichia pastoris* is able to add both *O*-linked and *N*-linked carbohydrate moieties to secreted proteins. The N-linked glycosylation pattern of *Pichia* is described as an N-acetyl glycose residue located on asparagines in the recognition sequence Asn-X-Ser/Thr, followed by (branched) mannose (3-18 mannose) glycosylation (Bretthauer and Castellino, 1999; Cereghino and Cregg, 2000; Montesino *et al.*, 1999). This glycosylation core can be subject to further extension, while the influence of the culture medium on glycosylation patterns has also been described (Gawlitzek *et al.*, 1995; Watson *et al.*, 1994).

Pichia pastoris can feed on methanol as a unique carbon source in the absence of glucose. Alcohol oxidase (AOX) with its very strong methanol dependent AOX promotor is responsible for methanol oxidation. Cloning of target genes downstream of this promotor therefore allows for their methanol-induced expression.

The pPICZAα vector was designed to enable insertion of the target gene directly downstream of the AOX1 promotor. The purified vector needs to be cut within the 5'AOX1 site region using SacI (for image of the vector cf. figure 2.21 below) in order to facilitate the crossover between plasmid and genomic DNA. After transformation of the pPICZAα target gene construct into competent *Pichia pastoris* cells a crossover between the vector and the genomic DNA at the AOX1 promotor (present in both the plasmid and the genomic DNA) will occur and thereby the target gene will be inserted into the genome upstream to the actual AOX1 gene (cf. figure 2.21).

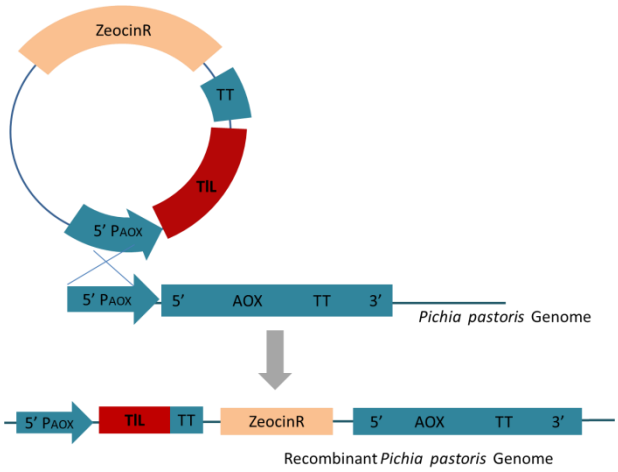

Figure 2.21: Crossover between the plasmid and the genomic DNA. The crossover occurs at the 5' AOX1 Promotor site and the plasmid DNA will therefore be inserted upstream of the AOX1 gene.

Since pPICZAα also carries an antibiotic resistance gene (Zeocin resistance) successful transformation can be observed through the ability of the clones to grow on YPDS agar plates with Zeocin. Moreover, Zeocin an antibiotic of the bleomycin family, intercalates with the DNA and causes strand breakage (Ehrenfeld *et al.*, 1987) and is therefore a broad-spectrum antibiotic, active against fungi and bacteria. After transformation the growth on Zeocin containing plates is indicative of successful yeast transformants. The resistance towards Zeocin is proportional to the amount of inserts. High copy strains can be identified by varying the concentration of Zeocin. Lastly, employing the pPICZAα vector, the target protein is produced

as a fusion product of the secretion sequence of the α-mating factor from *Saccharomyces cerevisiae*, which causes the desired protein to be excreted into the fermentation medium.

For the reasons cited above *Pichia pastoris* was chosen as the expression organism for TlL. The conditions for expression were taken from Naik and co-workers (2010), and were modified as convenient (*vide infra*).

2.2.4.2 Creation of the TlL variants and transformation into *Pichia pastoris*

Expression of the TlL gene has been described using both *Pichia pastoris* and *Aspergillus niger.* Due to the ease of application and in-house expertise *Pichia pastoris* was chosen as the host organism. The gene sequence was taken from Boel and co-workers (Boel and Huge-Jensen, 1995) and features a C-terminal secretion sequence. This allows for secretion of the protein into the fermentation medium and allows for simple yield of soluble lipase without the need to disrupt the cells. A synthetic gene, codon optimised for *Pichia pastoris*, was ordered from GeneArt (for sequence cf. § 4.3.1). The sequence was designed to have an EcoR1[2] restriction site at the 5' end and a Xho1 restriction site at the 3' end. The sequence was cloned using the MCS of pPICZAα and the EcoRI and XhoI restriction sites (Protocol cf. Materials and Methods § General molecular biological techniques). TlL was cloned into the pPICZAα vector directly behind the AOX promoter (cf. figure 2.22). The whole construct measures 4176 bp.

[2] The rules established by Roberts and co-workers (2003) for the nomenclature of restriction endonucleases was adopted

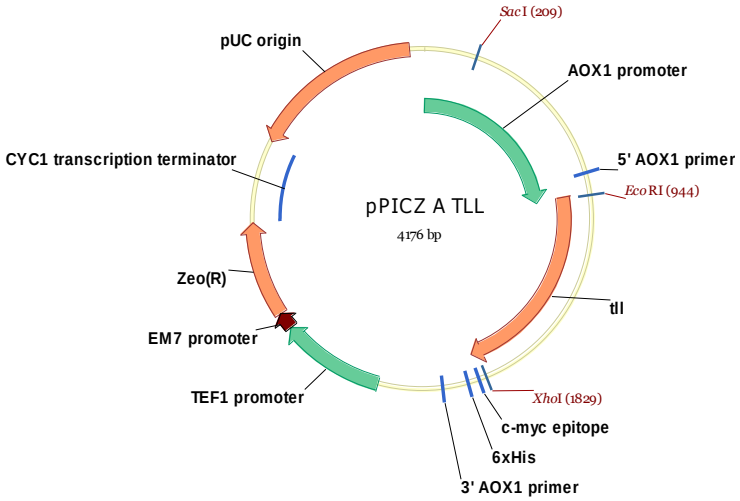

Figure 2.22: pPICZA_TlL, the Tl Lipase is cloned in 5'-3' orientation into the pPICZA vector behind the AOX1 Promotor, using the EcoRI and XhoI restriction sites. A SacI restriction site occurs only within the AOX1 promotor. The whole construct is 4176 bp large.

In order to create the TlL variants (cf. § 2.2.2) the relevant mutations were introduced using the QuickChange PCR method (cf. § 4.3.1, especially 4.3.1b). In case of multiple codons the codon was chosen according to *Pichia pastoris*' codon preferences.

After amplification the constructs were ligated and transformed into competent *Escherichia coli* XL1 Blue cells. Zeocin was used as a selection marker for both *Escherichia coli* and *Pichia pastoris* strains. The advantage of Zeocin is that it works as a selection marker for both fungi and bacteria although it is not as efficient for bacterial selection and requires application at higher concentrations to minimise false positives and contaminations. An empty plate at the same antibiotic concentration was kept for incubation under the same condition during each transformation step (both bacterial and fungal transformation) to monitor contamination.

Yeast transformation imposes some obstacles to high-throughput work. The growth period takes roughly 3 days and transformation efficiencies can be very low, requiring large amounts of plasmid DNA for every transformation step. Plasmids were isolated following an optimised miniprep protocol (on ice; cf. § 4.3.1) that ensured a 10-fold increase in DNA yield. At first X33 cells were made competent in house. The transformation efficiency of these cells was very poor. Therefore *Pichia Pastoris* X33 cells were made competent using the

EasyComp™ kit (Invitrogen) which increased transformation efficiency (cf. § 4.2.4). Transformation reactions were performed with all mutant constructs as well as with the wild type construct and an empty *Pichia pastoris* vector as negative control (cf. Table 2.2.3.2a).

Although in principle multiple inserts are possible after a transformation event the likelihood of a multiple insertion was considered relatively low in a transformation that already occurred with low efficiency. From each plate a clone was picked and re-streaked on a fresh agar plate containing the appropriate amount of Zeocin. Subsequently, glycerol stocks were prepared of these colonies.

2.2.4.3 Verification of the constructs

In order to verify that the transformants contained the desired sequence and no further modifications in the genomic sequence the DNA was isolated and sent for sequencing. In case of the pPICZAα plasmids isolation from *Escherichia coli* cells was straightforward. sequence analysis confirmed the correct sequence in all cases. In the case of the *Pichia pastoris* transformants, however, the matter was slightly more complicated. During the transformation process the plasmid recombines with the genomic DNA of the yeast and the target gene (and resistance marker) is included into the genomic DNA. Isolation of the genomic *Pichia pastoris* DNA proved to be challenging. Different methods for DNA extraction were explored. Both the QIAGEN blood and tissue DNA isolation kit and a method relying on osmotic shock and freeze-thawing did not yield the desired amount of DNA (Akada *et al.*, 2000). The use of phenol during the DNA extraction was avoided due to its toxicity in handling. The best outcome was with the use of lyticase to digest the cell wall of the yeasts followed by a quick freeze-thaw step which would burst the cells open. Although more successful than any other tested method even this process proved to be only partially successful if the cells used were not freshly grown.

In order to avoid sequencing the whole *Pichia* genome a PCR was run over the isolated genomic DNA using two sets of primers: AOX primers and gene specific primers were used to verify the insert (Invitrogen).

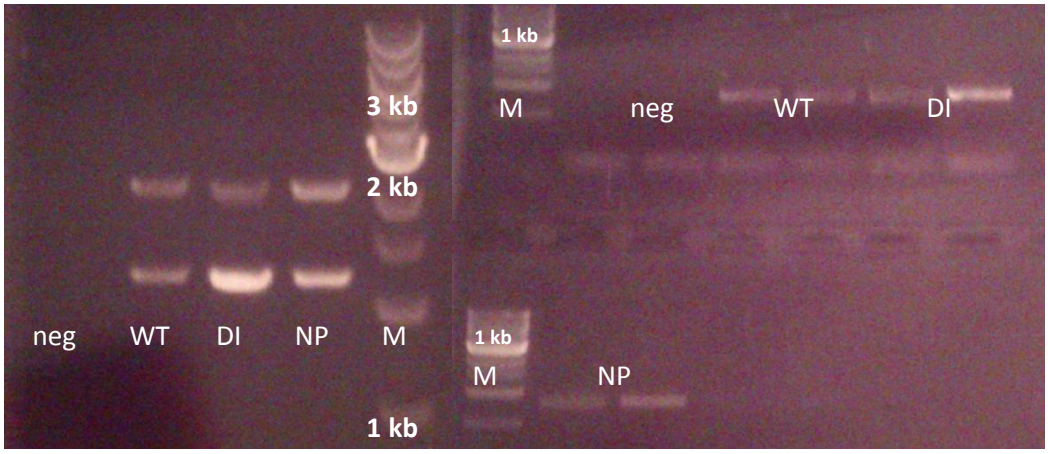

Figure 2.23: Colony PCR of extracted *Pichia pastoris* genome using differing primers.
left image: AOX primers; the AOX gene (2.2 kb) and the TlL gene (>1kb) have been amplified
right image: gene specific primers; only the TlL gene (<1 kb) has been amplified
Generuler 1 kb DNA ladder(thermo scientific) was used as marker (M)
Abbreviations: empty vector transformation control (neg), wild type TlL (WT) Asp57Ile variant (DI) Asn88Pro variant (NP).

From the results obtained in the PCR (cf. figure 2.23 Gel 1 lane 2) it can be seen that there is an insert in all the positive strains (cf. figure 2.23 Gel 1 lane 3-5). The TlL sequence was inserted correctly behind the AOX promotor (as can be seen by the double banding in the positive strains using the AOX primers). No amplification of the AOX gene is observed for the control strain (neg) which has been transformed with an empty vector (termed 'negative control' hereafter, possibly due to low yield during the extraction of genomic DNA. The identity of all positive constructs was verified through DNA sequencing (sequencing of amplified DNA from PCR with gene-specific primers, cf. § 4.3.1).

After the identity of all constructs had been confirmed the genes were expressed and purified following as described by Naik *et al*. (2010) with slight modifications (*vide infra*). The resulting proteins were characterised in terms of the biochemical and catalytic properties.

2.2.5 Analysis

2.2.5.1 Purification

Purification of TlL proved to be a challenge. The protein was secreted into the fermentation medium due to the C-terminal secretion sequence, however the protein concentration was very low on an analytical SDS-PAGE. Hypothetically multiple inserts can occur during a *Pichia pastoris* transformation. A clone with multiple inserts of the target gene would lead to a higher protein concentration in the medium. However, the transformations yielded very few clones (1-4 clones per transformation) and a screening for multiple inserts was therefore not feasible. The volume of the medium containing the protein was reduced using an Amicon concentration cell with a 15KDa molecular weight cut off (MWCO). The resulting concentrated protein solution was then dialysed against potassium phosphate buffer (0.1 M, pH 7.0) for 24 hours using a 15 KDa MWCO dialysis membrane (ratio of sample to dialysis buffer 1:100). The culminating protein solution was analysed by SDS-PAGE.

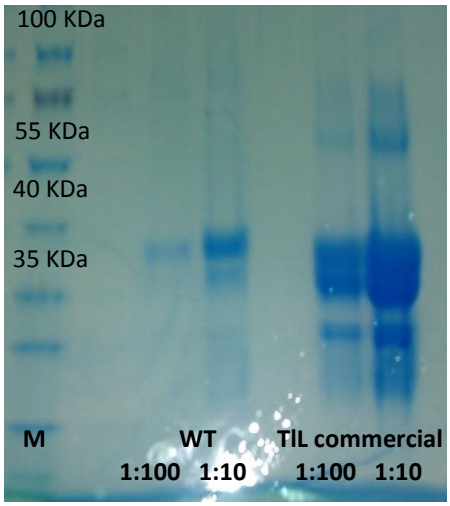

Figure 2.24: Comparison between in-house wild type TlL (WT) after the concentration step and the commercial Lipase (Lipolase 100 TL, Aldrich) on a 4-20% SDS PAGE, both enzymes were analysed in 1:10 and 1:100 dilutions from the stock solution; Thermo Scientific Spectra Multicolor Broad Range Protein Ladder as marker (M)

The wild type enzyme overexpressed in-house (WT) was compared to the commercial enzyme from Aldrich. The most dominant band for both enzyme preparations is the band a bit

above 35 KDa. TlL has a molecular weight of 30 KDa (calculated on the base of amino acid content), but in reality the enzyme is a glycoprotein. As such, the sugar residues will not only influence the molecular weight but also the movement of the lipase on a SDS gel. The difference between the calculated molecular weight and the apparent weight can therefore be explained easily. The commercial enzyme was more concentrated than the WT, but seemed less pure. The impurities present in the commercial enzyme at ~60 KDa, 70KDa and at ~20 kDa were absent in the samples of the wild type (WT) (cf. Figure 2.24), which could be due to an effect of the dilution as different protein concentrations were loaded on the gel. However comparison of the 1:10 dilution of the WT preparation and the 1:100 dilution of the commercial enzyme (cf. figure 2.24: TlL bands have a similar intensity which equals a similar relative amount) shows fewer impurities (less relative amount) in the WT preparation. This finding is again highlighted in figure 2.27. More interestingly, in both the commercial as well as in the in-house enzyme, there seems to be a double banding in the TlL region. An expression test with the negative control (empty vector transformation (cf. table 2.2.3.2a)) does not show the same banding pattern (cf. figure 2.24), which together with the fact that the double banding even appears in the commercial preparation, leads to the conclusion that the double banding is related to the TlL expression. Moreover, it is known (Cereghino *et al.*, 2002) that protein expression with *Pichia pastoris* expression strains can give rise to differently glycosylated proteins.

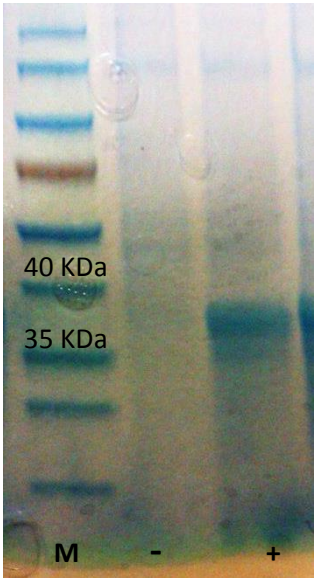

Figure 2.25: 4-20% SDS PAGE; comparison between negative control (-, strain transformed with an empty vector) and positive control (+, WT enzyme, in-house production), marker (M) thermo Scientific Spectra Multicolor Broad Range Protein Ladder. The double banding is clearly visible in the lane containing the positive control. Neither band appears in the negative control

The double banding that can be observed in figure 2.25 is likely to be the result of a different glycosylation pattern. Assuming that one band is more glycosylated than the other the difference in travelling distances on a gel could be explained. To test this hypothesis both bands were digested (Trypsin digest) and analysed by MS. A comparison of the masses obtained from the samples to the Mascot database returned positive hits for the lipase from *Thermomyces lanuginosus*[3].

Encouraged by these results, a sample of the lipase was treated with PNGase F (NEB Biolabs) which is an amidase that cuts between the innermost GlcNAc and asparagine residues of high mannose, hybrid, and complex oligosaccharides from *N*-linked glycoproteins. It cannot cut when the innermost GlcNAc residue is linked to an α1-3 Fucose residue. This was done to deglycosylate the lipases. If the double banding is the result of a different glycosylation pattern the double banding should merge into one distinct band after deglycosylation. The exact glycosylation pattern of the TlL is not known. It can only be deduced from literature (cf. § 2.2.3.1) that it will likely mainly consists of mannose and n-acetyl Glucosamine.

The PNGase digest as well as a series of positive and negative controls were run on a SDS-PAGE. Deglycosylation of the WT enzyme gave one single band. The slightly higher band, as seen in the untreated lane disappeared (cf. figure 2.26, WT (untreated) and rxn (after deglycosylation)). A control sample containing only the PNGase shows that on overlap of the PNGase with the lower band. However the higher band of TlL runs discernibly higher than the PNGase. (cf. figure 2.26, WT (untreated) and PNGase (PNGase control)). The staining method chosen here gives a slightly darker image and does not allow for clear distinction of the double banding. Nonetheless, comparison of the reaction (rxn) and untreated wild type (WT) shows that upon treatment with the N-PNGase the two TlL bands become one ('higher' band disappears).

[3] This experiment was performed by Dr. Martin Read, as part of the mass spectrometry service for the identification of proteins. http://www.manchester.ac.uk/research/martin.read/research

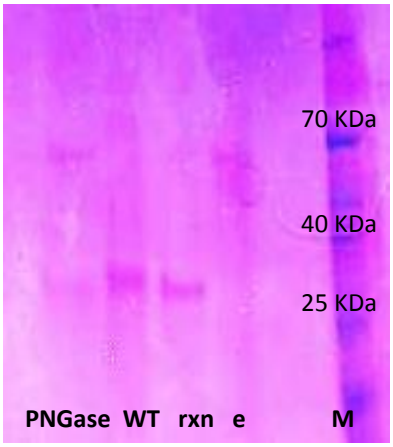

Figure 2.26: PNGase treatment of TlL-wt; the samples shown are the PNGase negative control (PNGase only), the wild type TlL (WT) and the deglycosylation reaction (rxn) as well as an empty lane (e) in which only Laemmli buffer was loaded. The marker (M) used was Thermo Scientific Spectra Multicolor Broad Range Protein Ladder. To properly stain all glycoproteins the gel was stained with a different staining agent (cf. § Materials and Methods) which destained poorly and gave a slightly purple gel.

After PNGase treatment the TlL runs as one discreet band, although the weight is still slightly above the expected 30 KDa. It is known that *Pichia pastoris* is able to add both *O*-linked and *N*-linked carbohydrates onto secreted proteins (Cereghino *et al.*, 2002). The deglycosylase used here, however, only removes N-linked sugar residues. The remaining band therefore may be the O-linked glycoform of TlL.

Glycoproteins have a tendency to poorly stain with Coomassie staining (Osset *et al.*, 1989). Since the use of a methanol/acetic acid Coomassie staining gave a strong background staining that could not be removed (cf. figure 2.26), a gel was left for 10 days in an InstantBlue staining bath was generally used in order to detect hidden proteins (cf. figure 2.27).

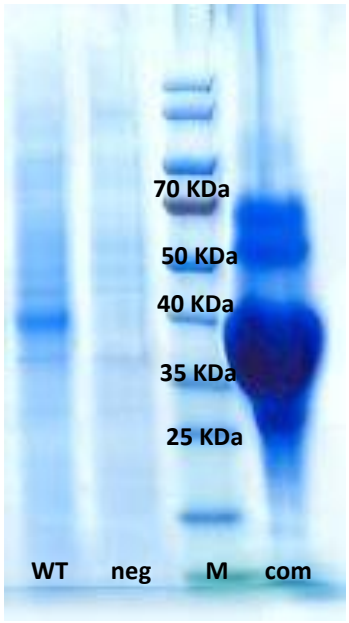

Figure 2.27: 10 day staining of a wild type (WT) sample compared to an empty expression and the commercial lipase (com). The marker (M) used was thermo Scientific Spectra Multicolor Broad Range Protein Ladder. This image highlights the capacity of glycoproteins to hide on an SDS-PAGE at shorter staining times (compare to figure 2.25).

From figure 2.27 it can be seen that the commercial lipase has several contaminants at ~50 KDa and ~70 KDa as well as at ~25 KDa, but also the in house produced KGH-TlL has several minor hidden contaminants which coincide with the bands obtained in the empty vector (negative) *Pichia* fermentation.

From the above results it becomes obvious that protein quantification from the crude extract is challenging. Coomassie-staining on an SDS-PAGE yields unclear images as a result of poor staining of glycoproteins under these conditions. The crude extract of both the negative control and the protein samples after concentration and dialysis had a yellow-brownish colour (cf. figure 2.28). This colouring interfered with any kind of Bradford-protein assay or measurement of absorption at 280 nm of the crude extract and did not allow for protein quantification at this stage. It was attempted to eliminate the colouring component through a desalting step with a PD_{10} column. Unfortunately, the colour persisted in the flow through.

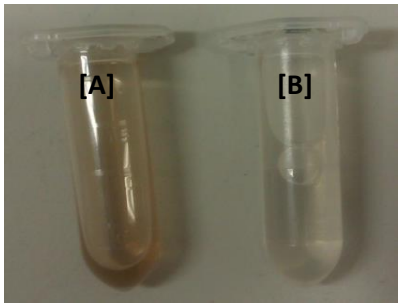

Figure 2.28: Observed remaining yellow-brownish colour in the protein solution of the wild type enzyme [A], disappearance of the colour after purification [B].

At this point it became evident that further purification of the lipase was required and any biochemical characterisation (including concentration determination) could only be done on purified protein. Purification was attempted following the procedure described in literature for the purification of the TlL (Naik *et al.*, 2010).

The first step described consists of hydrophobic interaction chromatography (HIC) using decyl-agarose as solid phase (Naik *et al.*, 2010). After the HIC chromatography the elution buffer (sodium borate buffer, pH 9.0 0.5 M, isopropanol (30%)) was exchanged for a low-ionic strength buffer (sodium borate buffer 0.01M, pH 9.0). This step was needed in order to reduce the background noise caused by buffer components in the following Bradford assay. A comparative SDS PAGE was run of all protein samples before and after the purification steps (cf. figure 2.29).

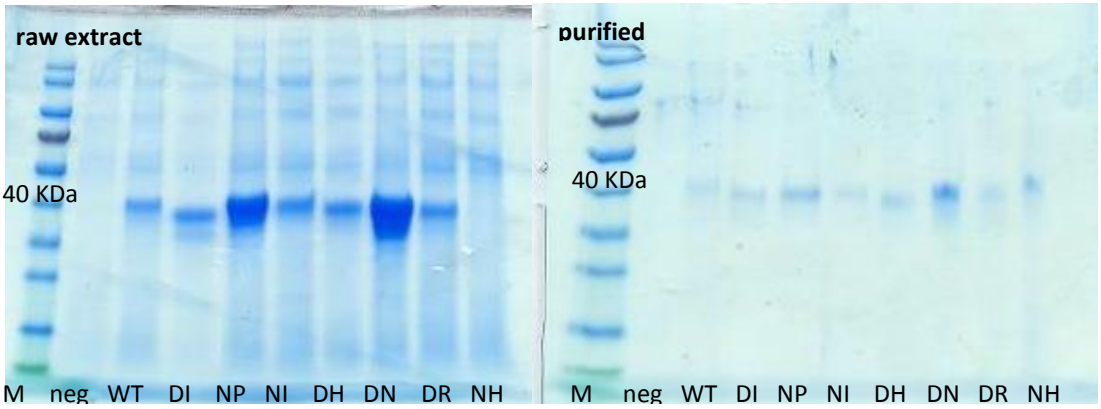

Figure 2.29: Raw extract and purified enzyme variants; the marker (M) used was thermo Scientific Spectra Multicolor Broad Range Protein Ladder, protein samples: negative control (neg), wild type (WT), Asp57Ile (DI), Asn88Pro (NI), Asn88Ile (NI), Asp57His (DH), Asp57Asn (DN), Asp57Arg (DR), Asn88His (NH).

It can be seen from figure 2.29 that a considerable amount of protein was lost in the purification step. Therefore it is not possible from the gels to ascertain that the samples are indeed pure since some contaminants may be invisible due to high dilution and poor staining. The Asn110His variant (cf. figure 2.29 NH) does not seem to have expressed properly (very faint band in the gel of the raw extract) but after purification a stain appeared on the gel slightly higher than expected. Probably the glycosylation (hiding bands on a gel, influencing the migration) is responsible for this finding. A negative control (expression of an empty vector strain) was performed and treated in the same way (cf. fig 2.27, lane 'neg'). The signals obtained in all assays were indeed not above average background noise (*vide infra*). The negative control (assay performed with the extract form the negative control expression after purification) was rigorously performed in all assays and the results obtained were subtracted from the data obtained using the different enzyme variants This was done to ascertain that the data obtained for the enzyme variants was a bias free, true representation of the variants activity.

This HIC purification step was done on a 1 mL scale for analytic purposes. It can be seen from figure 2.29 by comparing the raw extract and the purified protein the concentration of the protein diminished. The result obtained from the purified protein (in μg/mL) equals a smaller amount of protein in the original sample due to loss of material at each purification step, but since all samples have been treated equally the relative amount of protein remained will have remained constant. This information was further used as a relative guide to extrapolate to the non-purified protein samples to better approximate how much protein of each variant was present in crude samples. Although this method of indirectly measuring the protein concentration is not ideal, it was necessary in order to get an approximate protein concentration.

Purified variant preparations were used for general assay work, and the specific activities of each against para-nitrophenol butyrate (pNPB) as a model substrate were determined.

2.2.5.2 Specific activity

In order to further characterise the lipase variants, the specific activity of each was determined. A model substrate had to be used since UV/Vis spectrophotometric determination of the hydrolysis of the target ester *rac*-**48** is not possible, since neither substrate nor product had suitable absorption profiles.

A huge variety of different esters varying in acyl chain length are available for this purpose. For the present case p-nitrophenol butyrate (pNPB) was chosen as model substrate. Its stability in DMSO at room temperature makes it favourable to p-nitrophenol acetate (pNPA), which shows an increased tendency to autohydrolyse. Hydrolysis of the ester liberates the p-nitrophenolate (pNP) which is a bright yellow coloured compound with an absorption maximum at 405 nm (cf. figure 2.30). Activity-studies can thereby be monitored spectrophotometrically.

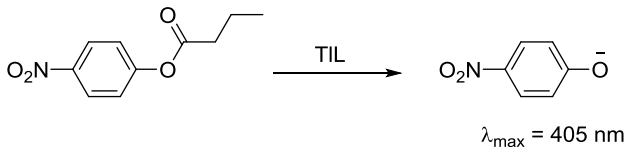

Figure 2.30: Principle of the *para*-nitrophenol butyrate (pNPB) assay, the lipase (TlL, *Thermomyces lanuginosus* Lipase) hydrolyses the ester and liberates *para*-nitrophenol (pNP) (pK_a = 7.2). The deprotonated species, *para*-nitrophenolate has a characteristic absorption maximum at 405 nm

Equation 10 relates the measured absorption to the concentration of substrate in the cuvette. At known path-length *l* the concentration is proportionally related to the measured absorption by ε, which was determined as 8448 M^{-1} cm^{-1} through linear regression of a standard curve (cf. § 4.4.1). The absorption coefficient is dependent on the composition of the medium, for a borate buffered system measured at 400 nm it is reported to be around 18,800 M^{-1} cm^{-1} and 19,200 M^{-1} cm^{-1} at a pH >10 (Bowers *et al.*, 1980). The difference between the measured specific absorption and the literature value is attributed to the lower pH of the measurement (pH 7.0) which was necessary to avoid autohydrolysis of pNPB.

$$A = \varepsilon c l \qquad \textbf{Equation 10}$$

The activity of an enzyme (in U) is defined as the conversion of 1 µmol pNPA to pNP per minute. Therefore it can be directly calculated from equation 11 divided by the time. The specific activity is a magnitude independent of the protein concentration and can be calculated as given by equation 2.2

$$\frac{dA}{dt} / \varepsilon \Big/_{c(Protein)} = specific\ Activity\ [\frac{U}{mg}] \qquad \textbf{Equation 11}$$

The specific activity was calculated for all variants and compared to the specific activity of the wild type enzyme and the purified commercial enzyme.

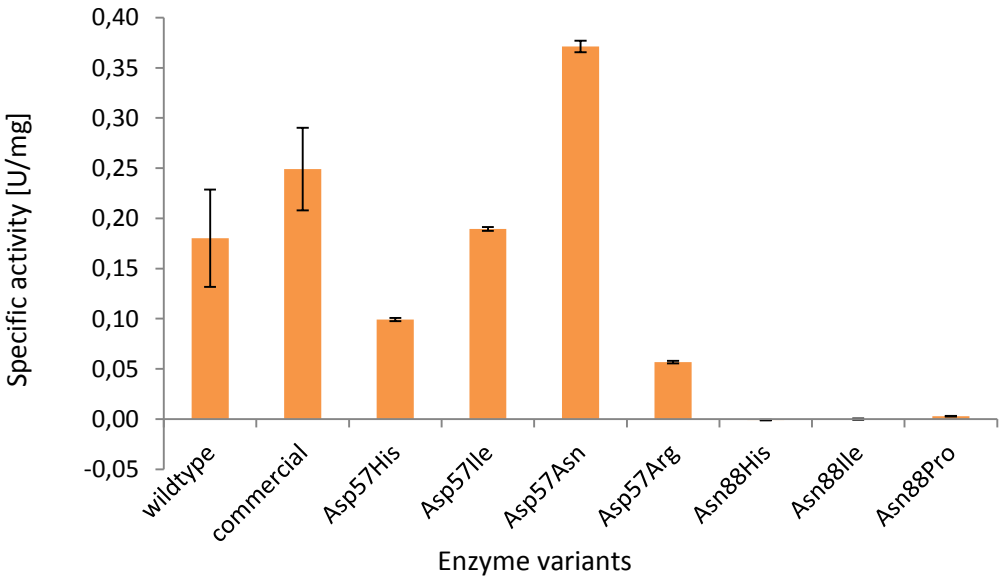

Figure 2.31: Specific activities of the wild type, commercial enzyme and enzyme variants, the specific activity was calculated from the change in absorption as per equation 2.29. The error is given as standard error

$$(standard\ error = standard\ deviation\ of\ the\ measured\ activity/\sqrt{3})$$

Figure 2.31 shows the results from the activity assay for all variants and wild type enzymes. The results will be discussed in detail in the following paragraphs. Overall, it can be seen that the Asn88X mutations all lost their activity towards pNPB. The wild type enzyme (in-house production) and commercial enzyme display a specific activity of 0.18 U*mg^{-1} and 0.25 U*mg^{-1}, respectively. The Asp57X mutations display a wide range of activities ranging from 0.06 U*mg^{-1} (Asp57Arg) to 0.37 U*mg^{-1} (Asp57Asn).

From the complete loss of activity, it can be concluded that Asn88 is important for the stability of the open conformation. The hydrogen bonds this residue establishes serve to keep the lid in the open conformation. With the introduction of histidine it was thought to increase the stabilising effect of asparagine, however the more sterically demanding imidazole ring is likely too bulky to form the required bonds with the backbone of Gly61 and Asp62 and thereby destabilises the open conformation (cf. figure 2.19). It is clearly visible that Asn88 plays a key role in stabilising the open conformation since all mutations that interrupt these hydrogen bonds formed by this residue results in total loss of activity under the assay conditions.

Shifting the focus to the Asp57X variants it was determined that Asp57 has some influence on enzyme activity. Introducing an arginine sidechain was intended as a way to 'push' Arg84 away to attain the A state (Arg84 switched towards the carbonyl backbone of Cys268). However it was shown that this mutation created a variant with reduced activity. A hypothesis for this finding is that minor conformational changes trigger the formation of an alternative salt bridge between Arg84 and Asp62 (a residue proximal to Asp57), preserving the influence of Arg84 on the closed state. Moreover introducing the Arg in position 57 creates an Arg rich region (Arg57, Arg48 and Arg81) which can feasibly have a negative effect on enzyme activity (cf. figure 2.32).

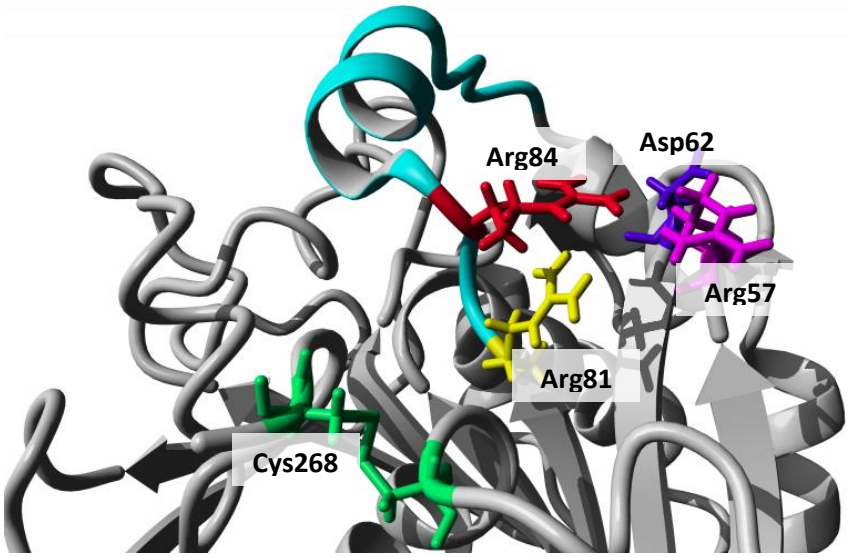

Figure 2.32: Arginine rich region in the Asp57Arg variant. A stabilising effect of the introduced Arg57 (pink) in combination with Arg84 (red) and Arg81 (yellow) is conceivable. Moreover a salt bridge between Arg84 (red) and Asp62 (purple) could stabilise the closed conformation. The model was created through a simple *in silico* change of the residue employing a resolved structure of the colsed conformation (1DT3) as scaffold. No further further energy minimisation has been performed on the model.

The introduction of an isoleucin residue serves to break any hydrogen bonds between Asp57 and Arg84, which were described to be responsible for holding Arg84 in the LA position. However, there is little difference in the activity between the wild type and the Asp57Ile variant (cf. figure 2.31) observed in the pNPB assay. This result questions the hypothesis that Asp57 is reponsible for the maintenance of the LA state (Brzozowski *et al.*, 2000).

An interesting finding is the Asp57Asn mutation. This variant seemed to show increased activity in the pNPB assay (twice as active as the wildtype enzym, cf.figure 2.31).

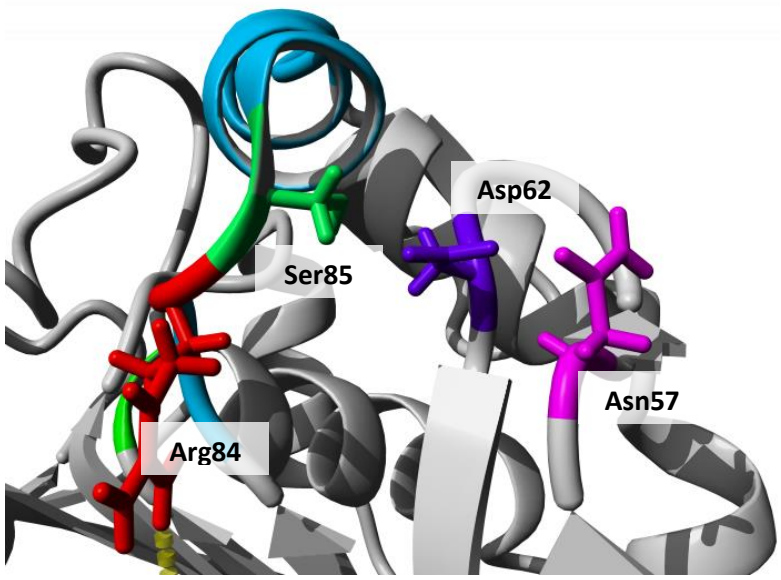

Figure 2.33: Interaction of the Asp57Asn variant. A stabilising effect of the introduced Asn57 (pink) enhances potential Asp62 (purple) -Ser85 (mint green) hydrogen bond which stabilises the open conformation of the lid (cyan helix). Arg84 (red) has switched its orientation towards its stabilising hydrogen bond with the mainchain carbonyl of Cys 268 (yellow dotted line). The model was created through a simple *in silico* change of the residue employing a resolved structure of the colsed conformation (1DTE) as scaffold. No further further energy minimisation has been performed on the model.

Since the influence of the hydrogen bonds formed between Asp57 and Arg84 to maintain the closed state has been ruled out (vide supra: interuption of all interactions in the Asp57Ile mutation yields a mutant with wildtype activity, while the Asp57Arg mutation creates a potentional alternative Arg84-Asp62 salt bridge which serves to stabilise the closed conformation), Asn57 must exert its function of stabilising the closed conformation in a indirct manner, interacting with a residue in its proximity thereby modulating the activity. In this

sense Asn57 may interact with Asp62 which upon close inspection of the crystal structure of the open conformation, forms a clear hydrogen bond to Ser85. An interaction between Asn57 and Asp62 can reinforce a conformation in that residue that is more conducive to binding with Ser85, thereby stabilising the open conformation.

2.2.5.3 pH profile

Encouraged by the results obtained with the wildtype enzyme (WT § 2.2.2), in a pH-screen of the standard reaction (cf table 2.9, § 2.1.4.3), pH profiling was performed for all enzyme variants inculding the commercial enzyme. This assay was performed on the standard substrate ester *rac*-**48** in order to assess the activity of the enzyme variants towards the target substrate. For practical reasons the crude, concentrated protein solution was employed in these trials, since it was shown that the negative control (fermentation with strain from empty vector transformation) did not show any catalytic activity (cf. table 2.2.4.4a entry 5). TlL is reported to be most active at high pH, the optimal pH range is reported to be between pH 8 and 12 (Neves Petersen *et al.*, 2001), while other sources state the pH optimum to be at pH 8 (Brzozowski *et al.*, 2000). In order to cover a broad range a pH screen was performed between pH 6 and 10 using a set of two different buffers overlapping at pH 8 to investigate secondary effects due to the composition of the buffers. Both wildtype and commercial enzyme were added to the reaction mixture (5 mL) containing an appropriate buffer and substrate ester *rac*-**48** as 2% w/v. The other variants were added in the percentual proportion to yield the same final amount of protein in each reaction (cf. table 2.11). It can be expected that the enzymes will show a different reaction profile to the one observed in the pNPA assay at pH 7 since the pNPA assay was performed using DMSO as a co-solvent (cf. § 4.4.1) It. has been shown before (cf. § 2.1.4.2) that the addition of a co-solvent can strongly influence the outcome of the reaction, therefore any change in reactivity between the pNPA assay and the assay using *rac*-**48** as a substrate will be due to the change in reaction conditions. No direct, absolute comparison can be made between the data from the pNPA assay and the pH assay, however it is expected that variants showing an increased activity in one assay will exhibit a similar behaviour in the the other.

Table 2.11: Protein concentrations obtained after the purification of the TlL variants. The protein concentration was determined in a Bradford assay

Entry	variant	concentration [μg/mL)
1	neg	6.3
2	WT	23.3
3	Asp57His	39.3
4	Asp 57Asn	115.6
5	Asp57Ile	30.0
6	Asp57Arg	23.9
7	Asn88His	14.5
8	Asn88Ile	19.0
9	Asn88Pro	63.9
10	commercial	1070

In order to relate the measured activity of the variants towards the target substrate *rac*-**48** (cf. §§ 2.2.5.2 and 2.2.5.3), to the activity of the wild type enzyme, the amount of protein was normalised so that any added volume of protein solution contained the same mass equivalents of protein as the wild type. The protein concentration measured in the purified preparation of the samples was taken as basis for these adjustments. Although the absolute amount measured in the purified samples does not equal the amount of protein present in the crude sample the relative amounts are accepted to be the same, since all samples were treated equally and the inevitable percentage loss during purification will be the same. This method of indirect measurement of protein quantities was necessary and imposed by the composition of the crude protein sample. The data obtained can therefore not be taken as an absolute value, the relative activities of the variants, however are truly comparable.

In the following, primarily the results obtained for the Asp57X variants will be discussed (cf. figure 2.34). It was investigated whether the results from the pNPB assay were validated in the reaction with the actual compound ester *rac*-**48**. Of particular interest was the conversion, since the primary aim of making mutations was to increase the conversion in this reaction. The assay test (set up as per standard reaction protocol: ester rac-48 (50 μg) in the

corresponding buffer (5 mL), addition of the protein solution to give an amount of protein equal to 100 µl of WT preparation) was run over the period of 48h, the reaction was stopped by extraction with MTBE (cf. § 4.4.2.3) and analysed (end-point determination). The results obtained are summarized in figure 2.34 and 2.33. However the pH dependency of enzyme activity observed has to be taken cautiously[4] due to several possibilities of experimental error that may influence the determination ofconversion and enantioselectivity in chiral HPLC. Therefore the data presented cannot be taken absolutely but rather indicatively. A clear yes-no answer for enzyme activity can be given. A pH dependency for each mutant is discussed below.

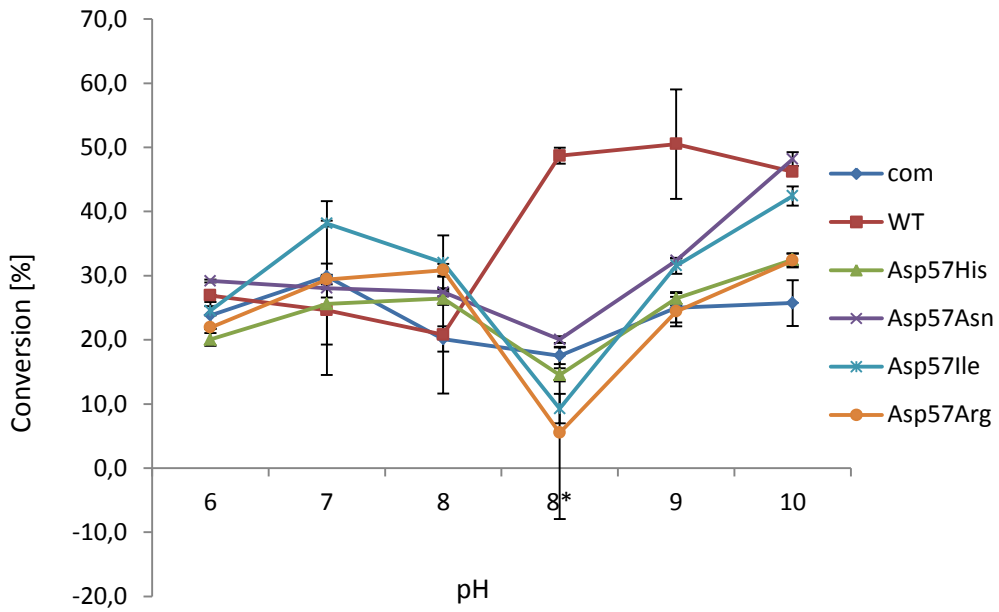

Figure 2.34: pH profile of the commercial TlL, wildtype and Asp57X variants in a HPLC monitored hydrolysis assay of ester *rac*-**48**. The assay was performed over a pH range from 6-10. The first three values (pH 6 –pH 8) were obtained in potassium phosphate buffer at the indicated pH. The last three values (pH 8 – pH 10) obtained in glycine/NaOH buffer at the indicated pH.

It is interesting to see, that an effect of the pH and buffer system can be observed in all cases. All enzyme variants proved to be less active in the phosphate buffered reactions than in the Glycine-NaOH buffered reactions, although a drop in reactivity was observed at Glycine-NaOH buffered reactions at pH 8, which can be due to the reduced buffer capacity of glycine at pH 8. The conversion increased with the pH and arrived at close to 50% at higher pH levels.

[4] The data combines the pipetting error during the setup, the fluctuation of stirring velocity and room temperature) between batches and the detection limit of the HPLC.

The enantiopreference of the variants remained stable ((*S*)-selective) in all cases. The enantioselectivity varied around an *E* value of 100 (data not shown): the *E* is stable and the enantioselectivity is not influenced by the changes made in the enzyme. The data obtained in the pNPB assays was mirrored in the pH screen towards the hydrolysis of ester *rac*-**48**. The most striking result is the observed shift in activity of the wildtype enzyme when the buffer is changed from phosphate to glycin. Using a phosphate buffer at low pH values the conversion reaches 25% after 48h. A shift to glycine buffer yields conversions of 50% for the wildtype enzyme. It can be seen from the discrepancy between the conversions attained using phosphate and glycine buffer at pH 8 that this change in activity is a result of the buffer system (the pH remains the same while the buffer system changes). From this result it can already be concluded that a glycine buffered system is preferable for this biotransformation. The observed dip in activity observed in all other variants is attributed to the reduced buffer capacity of Glycine at pH 8. It can be hypothesized that the wildtype enzyme is more stable towards small shifts in pH. Moreover, the same volume of commercial and wildtype enzyme were added in the respective reactions. It is clear from the data that the commercial enzyme is 40% less active towards the target ester *rac*-**48** than the wildtype enzyme. Considering that the commercial enzyme is about 50 times more dilute than the wildtype this makes the commercial enzyme a less attractive catalyst for the target transformation. This discrepancy in activity may be due to a reduced shelf life of the commercial enzyme.

The error bars at low pHs (6-8, phosphate buffered system) are to high to give reliable data, no clear pH dependecy can be assigned to the mutants. However it can be seen that the variants that were particularly active in the pNPB assay showed enhanced activity towards the target ester *rac*-**48**, too. The most promising candidate, apart from the wild type enzyme, was the Asp57Asn mutation, which reached the same conversion levels as the wild type at pH 10. Although it offers a lone pair at the nitrogen, Asparagine will not act as a H-bond acceptor to the extend Aspartate might do. This is mainly due to the fact that asparagine has a partial double bond character, where the lone pair is no longer available for interresidual contacts.

It can be concluded that the pH optimum was generally at pH 9-10. At physiologic pH the Arg84 will most likey be protonated, acting as a H-bond donor in the Arg84 - Asp57 interaction. The increase of the pH to basicicity will lead to both the arginine and the aspartate to be deprotonated (pK_a = 12.75 (Berg *et al.*, 2012)) and therefore will create a repelling interaction at high pHs leading the lipase to acquire the [A] conformation (cf. figure

2.16; the arginine has switched but the lid is still closed) giving a rationale for the activity of the lipase at high pHs.

Although no improvement of the mutants over the wild type enzyme was detected it could be proven that the wild type enzyme showed an enhanced activity over the commercial enzyme. Since it has been previously reported that the mutation of a single residue can alter the enantioselectivity (Holmquist *et al.*, 1993a) the enantioselectivity was determined in all cases but remained stable at an *E* of approximately 100.

The Asn88X variants proved to be inactive in the pNPB assay. However they were included in the pH screen since the pNPB assay was performed under conditions different from the standard reaction conditions (addition of DMSO and in phosphate buffer pH 7.0). Including the Asn88X variants in the pH assay (cf. figure 2.35) allows to determine wether the activity is pH dependend and the lack in activity determined in the pNPB assay was due to a non-optimal pH

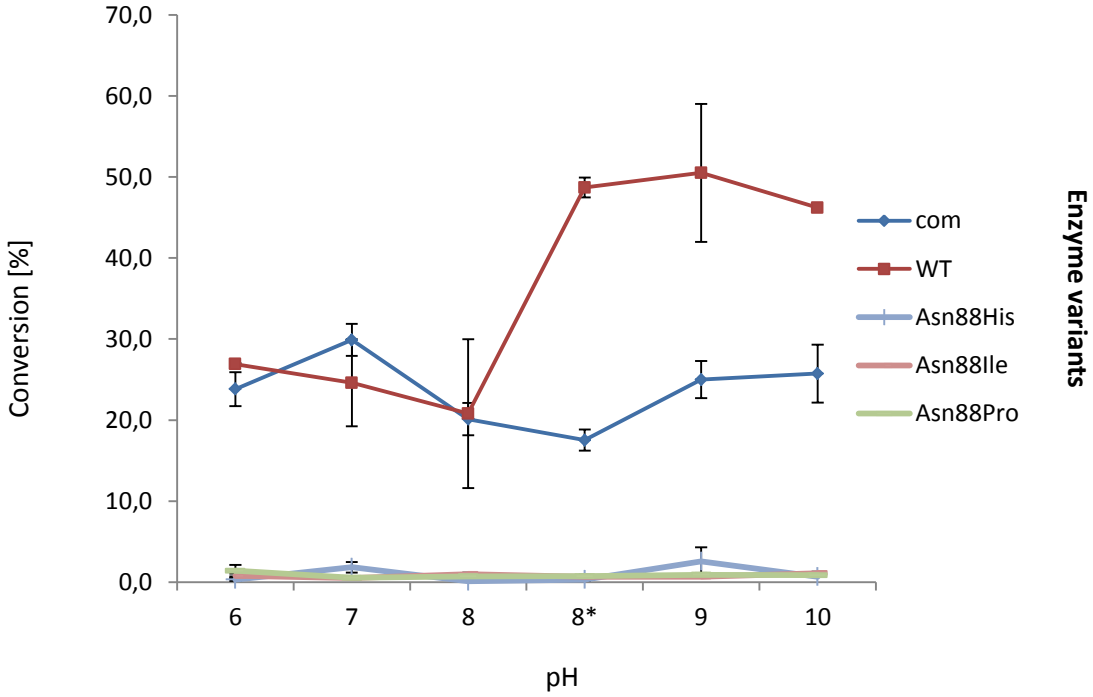

Figure 2.35: pH profile of the commercial TlL, wild type and Asn88X variants. The assay was performed over a pH range from 6-10. The first three values (pH 6 –pH 8) were obtained in potassium phosphate buffer at the indicated pH. The last three values (pH 8 – pH 10) obtained in glycine/NaOH buffer at the indicated pH

As expected, on the basis of the pNPB assay the Asn88X mutations did not show any activity. The conversion was around 1% after 44 hours. Conversion and enantioselectivity are indirectly measured via the enantiomeric excesses determined in HPLC. A blank reaction was

performed at pH 6 (phosphate buffer) and at pH 10 (Glycine-NaOH buffered) to determine the background hydrolysis of the ester under the extremes of the assay conditions. No background hydrolysis was observed (data not shown).

At this point it can be stated with certainity that the Asn88X mutations are fully inactive and therefore Asn88 residue is important for catalytic activity. The Asp57 residue on the other hand seems to influence the opening of the lid. More thorough tests with a more sensitive method of analysis will need to be performed to fully establish the importance of the residue, however it appears that variants disrupting the hydrogen bond with Asn84 lead to a relative increase in activity, while residues that could act as a H-bond acceptor even at high pH values reduced the activity of the enzyme at a pH where the wildtype enzyme showed full activity. The Asp57Ile mutation fully disrupted the hydrogen bond and lead to full activity even at pH 7 (results illustrated in figure 2.13).

Table 2.12: Summary of the pH assay; comparison of the wild type (WT) and variants in terms of pH optimum and maximal conversion attained at the optimal pH

Entry	Variant	pH optimum	buffer[a]	%c[b]
1	WT	9	G	50.4
2	Asp57His	10	G	32.5
3	Asp57Ile	7	P	42.4
4	Asp57Asn	10	G	48.2
5	Asp57Arg	10	G	32.4
6	Asn88His	n/a	n/a	< 1
7	Asn88Ile	n/a	n/a	< 1
8	Asn88Pro	n/a	n/a	< 1

[a] G indicates Glycine-NaOH buffer while P stands for Potassium phosphate buffer

[b] determined in chiral HPLC as determined as c = $\frac{ee_s}{ee_s + ee_p}$

2.3 CHEMO

2.3.1 Introduction

The ultimate goal of this thesis was the development of a biocatalytic process for application in pharmaceutical industry. Several factors that are of secondary significance at laboratory scale need to be considered when a process is transferred to industrial scale. The most important aspects taken into consideration during the scale-up of a process are (1) safety of the chemistry involved (2) cost of goods (CoGs) and of operations, and (3) management of the generated waste (Anderson, 2000). Moreover, European legislation for industrial processes requires sustainable and environmentally benign synthetic routes (for full discussion of green chemistry see § 1.1.1).

The present work therefore *per se* addresses two of the key issues of pharmaceutical processes: The application of enzymes as (chiral) catalysts in organic synthesis applies this principle of green chemistry in terms of environmental sustainability. There is no need for the use of non-renewable, expensive and potentially toxic chemical catalysts. Moreover the reactions can be carried out mostly in aqueous medium, which reduces the amount of solvents to be incinerated or recycled and the amount of organic by-products generated.

The subject of further optimisation of the current process is the reduction of production cost. Secondly, the further reduction of waste and a reduction in the use of toxic solvents (co-solvents and solvents used for downstream purification and extraction from the reaction medium) need to be addressed. These concerns were the second target (after the successful identification of a suitable biocatalyst cf. § 2.1) of the work presented and will be discussed below.

The main cost factor in the process discussed is the enzyme. Modification of the enzyme in order to increase the turnover rate has been discussed in the previous chapter (cf. § 2.2). This chapter will focus on the industrialisation and scale-up of the TlL mediated hydrolysis of compound *rac*-**48**. The first part will deal with the scale of the reaction with particular views on gram-scale reaction engineering in terms of temperature, co-solvents and reaction stoichiometry. Moreover the recyclability of the enzyme will be examined. The second part of this chapter will transfer the knowledge obtained in the scale-up experiments and apply them to flow chemistry in a reaction engineering approach.

2.3.2: Scale up

It was established in several trials that the reaction rate and enantioselectivity is strongly influenced by the temperature, since the small reaction volumes did not allow for even equilibration of the reaction medium to the set temperature (data not shown). The small-scale trials were therefore run at room temperature without temperature monitoring for simplicity and increased throughput (cf. § 2.1). Large scale reactions during the optimisation of the reaction parameters were run in an EasyMax™ apparatus, which allows a precise control of temperature and a reproducible stirring mode, either with a magnetic stirrer or a mechanical overhead stirrer (figure 2.36)

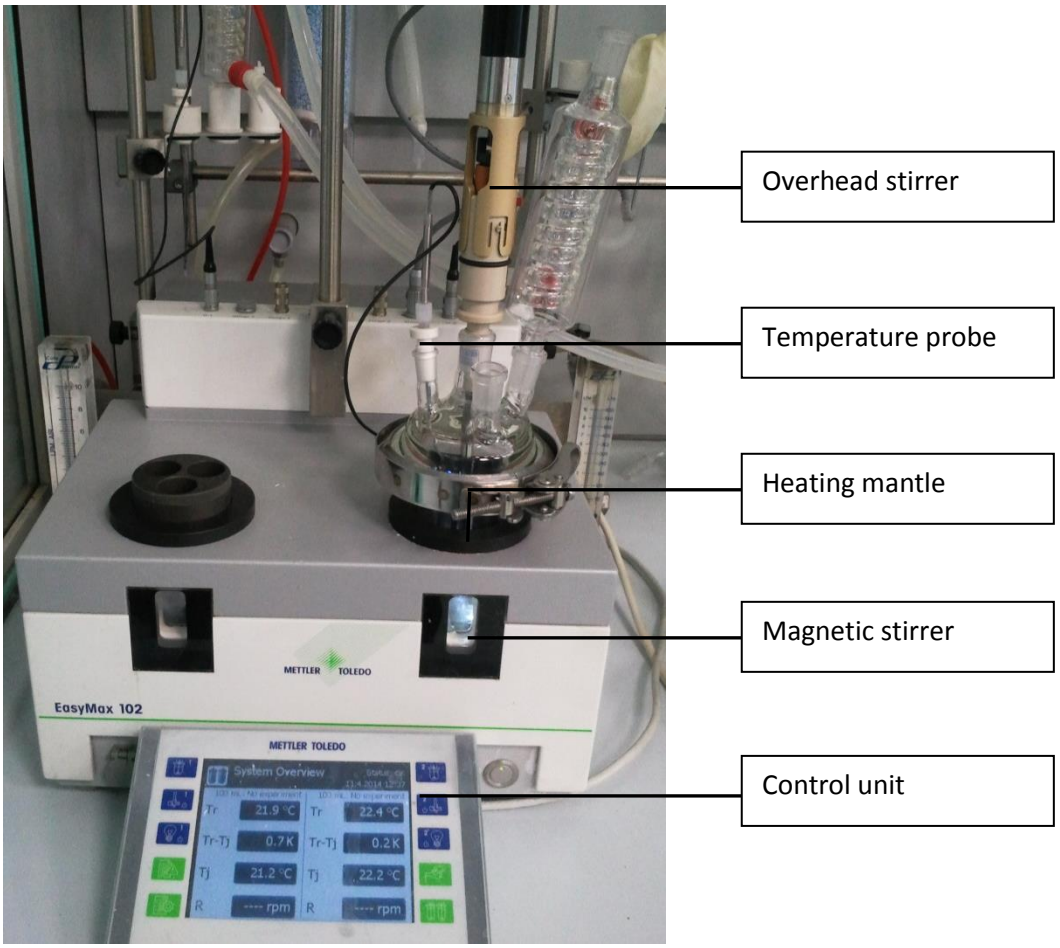

Figure 2.36: The EasyMax™ apparatus with an overhead stirrer, a probe for temperature control, a heating mantle for precise heating and a built-in magnetic stirrer. Temperature and mode of agitation can be controlled via the control unit.

Moreover the method of agitation can be changed using the EasyMax^{TM} equipment, and a thorough mixing can be attained even at large reaction volumes. Immobilised TlL on beads (cf. table 2.4, entry 40 (purchased in large quantities from Aldrich (Lipolase TL IM))), had not been employed and studied thoroughly since previously the use of magnetic stirring caused the beads to be ground and therefore the observed lower values of enantioselectivity and conversion could not necessarily be attributed to a reduced functionality of the enzyme but were possibly also influenced by the mechanical destruction of the beads. Using a stirring anchor (cf. figure 2.37) the reaction mixture could be stirred homogeneously without risking to grind the immobilised enzyme.

Figure 2.37: EasyMax^{TM} reaction vessel with stirring anchor and temperature probe

In order to study the parameters discussed (TIL immobilised on beads against liquid preparation of the TlL; temperature; stirring) a reaction volume of 50 or 100 mL was chosen as reaction volume (results collected in table 2.13).

Table 2.13: Comparison between the immobilised TlL (B) and the liquid preparation (L) (both purchased from Aldrich) in terms of conversion and enantioselectivity

Entry	% ee_s [a]	% ee_p [b]	% c [c]	E [d,e]	t [h]	liq /beads (L/B [g; mL]	Units [f]	subst (g)	vol [mL]	cosolv (mL)
1	96.4	96.4	50.0	221	24	L, 1.0 mL	10^5	0.5	50	na
2	77.0	95.8	44.6	108	23	L, 0.2 mL	$2x10^4$	0.5	50	na
3	48.8	97.1	33.4	112	23	L, 0.1 mL	10^4	1.0	100	na
4	74.4	76.4	49.3	17	24	B, 2.0 g	$2x10^4$	1.0	100	na
5	95.8	86.2	52.6	52	23	B 0.5 g	$5x10^3$	0.5	50	na

Conditions: ester *rac*-**48** (50 / 100 mg), lipase in different concentrations in Glycine-NaOH buffer (50 /100 mL); the reactions with the immobilised enzyme were stirred employing a stirring anchor (cf. figure 2.3.1a).

[a] determined by chiral HPLC

[b] determined by chiral HPLC

[c] determined as c = $\frac{ee_s}{ee_s + ee_p}$

[d] determined from ee_s and ee_p as in equation 8, § 1.1.2.2

[e] the absolute configuration was (1*R*,2*R*) for the ester **48** and (1*R*,2*R*) for the acid **32**

[f] Beads: 9820 Units/g (from CoA of specific lot) Liquid: >100000 Units/g (exact data not available from CoA). 1 Unit corresponds to the amount of enzyme that liberates 1 µmol of butyric acid per minute at pH = 7.5 at 40 °C (substrate tributyrin)

From table 2.3.1a it can be seen that the liquid preparation of the enzyme is 2 x more active towards the target ester *rac*-**48** than the immobilised enzyme (cf. table 2.13, entry 2 and entry 4). The observed difference in conversion between the reactions performed at small scale and in the EasyMax™ can be attributed to the more homogeneous stirring and a constant reaction temperature within the reaction mixture (cf. table 2.8 entry 5 and table 2.13, entry 1; same relative amounts of enzyme to substrate ester *rac*-**48** are employed).

Although table 2.13 suggests that the liquid preparation of the enzyme is more effective it has to be taken into consideration that the immobilised enzyme was developed to be recycled. While the liquid preparation of the enzyme has to be disposed of after every round of reaction (increase of waste, increase of production cost) the immobilised enzyme can theoretically be filtered and reused in the next round of reaction and thereby becomes more efficient for the target process on the long run. Taking the above into account the focus was

shifted to the immobilised enzyme (for recycling trials please cf. table 2.16).

Finally table 2.13 shows that when reducing the amount of catalyst two fold the reaction still goes to completion after 24h, but with increased enantioselectivity. This finding is indicative of a secondary effect (substrate inhibition) on the enzyme but at the same time highlights the enantioselectivity of the TlL. More importantly this result indicates a secondary effect caused by the ester on the immobilised enzyme and emphasizes the need for a co-solvent to wash the beads constantly over the course of the reaction in order to minimise the saturation of the enzyme with substrate.

2.3.2.1 Co-solvents

Upon addition of the ester *rac*-**48** to the reaction mixture it was noted (visual examination) that the ester immediately adsorbed to the beads, which raised the question of a possible modification of the conversion and enantioselectivity of the reaction due to substrate or product inhibition (*vide supra*). Moreover the extraction of the remaining product ester (1*R*,2*R*)-**48** at the end of the reaction is challenging and requires the use of a lot of solvent to wash the beads. Therefore the use of a co-solvent to constantly wash the beads during the course of the reaction was discussed (results collected in table 2.14).

Table 2.14: Use of co-solvents in the TlL mediated hydrolysis of ester *rac*-**48**

Entry	% ee_s[a]	% ee_p[b]	% c[c]	E[d,e]	t [h]	liq /beads (L/B [g; mL]	Units[e]	subst (g)	vol [mL]	cosolv (mL)
1	83.6	90.6	48	54	24	B, 1g	10^4	0.5	50	10 Hept
2	88.6	73.4	54.7	19	23	B, 2g	$2x10^4$	1	100	10 MTBE

Conditions: ester *rac*-**48** (50/ 100 mg), lipase in different volumes in Glycine-NaOH buffer (50-100 mL); the reactions with the immobilised enzyme were stirred employing a stirring anchor (cf. figure 2.37).

[a] determined by chiral HPLC

[b] determined by chiral HPLC

[c] determined as c = $\frac{ee_s}{ee_s + ee_p}$

[d] determined from ee_s and ee_p as in equation 8, § 1.1.2.2

[e] Beads: 9820 Units/g (from CoA of specific lot) Liquid: >100000 Units/g (exact data not available from CoA). 1 Unit corresponds to the amount of enzyme that liberates 1µmol of butyric acid per minute at pH = 7.5 at 40 °C (substrate tributyrin)

[e] the absolute configuration was (1*R*,2*R*) for the ester **48** and (1*R*,2*R*) for the acid **32**

Both substrate ester **48** and product acid **32** dissolve readily in MTBE which will allow for an efficient extraction of the compounds into the organic phase. In spite of these considerations it was shown that the use of MTBE as a co-solvent did not have a positive influence on the outcome of the reaction (cf. table 2.14, entry 4 and table 2.14, entry 2) in terms of both conversion and enantioselectivity. Csuk and co-workers have successfully employed TlL in a similar biotransformation using hexane as a co-solvent (1996). This method was followed in this work but due to its reduced toxicity in comparison to hexane (Buddrick *et al.*, 2013) heptane was used instead. It was shown that the use of heptane as a co-solvent has a beneficial influence on the reaction (cf. table 2.13, entry 4 to table 2.14 entry 1). It can be seen that when using heptane as a co-solvent the enantioselectivity of the process was increased 10 fold. The conversion, however, was uninfluenced by the use of a co-solvent. The use of a co-solvent will help to wash the unreacted ester off the beads and thereby reduce time of direct contact of the enzyme with ester **48**, which will help to mitigate secondary effects of the ester **48** effects on the enzyme, which were observed in previous trials (*vide supra*) and thereby allow the reaction to proceed with an increased enantioselectivity. Although the use of the co-solvent should increase the conversion rate by reducing the effects of substrate inhibition, secondary effects of the co-solvent on the enzyme as well as the reduced contact between substrate ester **48** and TlL may affect the conversion rate in a way that no overall change in conversion is observed.

2.3.2.2 Temperature

The influence of the temperature had been considered previously (cf. chapter 2.1.4.3) but had not been examined since the set-up of the small scale biotransformations did not allow for any studies on temperature. Using the EasyMax^{TM} (cf. figure 2.13) in a setup with the stirring anchor (cf. figure 2.37) the temperature inside the reaction mixture could be kept constant and therefore studies on the effect of the temperature on the reaction employing the immobilised enzyme could be performed. The reactions were performed without the addition of any co-solvent (results collected in table 2.15). Aliquots were taken at regular intervals to plot the conversion vs the temperature (cf. figure 2.38).

Table 2.15: Study on the effect of the temperature on conversion and enantioselectivity of the TlL mediated hydrolysis of *rac*-**48**

Entry	time [h]	T [°C]	% ee_s [a]	% ee_p [b]	% c [c]	E [d,e]
1	23	10	77.2	84.0	47.9	27
2	24.5	20	74.4	76.4	49.3	17
3	24	40	90.0	57.8	60.9	11

Conditions: ester *rac*-**48** (1g), immobilised lipase (2g) in Glycine-NaOH buffer pH 9.0 (100 mL); the reactions with the immobilised enzyme were stirred employing a stirring anchor (cf. figure 2.37).

[a] determined by chiral HPLC

[b] determined by chiral HPLC

[c] determined as c = $\frac{ee_s}{ee_s + ee_p}$

[d] determined from ee_s and ee_p as in equation 8, § 1.1.2.2

[e] the absolute configuration was (1*R*,2*R*) for the ester **48** and (1*R*,2*R*) for the acid **32**, determined by comparison to a enantioenriched standard in chiral HPLC

Table 2.15 indicates the effect of the temperature on conversion and enantioselectivity. The reactions were performed in the same way as the reactions in table 2.13. The result obtained in the reaction at 20 °C coincided with previous results (cf. table 2.15 entry 2 with table 2.13, entry 4). As was expected, the enantioselectivity increased when the reaction temperature decreased. The conversion rate however remained the same, highlighting the fact that the amount of enzyme can be significantly reduced (cf. table 2.15, entry 1). Increasing the temperature leads to a decrease in enantioselectivity and an increase of conversion rate above the desired 50% conversion (cf. table 2.3.2.2.a, entry 3). Aliquots were taken at regular intervals to observe the conversion over time. Although sampling was difficult due to the hetererogenity of the reaction, figure 2.38 gives an indication of the reaction rates at different temperatures.

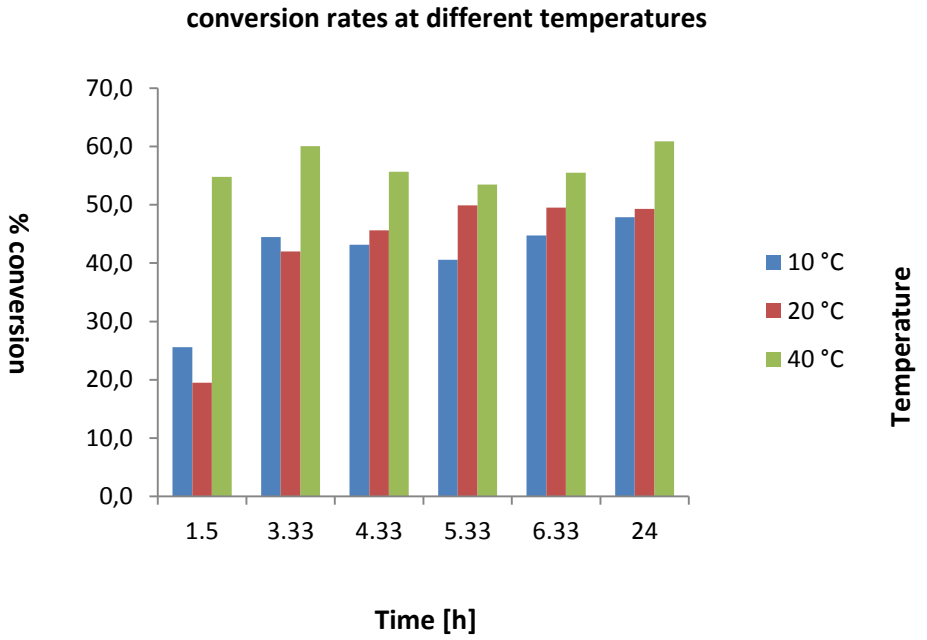

Figure 2.38: Conversion rates at different temperatures, aliquots taken at regular intervals to compare the rate of hydrolysis of reactions at different temperatures

Conditions: ester *rac*-**48** (1g), immobilised lipase (2 g) in Glycine-NaOH buffer pH 9.0 (100 mL); the reactions with the immobilised enzyme were stirred employing a stirring anchor (cf. figure 2.37).

Figure 2.38 represents the change of conversion over time. Aliquots were taken at regular intervals. While 50% conversion is only reached after around 24h in a reaction at 10 °C, it is clearly shown that the conversion reaches the desired 50% after 5h at a temperature of 20 °C. Good enantioselectivities are achieved in both cases. Increasing the temperature to 40 °C allows for a conversion of >50% after 1h, however the enantioselectivity decreases significantly (for enantioselectivities cf. table 2.15).

As a conclusion of the temperature experiments, it can be said that the best yield-enantioselectivity ratio is obtained at a temperature of 20 °C. The results obtained in combination with the results from the co-solvent experiments indicate that the reaction time can be shortened (or the amount of enzyme reduced) significantly in a stirred reaction at 20 °C.

2.3.2.3 Recyclability

The last step towards an industrial process, that is considered here, is the reduction of production costs. The main factor in this process is the amount of enzyme employed in each hydrolysis reaction. Although a decrease in the amount of the enzyme as a liquid formulation is clearly possible (cf. § 2.3.2.1 and § 2.3.2.2), its recycling at the end of the reaction is not feasible. When the liquid formulation is used, a stable emulsion is formed at the end of the reaction, which needs to be filtered on a filtration aid such as celite, generating large volumes of solid waste.

On the other hand, employing immobilised TlL (immobilised on Immobead 150) which consists of large beads (0.5 mm diameter) that can be easily filtered off at the end of the reaction. This not only allows for a quick and easy workup (filtering and washing of the beads; extraction of the enantiopure ester **48** from the medium) but also is an optimal condition for the re-cycling of the enzymes. The filtered and washed enzyme can be re-used in a next round of reaction. However, although this process already reduces the amount of the enzyme, the process is still lengthy and requires many different workup steps. Moreover the immobilised enzyme, although stable over a longer period is gradually ground to a fine powder even in the anchor-stirred reactor. Therefore a system had to be devised that allows for an easy separation of beads and reaction medium while keeping the beads safe from mechanical damage during the course of reaction. A construction similar to the one used by Mallin and co-workers (2013), was implemented.

Figure 2.39: Immobilised TlL wrapped in first aide gauze ('tea bag') as set-up for recycling experiments

The immobilised enzyme was wrapped in chemically inert first aide gauze (figure 2.39). In this way the enzyme was protected from external damage. The reaction could be easily stopped simply by taking the 'tea bag' of enzyme out of the liquid reaction medium and washing it in a mixture of heptane (to extract the remaining ester adsorbed to the beads) and fresh buffer at pH 9 (to extract the remaining acid trapped in the gauze). The reaction was set up at a 1g scale (substrate *rac*-**48**, 1g; enzyme in 'tea bag', 2g, in Glycine-NaOH buffer pH 9.0, 0.1M, 100 mL) and repeated six times. For the workup the 'tea bag' was quickly washed in hexane and fresh buffer prior to being added to a fresh reaction mixture. This set up allowed for several cycles of hydrolysis to be performed with the same batch of immobilised enzyme without any significant loss of enzyme activity or enantioselectivity (results collected in table 2.16). The apparent increase of enantioselectivity observed after several cycles is considered not significant and is probably due to an enrichment of optically active substrate and product by retention in the tea bag.

Table 2.16: Recycling experiments using the immobilised TlL in a 'tea bag'

Entry	cycle #	% ee_s [a]	% ee_p [b]	% c [c]	E [d,e]	yield [mg]
1	1	85.2	76.8	52.6	20	437
2	2	77.2	85.4	47.5	30	212
3	3	72.8	86.9	45.6	31	600
4	4	70.8	88.2	44.5	34	707
5	5	75.0	87.6	46.1	34	
6	6	74.9	88.7	45.8	37	811

Conditions: ester *rac*-**48** (1g), immobilised lipase (2g) in Glycine-NaOH buffer pH 9.0 (80 mL) with Heptane (20 mL); the reaction was stirred with a magnetic stirrer (500 rpm)

[a] determined by chiral HPLC

[b] determined by chiral HPLC

[c] determined as c = $\frac{ee_s}{ee_s + ee_p}$

[d] determined from ee_s and ee_p as in equation 1.1.16, § 1.1.2.2

[e] the absolute configuration was (1*R*,2*R*) for the ester **48** and (1*R*,2*R*) for the acid **32**

A matter that needed addressing was the retention of substrate and product in the enzyme parcel. Although a short washing step allowed for most of the used product to be recovered (cf. table 2.16) some remained in the parcel, as was established by comparison of

raw material and recovered product. In order to ascertain the initial loss of material (the percentage remained will be extracted at the last cycle, when the beads are stripped of any remaining substrate before disposal) a second reaction was set up in identical conditions but with a different workup. The teabag was quickly washed in heptane as described previously and the aqueous phase was extracted at both basic (pH 9) and subsequently acidic (pH 1) pH with hexane. The 'tea bag' was opened and the beaded enzyme was stirred in water: heptane (1:1) (pH 1) for 15 min. The enzyme was filtered off and the organic phase was washed with a basic solution (pH 9) and re-extracted with heptane. The organic phases were concentrated and analysed by chiral HPLC.

Table 2.17: Recovery of substrate and product after one cycle of reaction using the 'tea bag'

Entry	sample[a]	compound	% ee_s[b]	% ee_p[c]	% c[d]	E[e,f]	yield [mg]	% recovery[g]
1	RX, b	ester	82.4	80.6	50.6	24	232	23
2	RX, a	acid	82.4	80.6	50.6	24	131	15
3	B, b	ester	83.0	77.8	51.6	21	114	11
4	B, a	acid	83.0	77.8	51.6	21	79	9
5	total	na	na	na	na	na	na	59

Conditions: ester *rac*-**48** (1 g), immobilised lipase (2 g) in Glycine-NaOH buffer pH 9.0 (80 mL) with Heptane (20 mL); the reaction was stirred with a magnetic stirrer (500 rpm)

[a] origin of the sample, RX = reaction mixture, B = beads; b = basic extraction, a = acidic extraction

[b] determined by chiral HPLC

[c] determined by chiral HPLC

[d] determined as c = $\frac{ee_s}{ee_s + ee_p}$

[e] determined from ee_s and ee_p as in equation 1.1.16, § 1.1.2.2

[f] the absolute configuration was (1*R*,2*R*) for the ester **48** and (1*R*,2*R*) for the acid **32**

g calculated as mol% of the original amount of ester **48**,

From table 2.17 it can be seen that 20% of the product remains in the tea bag after one cycle of reaction (cf. table 2.17, entry 3 and 4). Moreover, adding the singular amounts of recovered product and substrate a total of 60% of the theoretical yield is recovered. The loss in product recovery can be attributed to the formation of micelles during the workup that contains parts of the acid **32** and the ester **48**.

The acid **32** can act as a surfactant due its amphiphilic character: the hydrophilic 'head' carboxylic group and the hydrophobic aryl cyclopropane group effectively makes this compound an ideal surfactant. The hydrophobic part of the surfactant tries to avoid contact with water. Micelle formation has been observed in the interface during the extraction. The observed interphase probably also contains some unbound enzyme or components form the immobilising agent. Some product was trapped (observed by NMR and HPLC analysis of the interface, full recovery and quantification was not possible) and is thought to be the cause for the loss in extracted reaction products. Several methods exist to dissolve micelles and further process development addressing this matter will lead to full recovery of acid and ester.

The result obtained in this set of experiments clearly indicated the possibility to reduce the amount of enzyme employed in the biotransformation. Moreover, it was shown that the mixing of the reaction medium (formation of a homogeneous mixture between the oily ester **48** and the reaction medium; addition of co-solvent to facilitate the mixture and to avoid saturation of the lipase by adsorption of the ester to the beads, cf. § 2.3.2) plays a crucial role in the development of a quick and effective process for the enantioselective hydrolysis of ester *rac*-**48**. It can be anticipated that the reaction could be accelerated if the contact between ester and enzyme could be prolonged without saturating the enzyme with adsorbed ester **48**. Since the catalyst is the most expensive compound in the process, the amount of the beads used needs to be kept as low as possible for the generation of a process feasible to be applied in pharmaceutical industry. This requirement was already explored using the 'tea bag' set up, which relies on the addition and removal of an empackaged enzyme.

2.3.3 Flow Chemistry

2.3.3.1 Introduction

Chemical engineering has brought about many different reactor types (Buchholz *et al.*, 2012). Principally they can be divided into batch reactors and flow reactors. Batch reactors (as used in § 2.3.2) are closed systems or semi-closed systems (fed-batch reactors with constant influx of substrates and efflux of products). Continuous stirring creates a homogeneous mixture within the reaction vessel while an internal probe allows for precise control of the reaction conditions (pH, temperature). The disadvantage of these systems is the need to stop the

process at the end of the reaction, separate the product from the reagents and then re-load the reactor for a new round of production. The applicability of the continuously stirred batch reactor system for the target biotransformation has been explored previously (*vide supra*). An interesting type of reaction which combines the recycling of the enzyme and the need for a high enzyme loading is the flow reactor system (cf. figure 2.40). Flow chemistry has come into the focus of chemical engineering because of its added efficiency (compared to other reaction set-ups) in a multistep, continuous, flow-based chemical processing. Flow tubes packed with the immobilized reagents and a mobile phase with the reagents in and a computer controlled pumping system allows for precisely controlled reactions with high turnover numbers. Many examples in literature (Baxendale *et al.*, 2009; Palmieri *et al.*, 2009) have successfully employed the flow chemistry set-up on macro- or microreactor (Valera *et al.*, 2010) scale.

Considering the limiting factors of the target biotransformation (cf. § 2.3.2.3) a more complex procedure combining the immobilisation and recycling of the enzyme with a re-iterative reaction was developed and will be discussed in the following. A set-up that would allow for this kind of reaction would ideally be a system similar to a liquid chromatography set-up, with the immobilised enzyme packed into a column as solid phase and the substrate (in co-solvent and buffer) as liquid phase (principle illustrated in figure 2.40).

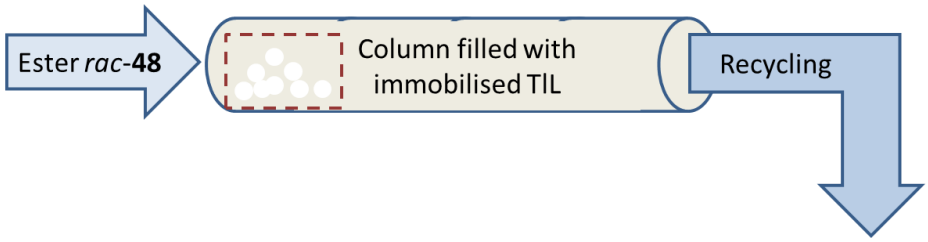

Figure 2.40: Schematic overview over the flow chemistry set-up: a column (in grey) was filled with the immobilised TlL (shown as white spheres in the cut-out (red dashed)). Ester rac-**48** was pumped into the column and the reaction products were collected and recycled at the end of the column.

2.3.3.2 Setup

The setup schematically illustrated in figure 2.36 was built using an empty HPLC column (250 mm x 4 mm) which was filled with the immobilised enzyme. Different amounts of enzyme were tested, to find the optimal packing. It was observed that the immobilising agent swells notably when it comes into contact with the mobile phase, causing a strong back pressure within the set up. Packing the column with 1 g of immobilised enzyme was found to be optimal.

Figure 2.41: Flow chemistry set up, the mobile phase was driven through the column containing the solid phase (immobilised TIL) using plastic syringes and syringe pumps. The two flows, via polypropylene tubing and plastic Swagelok fittings merged in a T-joint which then leads to the column. The effluent of the column was collected in a separating funnel.

The set-up, as illustrated in figure 2.41, consisted of the solid phase (immobilized TlL) packed into a HPLC column, the mobile phase was pumped through the system using polypropylene tubing and syringe pumps. Thorough mixing was attained by mixing the two flows (syringe a: Glycine-NaOH buffer (10 mL, 0.1 M) pH 9.0; syringe b: heptane (10 mL) and substrate ester *rac*-**48** (500 mg)) via a T-joint which then lead to the column and was monitored by adding a red food dye to the buffer in syringe a (figure 2.42).

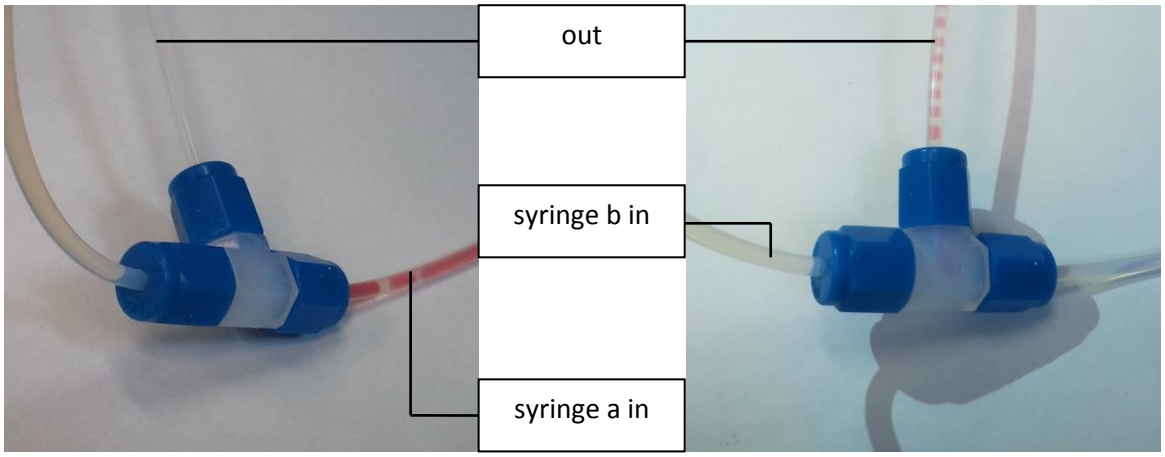

Figure 2.42: Mixing through the T-piece, an equal mixing of the liquids can be observed after both flows simultaneously passed through the T-piece.

Figure 2.42 illustrates the mixing of both components of the mobile phase after their passage through the T-piece. The mobile phase will be mixed even more efficiently within the column due to the turbulent flow through the spaces between the beads.

2.3.3.3 Results and Discussion

The mobile phase was chosen to be a 1:1 mixture of buffer and co-solvent (heptane). The substrate ester *rac*-**48** was dissolved in heptane (500 mg in 10 mL, which equals a concentration of 25 mg/ml within the column). The addition of 50% co-solvent was done in order to allow the beads to be constantly washed lest the adsorption of the ester to the beads caused any substrate inhibition (*vide supra*). The eluent was collected in a separating funnel as two distinct phases. Choosing a flow rate of 0.25 mL in each pump the run completed after 40 min. After each run, the column was washed with pure buffer and heptane to re-equilibrate and the the organic and aqueous phases were separated and loaded again in the syringes.

Three re-iterative cycles (each of 40 min) were performed and both the organic and

the aqueous phase were analysed by HPLC after each run (results collected in table 2.41). The aqueous phase contained the undesired (1*S*,2*S*)-acid **32** whereas the organic phase contained the desired ester with an increased optical activity (increase of (1*R*,2*R*)-ester **48**).

Table 2.18: Conversion and enantioselectivity in the flow chemistry setup of the TlL mediated hydrolysis of *rac*-**48**

Entry	Run n°	% ee_s [a]	% ee_p [b]	% c [c]	E [d]
1	1	17.5	96	17	58
2	2	30.5	95.5	24	58
3	3	41	90	31	29

Conditions: flow chemistry; two pumps for both components of the mobile phase, pumping rate of 0.25 mL/min

solid phase: column packed with immobilised lipase (1g),

mobile phase: Glycine-NaOH buffer pH 9.0 (10 mL) and ester *rac*-**48** (500 mg) dissolved in Heptane (10 mL)

[a] determined by chiral HPLC

[b] determined by chiral HPLC

[c] determined as c = $\frac{ee_s}{ee_s + ee_p}$

[d] determined from ee_s and ee_p as in equation 1.1.16, § 1.1.2.2

[e] the absolute configuration was (1*R*,2*R*) for the ester **48** and (1*R*,2*R*) for the acid **32**

The first run (table 2.18, entry 1) occurred with very good conversion (17% in 40 min). A dpubling of conversion was expected in the subsequent runs, however only an increase of +7% was observed (cf. table 2.18, entry 2 and 3). This phenomenon can be explained by the set-up of the reaction. In order to simulate a flow through a set of multiple enzyme-packed columns the effluent was directly recycled: the organic and aqueous phases were separated and re-loaded into the syringes for a new run. Although a drop in pH to pH 6.5 was noted after the first run the aqueous phase was recycled directly to simulate a continuous reaction. The pH was adjusted back to pH 9 only in the 3rd run. Probably the drop in conversion is a mixture of a product inhibition and a pH effect on the stability of the enzyme and the beads. This can be circumvented in the future by exchanging the buffer for a fresh Glycine-NaOH buffer pH 9.0 for each new run, since only the undesired acid **32** is contained in the aqueous phase.

It is noteworthy that the enantioselectivity reached higher values than those obtained in

previous trials and only dropped to the value obtained in batch (cf. § 2.3.2) after the 3rd run. The third run was performed after a 12h resting period. It can be hypothesized that the packing in the column is still too high and the beads experienced a huge pressure, which gradually lead to the inactivation of the enzyme.

In order to determine the actual mean residence time of the substrate in the column (which equals the true reaction time) the buffer was spiked with red food dye. Pure heptane and the dyed buffer were pumped through the system at the same flow rate used in the hydrolysis experiment. The eluent was collected in test tubes and the entry-exit times were measured collecting one fraction every 1 minute (cf. figure 2.43).

- First colour out: 4 minutes
- Last colour out: 10 minutes
- Peak of the colour: 5-6 minutes

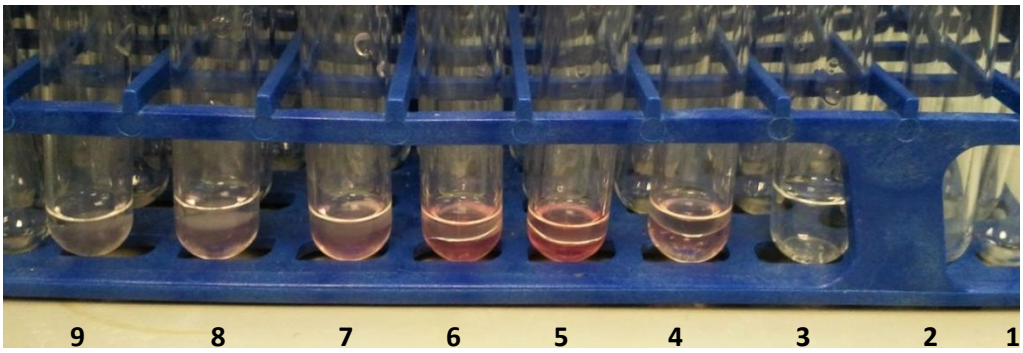

Figure 2.43: Fraction collection of colored eluent, each test tube (numbered) equals the flow-through of one minute. The peak of the dye at 5-6 min can be clearly observed.

2.3.4 Conclusion

The data collected within the trials described above indicates that the target process can be scaled up to industrial scale. It has been shown that the reaction and conditions determined at laboratory scale can easily be brought to gram-scale (cf. § 2.3.2.2). Furthermore, the recyclability of the enzyme has been extensively studied (cf. § 2.3.2.3), and it has been demonstrated that a recycling of the enzyme is possible and technically accomplishable.

There is scope for further process design and improvement. Although the conversion rate is very good (17% conversion after 40 min) the drop in conversion in the subsequent rounds of reaction needs to be accounted for. A possible way to adress this issue would be the exchange of the aqueous phase with fresh buffer. Like this, the unwanted acid (1*S*,2*S*)-**31** will be removed and the equilibrium will be pulled towards product formation. Moreover this will help to avoid product inhibition of the enzyme. The set-up may need further improvement in terms of column-length and/or sequential colums as well as in terms of reaction conditions. As the pressure builds up within the column it is likely that the enzyme partially decomposes. A larger amount of catalyst leads to a reduced time of reaction but may result in a high internal pessure. Careful adjustment of the conditions to favour an increase in conversion rates is still required. The distribuition of the catalyst over several colums, monitored exchange of the mobile phase and the establishment of the optimal ratio between buffer and co-solvent need to be further adressed and will eventually permit a smooth and elegant enantioselective hydrolysis of the enzyme on gram- and kilogram-scale.

As a conclusion it can be said that the results obtained in the flow chemistry trial (§ 2.3.3) build an encouraging base for further process development. The reaction time has been shortened significantly and the work-up and generation of waste has been reduced: there is no need for extraction and washing steps, the organic phase can directly be concentrated (recovering heptane) to yield the desired ester (1*R*, 2*R*)-**48**. The waste created is mostly aqueous with no further organic solvent waste. The acid contained in the aqueous phase can be easily re-extracted and disposed of separately. Most importantly, the set-up allows for a multiple-recycling step of the enzyme which reduces the cost of the catalyst. A scale-up to industrial scale is indeed feasible and will lead to a greener and more environmentally sustainable route towards the target API.

3 Conclusions and Outlook

3.1 Summary

The purpose of the work presented was the identification, development and implementation of a biosynthetic route towards an API. The research was based on Ticagrelor as API and its cyclopropyl subunit was the target compound in this research. Different biocatalytic routes towards the cyclopropyl amine (1*R*,2*S*)-26 were developed and tested on small scale and on gram scale.

The approach involving the ketoreduction of the tica ketone **52** had to be stopped because a competing patent claiming the same route was published concomitantly. The approach chosen then for further process development was a lipase-mediated hydrolysis of ester **48**. This approach was compared to a bacterial amidase mediated hydrolysis of the corresponding amide **49**.

After initial screens, *Thermomyces lanuginosus* lipase (TlL) was determined to be the most promising candidate for a successful kinetic resolution of the starting material (*rac*-**48**) yielding the desired (1*R*,2*R*)-ester **48** with >95% *ee*. The critical parameter in this approach was the reaction rate of the reaction. Different methods to increase the conversion of TlL in the target reaction were tested using the commercially available lipozyme 100 TL. The effect of the reaction conditions was thoroughly examined in §§ 2.1.4.2 and 2.1.4.3. It was found that the composition and pH of the buffer had a strong impact on the conversion. A Glycine-NaOH buffer (0.1M, pH 9.0) and a catalyst:substrate loading of 2:1 (w/w) gave the best result in a stirred reaction at room temperature (45 % conversion after 48h small scale, and 50% conversion after 24h on gram scale) .

A rational protein design strategy focussing on improving the opening mechanism of the lid of TlL was studied in § 2.2. Different enzyme variants were created with the purpose of finding a residue that would encourage the lid to attain the open position, assuming that an open lid would increase the conversion rate. The target residues were identified through analysis of the resolved crystal structures and subsequently mutated in order to investigate the influence of this residue on the overall performance of the lipase towards the target compound. Focussing on two different locations with three and four mutations in each case, in combination with a structure based analysis of the open and closed conformation (Brzozowski *et al.*, 2000), the studies performed within this research give an indication which positions are

vulnerable to modifications and which positions could possibly be changed. Target residues were chosen as a consequence of their proximity to the hinge of the lid and their ability to create salt bridges either in the open or the closed (or both) conformation of the lipase. It was found that mutating Asn88 in centre of the lid destroys the enzymes' activity towards both the model compound *para*-nitrophenol butyrate and the target ester *rac*-**48**. Mutations at position 57 (Asp57X) on the other hand had a low impact on the overall activity of the mutant causing a reduction by a factor of two in the Asp57Arg variant and an increase by a factor of two in the Asp57Asn variant.

Finally, the reaction employing the commercial enzyme was brought to gram-scale in § 2.3.2 and the recyclability of the enzyme was studied in § 2.3.3. It was found that commercially available immobilised lipase (TlL Immobead 150) could be recycled multiple times in a quick and easy set-up employing the lipase in a 'tea bag'. Moreover, the possibilities of a flow chemistry set-up were explored. The results obtained in the trials (§ 2.3.4) build an encouraging base for further process development. The reaction time was shortened significantly (17% conversion in 40 min as opposed to 45% conversion after 48h on small scale) and the work-up and generation of waste has been reduced. Most importantly, the set-up allows for a multiple-recycling step of the enzyme which reduces the cost of the catalyst.

3.2 Outlook

3.2.1 reactions employing the commercial enzyme

Once the optimal conditions for the TlL mediated enantioselective hydrolysis of ester *rac*-**48** were determined, the focus was laid on the preliminary studies for industrialisation of the process. The scale-up to gram scale and the flow chemistry indicated the feasibility of a scale-up to industrial-scale. The work presented here is a preliminary study on conditions, mode of stirring and recyclability. In order to include the biocatalytic step into the actual synthetic route, process development to enable a kg-scale needs to be done. A recycling-system similar to the one employed in § 2.3.3 needs to be developed and tailored to the requirements imposed by a kg-reactor in a fashion similar to the one used by Mallin *et al*. (2013).

The flow chemistry experiments represent another potential reaction mode for the target biotransformation. Especially in this case, further development of the reactor is imperative. Further work will be required to determine the optimal conditions for this particular set up. Moreover the system needs to be revisited in terms of the assembly: the specification of the column (length, diameter, packing) as well as the reaction mode (sequential versus repetitive) need to be discussed and tested.

3.2.2 study of the enzyme variants

The rational protein design approach focussing on the increase of conversion rates through selective modification of several residues in the lid of the lipase yielded information on the residues that are important for activity. An exhaustive study including all proteinogenous amino acids in a site-saturation mutagenesis experiment could give rise to an enzyme variant with significantly increased activity. Establishment of a high-throughput screen of an increased number of mutants would allow for a comprehensive study of the amino acids connected to the functioning of the lid. *Pichia pastoris* (or alternatively *Aspergillus niger* (Boel and Huge-Jensen, 1995)) however, is not an ideal expression system for high-throughput screening, since the process from mutation to expression of the new variant is laborious and time-consuming. *Escherichia coli* expression of TlL would need to be explored for this purpose. This approach, however, is only feasible if the glycosylation of TlL is not needed for its activity, since *Escherichia coli* expression does not allow for glycosylation of proteins. An alternative option would be *in silico* screening for a suitable candidate to obtain a reasonable number of variants. Finally, with TlL-variant tailored to the target reaction in hand, immobilisation and recycling of this enzyme (*vide supra*) can be further addressed.

3.3 Conclusions

The results obtained build an encouraging base for further process development. A scale-up from laboratory scale to gram scale was successfully applied and indicates that a scale up to industrial scale is within reach. This will lead to a greener and more environmentally sustainable route towards the target API. The present research was a case study to demonstrate applicability of biosynthetic chemistry to central problems in industrial chemistry. It was shown that the combination of retrosynthetic analysis and biotechnology skills allowed for the design of several greener routes towards an API. A precursor molecule was obtained

with an E of 100 at a conversion of 50% in a two-step synthetic route. The alternative route currently applied in industrial synthesis comprises a multi-step reaction and yields the desired compound in low yields with poor enantioselectivity, requiring a recrystallization step in order to obtain the (1*R*,2*R*)-acid with high optical activity.

Ultimately, this research has contributed to making the synthetic route towards Ticagrelor more environmentally sustainable. The need for the use of toxic unsustainable and sterically demanding auxiliaries (cf. § 1.2.2) has been eliminated. Moreover the waste (cf. 1.2.2 in particular figure 1.14) has been greatly reduced. Most of the waste produced is aqueous and the need for the use of large quantities of organic solvents has been substituted by the use of heptane as the only solvent for the reaction and extraction of products. The principles of green chemistry have been applied to the case studied: Waste prevention (solvent waste, reaction steps) and atom efficiency (no need for chiral auxiliaries) have been achieved, while the use of toxic and hazardous chemicals (e.g. diazomethane) has been avoided. The auxiliaries used in this process are innocuous and are derived from a sustainable source (isolated enzymes). The synthesis has been significantly shortened using a catalyst that can be recycled and employed in catalytic quantities.

Overall this research has helped to render a synthetic route towards a highly sought-after API greener and is a step in the direction of sustainable and environmentally benign organic synthesis.

4 Material and Methods

4.1 General

4.1.1 Reagents and Solvents:

The reagents were bought from Aldrich or Alfa Aesar and NEB or Invitrogen (for restriction enzymes, polymerases and electrophoresis markers) and were employed without further purification. The solvents were provided by Merck and Aldrich. The solvents of HPLC grade (hexane and 2-propanol) were provided by Aldrich and Romil.

4.1.2 General Experimental Techniques:

Thin Layer Chromatography (TLC): Silicia coated, aluminium supported chromatography plates of a thickness of 0.25 mm with integrated UV developer (F_{254}) were purchased from Merck. An aqueous solution of 1% $KMnO_4$, 5% K_2CO_3 and 5% KOH and/or UV light were used as developing agents.

Melting Points: The melting points were determined in open capillaries using a Stuart SMP10 instrument and have not been corrected.

Nuclear Magnetic Resonance Spectroscopy (NMR): Proton (^{1}H-NMR) and carbon (^{13}C-NMR, with proton decoupling and DEPT 135) spectra were measured using the Bruker spectrometers AV-AV-400 (^{1}H, 400.13 MHz; ^{13}C, 100.63 MHz). $CDCl_3$ and CD_3OD were used as solvents. Chemical shifts are given as δ values in parts per million (ppm), taking the chemical shift of tetramethyl silane as reference. The ^{1}H-NMR spectra were calibrated with the signal of the residual solvent partially- or non-deuterated ($CHCl_3$, 7.26 ppm; CHD_2OD, 3.31 ppm) and ^{13}C-NMR spectra were calibrated with the signal of the respective deuterated solvent ($CDCl_3$, 76.95 ppm; CD_3OD, 49.0 ppm). The multiplicity is described as observed, therefore, in cases when the coupling constants in dimensions of 1 Hz could not be evaluated precisely, signals which are e.g. formally doublets of doublets are indicated as simple doublets.

High Performance Liquid Chromatography (HPLC): The enantiomeric excesses of the different compounds examined were determined by HPLC analysis using columns with chiral coating and an Agilent 1100 system with a UV detector. Chiralcel OJ-H and OD-H were used in the conditions indicated in table 4.1

Table 4.1: HPLC conditions for the different compounds discussed within this report

Entry	compound	column[a]	H:IPA[b]	0.1 % TFA	T [°C]	flow rate [mL / min]	t_R [min][c]
1	acid	OJ-H	95:5	yes	20	1	9.7 / *12.4*
3	amide	OJ-H	95:5	no	20	0.8	43.8 / *49.2*
5	alcohol	OD-H	90:10	no	20	1	24.6 / *26.6*
7	ester	OJ-H	95:5	yes	20	1	6.3 / 6.9

[a]OJ-H refers to a Chiralcel OJ-H column and OD-H to a Chiralcel OD-H column

[b]H:IPA gives the ratio between hexane and 2-propanol in the mobile phase

[c]the retention time given in *italics* refers to the (*S*)-enantiomer, peaks were assigned to the respective enantiomers by comparison to a sample with known absolute configuration

Mass Spectrometry: spectra were taken in varying conditions in a HPLC MS tandem mass spectrometer by Atmospheric Pressure Ionisation -Electron Spray Mass Spectroscopy (ESI).

4.1.3 Buffers and media

Potassium phosphate buffer 100 mM, pH 6.0-pH 8.0

Potassium hydrogen phosphate (13.6 g) was dissolved in dH_2O (1L) and the desired pH was attained by titration with KOH. The buffer was sterilised where needed.

Glycine-NaOH buffer 100 mM, pH 8.0-10.0

Glycine (7.5 g) was dissolved in dH_2O and the desired pH was attained by titration with NaOH.

.

Tris buffer 50 mM, pH 7.5

For 100 mL of buffer Tris (0.6 mg, 5 mmol) and NaCl (0.88 g, 15 mmol) were dissolved in distilled H_2O (80 mL). The pH was adjusted to pH 7.5 and the solution was brought to a total volume of 100 mL.

HEPES Buffer 0.2 M, pH 7.5

For 100 mL of buffer 2-(4-(2-Hydroxyethyl)-1-piperazinyl)-ethansulfonic acid (4.76 g)

was dissolved in 90 mL H_2O. The pH was adjusted to 7.5 and the solution was brought to a total volume of 100 mL.

TAE-buffer (10 X stock)

Tris base (48.4 g), glacial acetic acid (11.4 mL) and EDTA disodium salt (3.7 g) were dissolved in H_2O (800 mL). The solution was made up to a total volume of 1 L. The buffer was diluted appropriately for use in gel-electrophoresis

HIC washing buffer

Sodium tetraborate decahydrate (9.534 g, 50 mM) was dissolved in dH_2O (0.5 L) and the pH was adjusted to pH 9.0.

HIC elution buffer

2-propanol (3 mL) was added to the HIC washing buffer (7 mL). The solution was freshly prepared prior to use.

HIC sample buffer

The HIC washing buffer was diluted 1:10 with dH_2O

Laemmli buffer, DNA Sample buffer and Restriction Enzyme buffers and SOC medium

Sample and restriction enzyme buffers were purchased NEB or Invitrogen

Alternative Coomassie Staining

Fixing solution: Methanol (100 mL) and glacial acetic acid (20 mL) were added to 80 mL dH_2O.

Staining solution: Coomassie Brilliant Blue (1g) was added to premixed fixing solution (100 mL)

Destaining solution: Methanol (40 mL) and glacial acetic acid (10 mL) were added to 40 mL dH_2O.

The gel was fixed in fixing solution for 1 hour with gentle agitation and was then transferred to a staining solution bath. The gel was stained for 20 min with gentle agitation and then destained using the destaining solution. The destaining solution was

exchanged several times until the background was fully destained.

LB-medium / agar

Aqueous solution (1 L) of bactopeptone (10g), yeast extract (20g), $MgSO_4 * 7\ H_2O$ (10 g) (Bertani, 1951). Addition of agarose (15 g) led to the corresponding liquid agar. All components were mixed and autoclaved. The liquid agar was poured on sterile petri plates and left in the fume hood to solidify for 5 hours. The agar plates were prepared as needed and never stored.

Low salt LB medium / agar

Aqueous solution (1 L) of trypton (10 g), NaCl (5 g) and yeast extract (5 g). The components were dissolved in H_2O (950 mL) and the pH was adjusted to 7.5 with 1N HCl. The solution was brought to a total volume of 1 L. Addition of agarose (15 g) lead to the corresponding agar.

YPD(S) medium / agar

The medium was prepared and autoclaved as two different solutions:

Solution 1: Yeast extract (10 g), peptone (20 g) and sorbitol (182.2 g for YPDS medium) were dissolved in H_2O to yield a total volume of 900 mL.

Solution 2: Glucose (20 g) was dissolved in H_2O (100 mL).

Both solutions were autoclaved separately and stored as separate solutions until used. Addition of agarose (20 g) yielded the corresponding agar. Zeocin (25 mg / mL if not indicated otherwise) was added when needed.

Pichia fermentation medium (modified from (Naik et al., 2010))

Yeast extract (10 g), peptone (20 g) sorbitol (10 g) and yeast nitrogen base (3.4 g) were dissolved in 0.05 M potassium phosphate buffer pH 6 to yield a total volume of 1 L.

Liquid culture medium for Rhodococcus rhodochrous

The culture medium was prepared in two different batches (Kakeya *et al.*, 1991).

Medium I: D-glucose (15 g), yeast extract (1.0 g), KH_2PO_4 (0.5 g), K_2HPO_4 (0.5 g) and distilled water *ad* 800 mL. The pH was adjusted to 7.2 with KOH aq. 3 M and the solution was brought to a final volume of 950 mL.

Medium II: ε-caprolactam (5.0 g), $MgSO_4 * 7\ H_2O$ (0.5 g) and distilled water *ad* 50 mL.

Both components were prepared separately and autoclaved to sterility. After they cooled down to room temperature they were mixed under sterile conditions and sealed to be stored.

S*olution for the preparation of competent cells*

The solutions were prepared and autoclaved in two different batches:

(I) $MgCl_2$ (4.066 g) was added to dH_2O (200 mL) and autoclaved to sterility.

(II) $MgCl_2$ (755 mg) and glycerine (12 mL) were added to dH_2O (68 mL) and autoclaved to sterility.

Antibiotics

Zeocin was bought from Melford and stored as an aqueous solution (100 mg / mL) at -20° C. The antibiotic was added to the cultivation media to yield a final concentration of 25 µg / mL.

4.2 Microbiology

4.2.1 General microbiological techniques:

Sterilization: All material that had been or would be in contact with the microorganism was sterilized in thorough autoclavation at 115 °C for 20 min. As an exception, biotransformations were performed with glassware and buffer solutions which had not been sterilized previously. Plating of the bacteria as well as inoculation of the bacteria in culture medium was performed on the bench next to an open flame.

Measurement of the Absorbance of the Bacterial and Fungal Suspensions: The bacterial suspension in phosphate buffer was measured in a 1 mL cuvette in 1:10 dilution in

culture medium or phosphate buffer against a blank of 1 mL of culture medium or phosphate buffer, respectively.

Storage of the Microorganism: The bacteria and yeasts (and all mutants thereof) are stored as a glycerol stock solution (50% v/v) of a culture grown to approximately OD_{650} = 3 at -80 sterile screw top tubes. Streaking of the stock solutions on agar plates of the appropriate medium in sterile conditions was used to obtain large quantities of bacteria easily accessible for microbiological experiments. These cultures were freshly prepared every month and were kept sealed at 4° C.

4.2.2 Rhodococcus rhodochrous:

Rhodococcus rhodochrous IFO 15564 was bought from the 'Institute for Fermentation', Osaka / Japan, where it is registered under the code cited above.

Cultivation of Bacteria: The culture medium (100 mL in a 250 mL Erlenmeyer flask) was inoculated with small quantities of bacteria from the agar plates. The bacteria were incubated (shaking at approx. 1 * g, 26°C) until reaching the stationary phase and were then transferred into phosphate buffer (100 mL) through a washing step (centrifugation at 4600 * g, 3 min). The suspension was kept in the shaker to homogenize for 10 min. and absorbance of the suspension was measured (see below). This suspension was finally diluted with phosphate buffer to yield the bacterial suspensions needed for biotransformation.

4.2.3 Escherichia coli:

Storage of the Microorganism: Competent *Escherichia coli* XL1 Blue were used as cloning strains and prepared in the laboratory or purchased from Invitrogen and stored at -80 °C.

Preparation of competent Escherichia coli XL1 blue: Escherichia coli XL1 Blue cells were grown overnight on LB agar without any antibiotics. A single colony was picked and

transferred to a flask containing LB medium without any antibiotic (5 mL) and shaken overnight at 37 °C. A fresh batch of LB medium (200 mL) was inoculated with at a 1:100 dilution of the overnight culture and grown at 37°C until it reached an OD of 0.5. The culture was transferred to sterile falcon tubes and chilled on ice for 15 min. The cells were spun down at 4000 rpm in a pre-cooled rotor for 10 min. The supernatant was discarded and the cells were resuspended in half of the original volume of prechilled $MgCl_2$ solution. The cells were left on ice for 30 min and were then centrifuged as above. The supernatant was discarded and the cells were resuspended in 1/20 of the original volume of $MgCl_2$/Glycerol solution. The suspension was pooled in one tube and chilled on ice for 1h and subsequently aliquoted (100 µL) into pre-chilled Eppendorf tubes and stored for further usage at -80 °C.

Cultivation of Bacteria: *Escherichia coli* cells were grown in low salt LB medium (antibiotics added when appropriate) at 37 °C for 16 h. Liquid cultivations were shaken at 1 * g, cultivations on agar plates were performed without shaking.

Transformation: The competent cells were thawed on ice and aliquots (50 mL) were transferred into sterile eppendorf tubes. DNA solution (1 µL) was added to the cell suspension and the mixture was incubated on ice for 30 min. A heat shock was performed at 42°C for 45 seconds and the cells were left on ice for another 2 min. Sterile SOC medium (250 mL) was added to the cells and they were incubated at 37°C for 1 h. The cells were plated on los salt LB medium and left to grow 16 h at 36°C.

4.2.4 Pichia pastoris:

The *P. pastoris* X33 cells were purchased from Invitrogen.

Competent cells: Competent *Pichia pastoris* cells were obtained from a 200 ml YPD grow-up of Pichia pastoris X33 cells (OD 0.8) using the EasyComp™ Kit, as per manual. The cells were aliquoted and stored at -80°C (slow freezing).

Cultivation of Yeasts: Fresh cultures were streaked out from the glycerol stock on YPD agar plates. The plates were left to grow at 30°C for three days until colonies formed.

Transformation: Linearized pPICZ-DNA (5-10 μg) was added to an aliquoted sample of competent *Pichia pastoris* cells. The transformation was performed as per Pichia Pastoris EasyComp™ manual. After transformation the cells were incubated without shaking for 1 h at 30°C and the bacterial suspension was then spread out on YPDS plates containing Zeocin (100 mg / mL). The plates were incubated for three days at 30°C. During the transformation the AOX gene will not be deleted but the TlL gene will be inserted upstream of the AOX (Invitrogen)4, flanked by the 5' and 3' primers of the AOX gene, in between the AOX promoter (which controls its expression) and the genomic AOX gene. Therefore a PCR with the AOX primers verifies the correct insertion of the TlL gene by yielding two constructs (TlL (1000 bp) and AOX (2.2 bp)).

Fermentation: Fermentations were carried out in 1L Erlenmeyer flasks containing modified *Pichia* fermentation medium (300 mL). The medium was inoculated and shaken for 24 h at 0.6 * g and 27.5 °C. The cells were then induced with the daily addition of 1% (3 mL) methanol for six days. An aliquot (1 mL) was taken each day. The cells were spun down in a table top centrifuge at 16000*g and the supernatant was stored at -20 °C for activity assays.

Concentration: The fermentation suspension was spun down at 4000 g and the supernatant was passed through firstly through a 0.4 kDa molecular weight cut-off (MWCO) filter and subsequently through a 0.4 μm stirred ultrafiltration cell. The solution was subsequently concentrated to 1/15th of the original volume using a 10 kDa MWCO Amicon filter under nitrogen pressure. The protein solution was stored at 4 °C and -20 °C for further usage in biotransformations or further purification steps (cf. §4.3.2)

4.3 Molecular biology

4.3.1 General molecular biological techniques

Synthetic gen: The synthetic gene for TlL_KGH has been ordered from GeneArt and has been optimised for expression in *Pichia pastoris*. The Gene is flanked by an EcoRI restriction site at the 5' end and a XhoI restriction site at the 3' end. The sequence is given below in 5'-3' direction with the signal sequence highlighted in blue and the propeptide highlighted in orange:

Gaattcaaaatgagatcctccttggttttgttcttcgtttccgcttggactgctttggcttccccaattagaagagaggtttccca
ggacttgttcaaccagttcaacttgttcgctcagtactccgctgctgcttactgtggtaagaacaacgatgctcctgctggaact
aacatcacttgtactggtaacgcttgtccagaggttgaaaaggctgacgctactttcttgtactccttcgaggattctggtgttg
gtgacgttactggtttcttggctttggacaacactaacaaattgatcgttttgtccttcagaggttccagatccatcgagaactgg
atcggtaacttgaacttcgacttgaaagagatcaacgacatctgttccggttgtagaggtcacgacggtttcacttcatcttgga
gatctgttgctgacactttgagacagaaggttgaggacgctgttagagaacacccagactacagagttgtttttactggtcact
ccttgggtggtgctttggctactgttgctggtgctgatttgagaggtaacggttacgacatcgacgttttctcttacggtgctcca
agagttggtaacagagctttcgctgagttcttgactgttcagactggtggtactttgtacagaatcactcacactaatgacatcg
ttccaagattgccaccaagagagttcggttactctcactcttctccagaatactggatcaagtccggtactttggttccagttact
agaaacgacatcgttaagatcgagggtatcgacgctactggtggaaacaaccagccaaacattcctgacattccagctcact
tgtggtacttcggtttgatcggtacttgtttgtaactcgag

Vector: The pPICZAα vector (Invitrogen) was used as a cloning vector. The TlL Gene was cloned behind the AOX-Promotor region using the EcoR1 and XhoI restriction sites of the MCS.

Miniprep and Gel Extractions: Miniprep and gel extractions have been performed as per protocol of the Quiagen Kits. In addition to the quick protocol, the lysis was done on ice (exception buffer II which needs to be handled at RT) to increase the yield in DNA. The elution buffer was heated to 70°C to enhance the elution efficiency.

Extraction of genomic DNA from Pichia pastoris: Colonies were grown on YPD-agar with Zeocin (100 mg / mL). A colony was picked and dissolved in dH_2O (10 µL) and a lyticase solution was added (5 µL of a 1U/µL solution). The sample was gently mixed and incubated at 30°C for 10 min. It was then frozen at -80°C freezer for 10 min and

subsequently spun down at 10000 rpm for 10 min. The supernatant was directly taken for the PCR. The sample was not stored as PCRs run with samples older than 5h gave no amplification.

PCR: The parent DNA (1 µL) was added to a pre-mixed PCR reaction mixture containing 5x buffer (10 µL), forward/reverse primer in 1:10 dilution (1.25 µL each), dNTP mix (2 µL) water (34.5 µL) and the Phusion Enzyme (polymerase, 1 µL). Primers and dNTPs were aliquoted in appropriate amounts, stored at -20°C and thawed prior to use. The remaining samples were disposed of. No PCR component was subjected to thaw-freeze cycles. The polymerase stock was kept at -20°C and never removed from this environment. The PCR was run in 15 (plasmid DNA) or 30 (genomic DNA) cycles as follows:

Temperature [°C]	Time [sec]	
98	30	
98	30	15 x (plasmid DNA)
Melting temp-5	30	30 x (genomic DNA)
72	60/kb	
72	600	
4	∞	

QuickChange PCR: The primers for the QuickChange PCR were constructed to be 35-40 bp long, with an approximate 20 bp left and right of the introduced mutation. The forward and the reverse primers are complements of each other. Care was taken to make the primers end on three purine bases within the last five bases. The melting temperature of the primers was chosen to be around 70°C. The codon change was introduced in accordance with the codon preference of the host organism. The PCR was set up as described in the general method (*vide supra*).

Colony PCR: Genomic *Pichia pastoris* DNA (1 µL) was added to the PCR mix. PCRs were run with two sets of primers:

Table 4.2: Primers used for gene amplification and sequencing

Entry	Primer	Sequence [5'-3']
1	AOX forward	GACTGGTTCCAATTGACAAGC
2	AOX reverse	GCAAATGGCATTCTGACATCC
3	gene specific forward	TATCCATGGAGGTTTCCCAGGACTTGTTC
4	gene specific reverse	ATATCTCGAGATACAAACAAGTAC

Table 4.3: QuickChange™ PCR primers and constructs for the generation of mutants, the mutation is highlighted in red.

Entry	Construct / Primer FW	Tm [°C]	strain	Variant
1	empty vector, pPICZα	na	neg	negative
2	WT sequence, pPICZα_TIL	na	WT	WT
3	pPICZα_TIL_D57H / cttgtactccttcgagcattctggtgttggtgacg	72	DH	Asp57His
4	pPICZα_TIL_D57I / cttgtactccttcgagatttctggtgttggtgacg	71	DI	Asp57Ile
5	pPICZα_TIL_D57N / cttgtactccttcgagaattctggtgttggtgacg	71	DN	Asp57Asn
6	pPICZα_TIL_D57R / cttgtactccttcgagcgttctgggttggtgacg	73	DR	Asp57Arg
7	pPICZα_TIL_N88H / ggttccagatccatcgagcactggatcggta	71	NH	Asn88His
8	pPICZα_TIL_N88I / ggttccagatccaatcgagatctggatcggta	68	NI	Asn88Ile
9	pPICZα_TIL_N88P / ggttccagatccatcgagccctggatcggta	71	NP	Asn88Pro

Sequencing: All samples have been sent off for sequencings to GATC. All plasmid sequencings experiments were performed in 5'-3' and 3'-5' direction with the exception of the PCR product from the genomic DNA of *Pichia pastoris,* which were sequenced only in forward direction. For sequencing of the pPICZAα vectors AOX primers were employed. The gene specific primers were used for sequencing the TIL gene (PCR product form the genomic DNA of *Pichia pastoris*).

Gel electrophoresis: For a 0.8% agarose gel agarose (0.4 g) were dissolved in 1x TAE buffer (50 mL) and microwaved briefly to dissolve the agar. Solution was cooled down to 60°C and CybrSafe Dye (5 µL) was added. The samples (50 µL) were loaded in 6x loading buffer and 1 kb DNA ladder (20 µL) was loaded as a standard. The gel was run for 30 min at 120 V.

Alcohol precipitation: 1/10 Volume of 3 M Sodium Acetate buffer pH 5.2 (purchased from Aldrich) and 2.5 Volumes of 100% Ethanol were added to a diluted sample of plasmid

DNA (from Gel Purification). The solution was incubated ideally over night at -20 °C and was then centrifuged at 14000 * g for 30 min. The supernatant was discarded and the sample carefully washed with 90% ethanol (200 µL) and centrifuged again at 14000 * g for 5 min. The supernatant was removed and the sample left to dry and then resuspended in the appropriate amount of water.

Ligation: The vector (150 ng) was mixed with a three-fold molar excess of insert and 10 µL Quick ligation buffer. T4 DNA ligase (1 µL) was added and the mixture incubated at 25°C for 10 min. It was then chilled on ice and used for transformation. The excess sample was stored at -20°C.

Restriction Digest: Restriction enzyme 1 (2 µL) and Restriction Enzyme 2 (where applicable – 2 µL) were mixed with the appropriate NEB buffer (5 µL) and BSA (where applicable – 0.5 µL). The vector DNA (2 µg) was added and the solution brought to a total volume of 50 µL with H_2O. The mixture was incubated for at least 3 h at 37°C.

4.3.2 General protein preparation techniques

Purification: To the concentrated and dialysed supernatant from the fermentation (1 mL) was added NaCl (116 mg, 2M). A 6% cross linked agarose gel functionalised with decyl groups (HIC decyl agarose) (1 mL) was equilibrated with HIC washing buffer (sodium borate buffer, 0.05M, pH 9.0). The protein sample was added to the HIC agarose and gently shaken at 5°C for 1h. The supernatant was eluted and the protein bound to the agarose beads was washed three times with HIC washing buffer (3x 1 mL). HIC elution buffer (washing buffer with an additional 30% 2-propanol; 2 mL) was added to the protein on the agarose beads and the sample was incubated 10 min at room temperature. The flow-through was collected and transferred to a PD_{10} column pre equilibrated with sample buffer (sodium borate buffer 0.01 M, pH 9.0). The flow-through was discarded and sample buffer (3.5 mL) was added. Three fractions (1 mL each) were collected for further analysis. Bradford analysis (*vide infra*) revealed that the total protein was eluted in the 3rd fraction. Therefore the protein has not been diluted during the purification step (start volume = end volume).

Storage of the raw protein: The remaining raw protein solution was aliquoted (2 mL) and

stored at -20°C for further use.

Bradford assay: The Bradford assay was done in triplicate in a microtiter plate. Protein solution (50 µL) was mixed with Bradford reagent (250 µL) and analysed at 595 nm. A standard curve was set up in sodium borate buffer (0.01M pH 9.0) using BSA as a reference protein. The standard curve was taken over a range of 0-100 µg BSA/ mL (0, 2.5, 5, 10, 15, 20, 25, 30, 40, 50, 60, 70, 80, 90, 100 µg/mL). Linear regression gave a zero reading at 0.5181 mAU ('blank') and a proportional factor of 0.005.

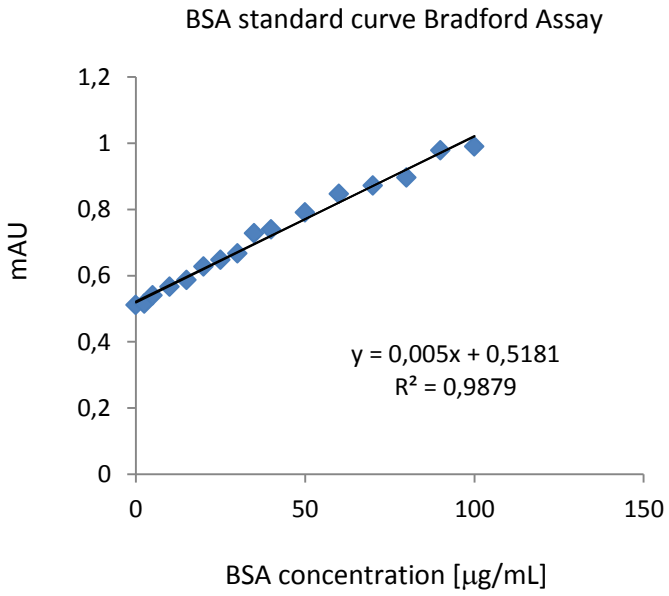

Figure 4.1: Standard curve for the Bradford assay over a concentration range of 0 to 100 µg/mL. The curve was within the linear range of the Bradford assay at 595nm (y-axis, 0.1-1 mAU) and was fitted as y = 0.005x + 0.5181 with 0.5181 being the blank reading which had to be subtracted from all future readings. 0.005 is the proportional factor that relates absorption to concentration. The concentration was determined according to the Lambert-Beer equation: $A = \varepsilon c l$ which relates the concentration to the Absorption in a cuvette of defined path length *l*.

SDS-PAGE: Precast NuSep 4-20% 10 well gels were used. The appropriately diluted sample was heated for 10 min at 95°C and loaded onto the gel. The samples (20 µl) were loaded in 10x Laemmli buffer and PageRuler prestained Marker loaded as a standard. The gel was run for 30 min at 150 V.

PAGE staining: The gels were usually stained with InstantBlue™. The incubation of the gels in

InstantBlue™ was generally 1 h (unless otherwise indicated). Where indicated, the gels were stained with an alternative more sensitive coomassie stain (composition of staining solutions cf. § 4.1.3).

Protein identification by trypsin digestion and mass spectrometry (Lovric, 2011): Coomassie stained protein bands were excised from acrylamide gels. The gel slices were then diced into cubes of approximately 1 mm^3. The gel cubes were then hydrated before the stain was extracted with alternate hydration and dehydration steps (dehydration/hydration/dehydration) in acetonitrile and ammonium bicarbonate (50 mM, 1:1). Following the final dehydration step mass spectrometry grade trypsin (20 mL), diluted in ammonium bicarbonate (50 mM) as directed by the manufacturer was added to the gel cubes. The digestion was performed at 37 ^{0}C overnight. Following manual removal of the liquid from the digest, water (40 mL) was added to the gel cubes to obtain the maximum yield of the tryptic peptides. The combined extracts are centrifuged in a microfuge at 13000 rpm for 10 mins to pellet any particulate matter. The supernatant (35 μL) is placed in vials on the inline HPLC (10 μL – 15 μL used for each run). Tryptic peptides were subjected to LC/MS/MS, separated on a nano-flow HPLC (Dionex) using a C18 column (LC Packings, Acclaim Pep Map 100 - a C-18 pre-column was also used). A nano-spray injection was employed to introduce samples into a Brucker Esquire 3000plus ion trap mass spectrometer. The spectrometer was used in positive ion mode, the flow rate was 200 nl/min, 'Picotip' fused silica emitters (needles) with a 360 μm diameter and 10 μl tip diameter (Presearch Ltd FS360-20-10-D-20) were used for the nano-spray ionisation. The mass spectrometry data was subjected to protein database searches using the Mascot MS/MS ion search software (Matrix Sciences). For a strong signal about 1 pmol of peptide was used. Sensitivity is about 50 fmol. The buffers for the C-18 ion exchange gradient are: Buffer A is formic acid (0.1%), Buffer B is acetonitrile (90%) and formic acid (0.1%).[5]

Deglycosylation: TlL (~ 5 μg)was mixed with 10X Glycoprotein Denaturing Buffer (1 μL) to a total volume of 10 μL. The protein was denatured at 100°C for 10 minutes. 10X G7

[5] This experiment was performed by Dr. Martin Read, as part of the mass spectrometry service for the identification of proteins. http://www.manchester.ac.uk/research/martin.read/research

Reaction Buffer (2 µL), 10% NP-40 (µL), PNGase F (0.5 µL) were added and the reaction volume was brought to 20 µL with dH_2O. The reaction was incubated at 37°C for 1 hour prior to analysis via SDS-PAGE.

4.4 Biotransformations and Assays

4.4.1 Assays

Para-nitrophenol butyrate (pNPB) assay: The absorption of para-nitrophenolate (pNP) is measured in triplicate over a concentration range of 0.02 mM to 0.1 mM in 0.01 mM steps. pNP in DMSO (100 µL) is mixed with potassium phosphate buffer (pH 7.0, 0.1 M; 850 µL) and sodium borate buffer (0.01 M, pH 9.0, 50µL) and the resulting absorption is measured at 410 nm (Khalameyzer *et al.*, 1999) in a PP cuvette with a path length of 1 cm. The slope of the resulting calibration curve is the molecular absorption factor and was determined to be 8448 M^{-1} cm^{-1} (cf. figure 4.2). The difference of the measured value to the literature value (17,700 M^{-1} cm^{-1}) is attributed to the addition of DMSO to the reaction medium

The assay is performed in triplicate under the same conditions as the standard curve. pNPB in DMSO (1 mM solution, 100 µL) is mixed with a solution made up of potassium phosphate buffer (0.1 M, pH 7.0; 850 µL) and the protein solution in the appropriate dilution in sodium borate buffer (0.01M pH 9.0; 50 µL). The change of absorption is measured in a Perkin Elmer spectrophotometer at 410 nm. The activity is determined through linear regression of the initial reaction rate (t_R = 300 sec). Specific activities are calculated using equation 2.2.4.3b and the concentrations obtained in the Bradford assay (*vide supra*).

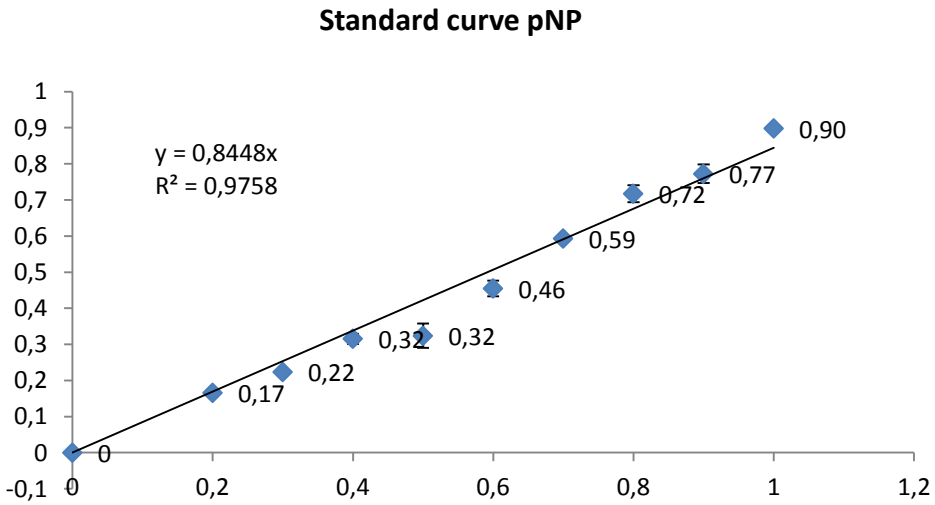

Figure 4.2: Calibration for pNP at λ = 410 nm over a concentration range of 0 to 1 mM, the molecular absorption factor is the slope of regression line. Linear regression yields ε = 8448 M^{-1} cm^{-1}.

4.4.2 Biotransformations

4.4.2.1 Ketoreduction

Conditions for the KRED (Codexis) enzymes

Reactions were performed in 100 mM potassium phosphate buffer (pH 7) with 5 g/L ketone 9 in 10% co-solvent, 5g/L ketoreductase, 1 g/L GDH, 1 g/L NADPH, 1.25 molar equivalents of glucose. Unless indicated otherwise, the co-solvent was DMSO. For the alternative co-factor recycling system using ketoreductase and 2-propanol, reactions were set up as described above without the addition of Glucose and GDH. IPA was used as a co-solvent. Reaction times varied between 1 h and 65 h.

Conditions for the AHDs (Johnson Matthey)

Reactions were performed in 100mM potassium phosphate buffer (pH 6.6) with 2.5 g/L

ketone 9 in 10% DMSO, 2.5 g/L ketoreductase, 0.5 g/L GDH, 0.5 g/L cofactor, 1.25 molar equivalents of glucose. The reactions were stopped after 25 h and 104 h.

Conditions for the AHDs (W. Kroutil)

The lyophillised enzymes were rehydrated in buffer for 30 min prior to the addition of the substrate. For ADH-A, ADH-T and SyADH reactions were performed in 50 mM Tris HCl buffer pH 7.5 with 8 g/L ketone 9 in 5% IPA, 37g/L ketoreductase, 0.7 g/L NADH. For RasADH screens were performed in 50 mM Tris HCl buffer pH 7.5 with 8 g/L ketone 9, 37 g/L ketoreductase, 0.7 g/L NADPH, 1 g/L, 2 molar equivalents of glucose.

Workup:

The reactions were stopped in all cases by extraction of the aqueous phase with two volumes of MTBE (by centrifugation at 1300 * g, 10 min for small scale 1 h for large scale). The organic phase was dried over $MgSO_4$ and the crude was analysed using a Chiralcel OJ-H column (H:IPA 9:1, 20 °C, 1 mL / min, 43 bar).

4.4.2.2 Amidase-mediated hydrolysis of compound *rac*-**49**

A suspension of arrested cells in a 0.1 M phosphate buffer at pH 7.0 was used for all biotransformations performed. The bacterial solutions employed showed an OD_{650} of 1.5, 1.2, 0.5 and 0.25, respectively. The substrate was added to the bacterial solution in 10% (w/v) ethanol to obtain a final concentration of 0.1 % (w/v). The reactions were performed for 22 hours and were then stopped by centrifugation and decantation of the supernatant. The resulting aqueous solution was basified with $NaHCO_3$ and extracted with DCM by shaking and centrifugation. Subsequently the resulting aqueous phase was acidified (1 N HCl) and again extracted with AcOEt. The organic phases were dried over $MgSO_4$ and the solvent evaporated in a rotary evaporator. The compounds were dried under vacuum and could be isolated in pure state with yields of ≥ 90%.

4.4.2.3 Lipase- mediated ester hydrolysis of compound *rac*-**48**

Small scale reactions were performed in MTBE or phosphate buffer (pH 7.0 0.1M) without any co-solvent in a 2 mL Eppendorf tube. The substrate ester *rac*-**48** was added to the

solvent (0.5 mL) as a 1 wt% (5 mg) solution. The enzyme was added to give a 5 wt% (25 mg enzyme e suspension) solution. The reactions were left to shake in an orbital incubator at 30°C (18°C) over a range of 5 to 22 h.

Medium scale reactions were performed in the appropriate buffer without any co-solvent in a 10 mL flask. The substrate ester *rac*-**48** was added as a 1 wt% (50 mg) solution to the solvent (5 mL). The enzyme was added to give a 2 wt% (100 mg enzyme suspension) solution unless otherwise indicated. The reactions were stirred at room temperature (18°C) for the time indicated with each experiment.

Gram-scale reactions were performed in Glycine-NaOH buffer (pH 9.0, 0.1M) with or without co-solvent using the EasyMax^{TM} equipment. The substrate ester *rac*-**48** and enzyme (liquid preparation or beads) were added to the buffer as indicated for each experiment.

Workup: The reaction medium was acidified (pH ~1.0 with HCl (1N)). Organic solvent (MTBE (small and medium scale reactions) or hexane (gram scale reactions), 1 volume equivalent) was added and the reaction mixture was extracted through vigorous shaking or stirring for 5 min. The phases were separated and the organic phase was dried over $MgSO_4$ and used for further analysis.

The HPLC samples were prepared from the crude organic phase and were filtered over cotton wool and $MgSO_4$ prior to injection. The crude was analysed using a Chiralcel OJ-H column (H:IPA 95:5 + 1% TFA, 20 °C, 1 mL / min, 45 bar).

Flow chemistry: for setup and conditions cf. §2.3.4.2

4.5 Computational analysis of TlL

All models and images of TlL and variants were made with YASARA using the 1dte (opened conformation) and 1dt3 (closed conformation) pdb files. No energy minimisation was performed on the models of the variants. Amino acid substitutions were chosen comparing published positions to residues in the 1dte and 1dt3 pdb files determined through analysis with YASARA.

4.5 Chemical analysis

(±)-trans-2-(3,4-difluorophenyl)cyclopropanecarboxylic acid **31** $C_{10}H_8F_2O_2$

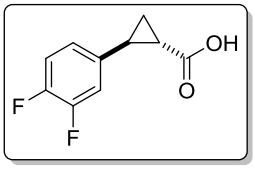

Kindly provided by CHEMO

GC-MS (EI) *m/z*: $[M]^+$ calc. for $C_{10}H_8F_2O_2^+$: 198.2; found: 198.0.

δ_H (400 MHz, $CDCl_3$): 1.36 (1H, dt, ^3J 9.3 Hz, ^3J 5.0 Hz, ^2J 4.9 Hz , 3-H); 1.67 (2H, m, ^3J 8.5 Hz, ^3J 6.5 Hz, ^2J 4.9 Hz, 3-H), 1.86 (1H, ddd, ^3J 8.5 Hz, ^3J 5.2 Hz, ^3J 4.1 Hz , 2-H), 2.55 (1H, ddd, ^3J 9.3 Hz, ^3J 6.5 Hz, ^3J 4.1 Hz , 1-H), 6.83 (1H, m, ^3J 8.5 Hz, ^4J 4.5 Hz, ^4J 2.2 Hz, 6-C‘), 6.90 (1H, ddd, ^3J 11.3 Hz, ^4J 7.4 Hz, ^4J 2.2 Hz, 2-H’) 7.07 (1H, dt, ^3J 10.4 Hz, ^3J 8.3 Hz. 5-H’).

δc (400 MHz, $CDCl_3$): 17.29 (3-C) 23.84 (1-C), 25.21 (d, ^4J 1.4, 2-C), 115.31 (d, ^2J 18 Hz, 2-C’), 117.1 (d, ^2J 17.31 Hz, 5-C’), 122.45 (dd, ^3J 6.0 Hz, ^4J 3.6 Hz, 6-C’), 136.48 (dd, ^3J 6.0 Hz, ^4J 4.0 Hz, 1- C’), 149.2 (dd, ^1J 247.4 Hz, ^2J 11.4 Hz, 4-C’) 149.6 (dd, ^1J 247.4 Hz, ^2J 11.4 Hz, 3-C’) 179.21 ($C_{carbonyl}$).

$[\alpha]_D^{20}$ = +323.2 (*c 0.*44 in $CHCl_3$)

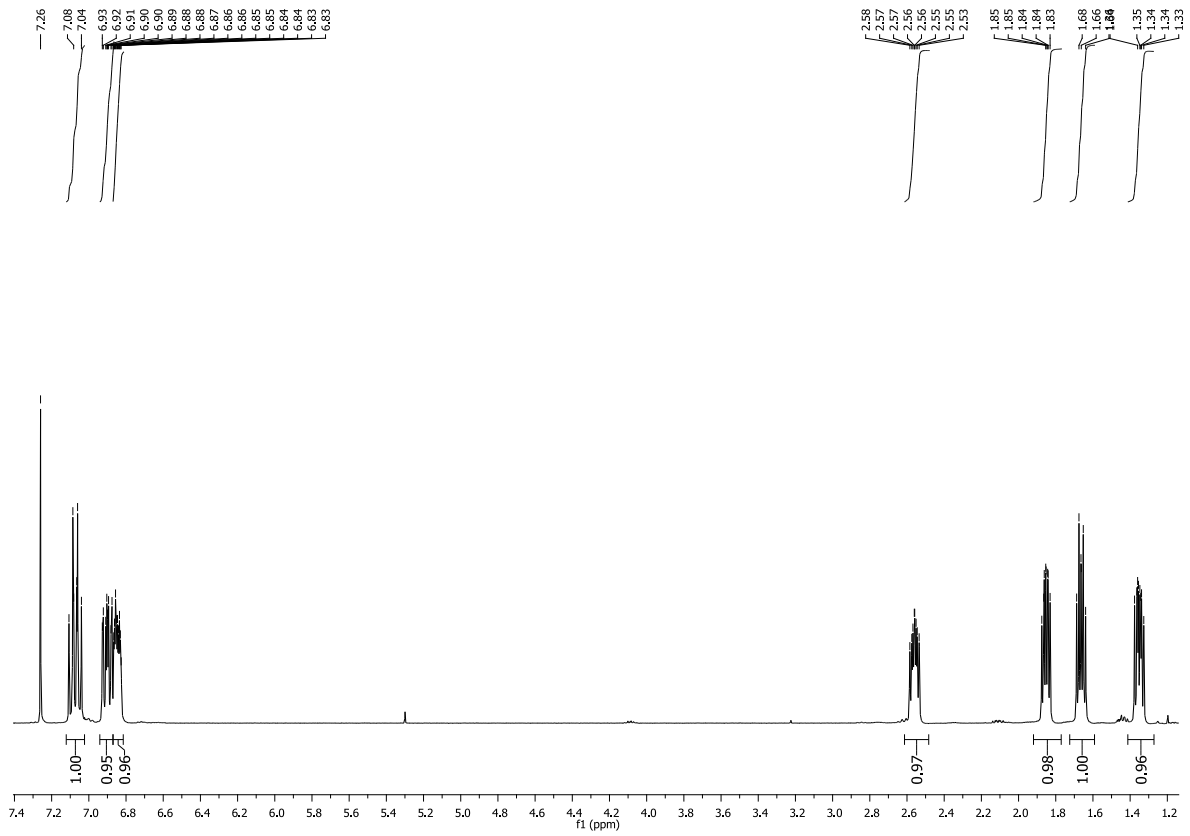
7.26
7.08
7.04
6.93
6.92
6.91
6.90
6.90
6.89
6.88
6.88
6.87
6.86
6.86
6.85
6.85
6.84
6.84
6.83
6.83
2.58
2.57
2.57
2.56
2.56
2.55
2.55
2.53
1.85
1.85
1.84
1.84
1.83
1.68
1.66
1.35
1.34
1.34
1.33
1.00
0.95
0.96
0.97
0.98
1.00
0.96
f1 (ppm)

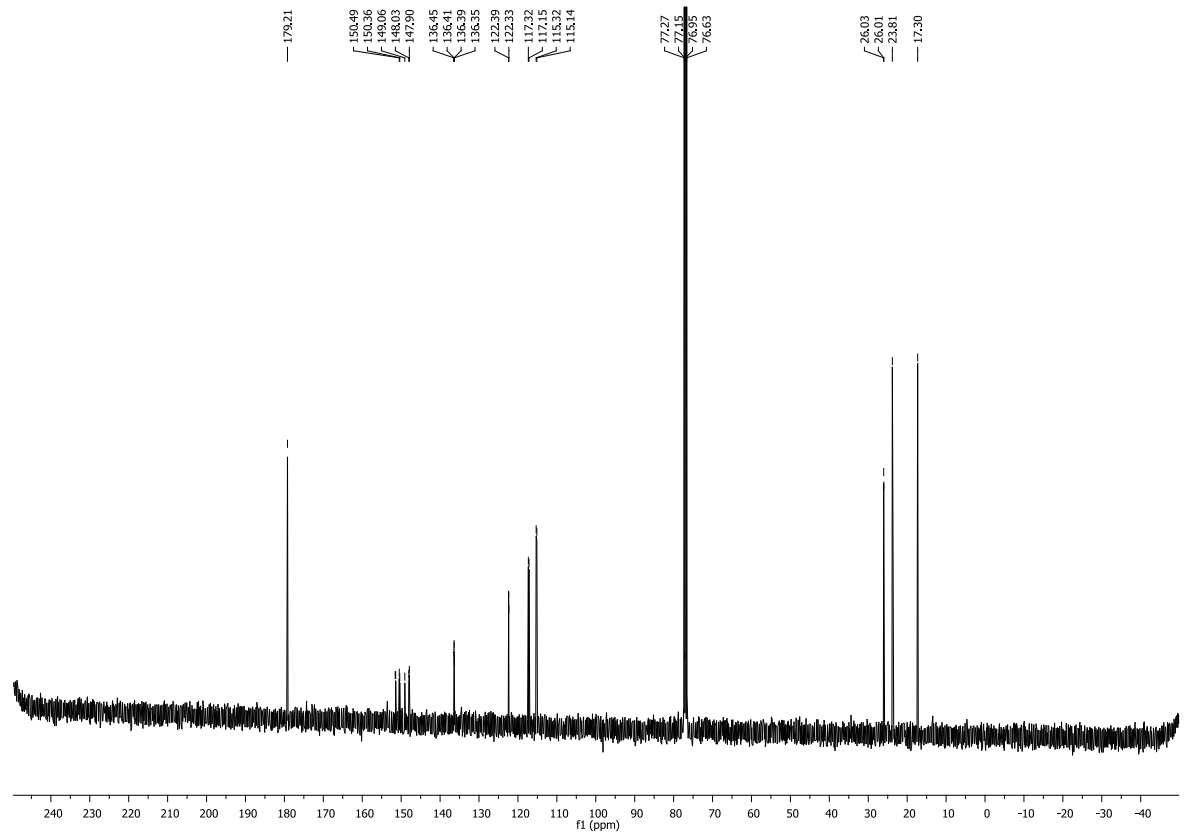
179.21
150.49
150.36
149.06
148.03
147.90
136.45
136.41
136.39
136.35
122.39
122.33
117.32
117.15
115.32
115.14
77.27
77.15
76.95
76.63
26.03
26.01
23.81
17.30
f1 (ppm)

(±)-trans 2-(3',4'-difluorophenyl)cyclopropanecarboxamide **49** $C_{10}H_9F_2NO$

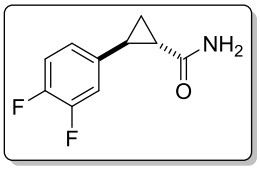

Kindly provided by CHEMO.

GC-MS (EI) *m/z*: $[M]^+$ calc. for $C_{10}H_9F_2NO^+$: 197.2, found: 197.1.

δ_H (400 MHz, $CDCl_3$): 1.23 (1H, ddd, ^3J 10.6 Hz, ^3J 6.6 Hz, ^2J 6.6 Hz , 3-H); 1.59-1.65 (2H, m, ^3J 10.6 Hz, ^3J 8.4 Hz, ^3J 4.4 Hz, ^2J 6.8 Hz , 2-H, 3-H), 1.59-1.65 (1H, dt, ^3J 8.7 Hz, ^3J 6.4 Hz, ^3J 4.8 Hz , 1-H), 5.73 (2H broad, NH_2) 6.81-6.84 (1H, m, ^3J 8.2 Hz, ^4J 4.4 Hz, ^4J 2.2 Hz, 5-H'), 6.87 (1H, ddd, ^3J 11.3 Hz, ^4J 7.2 Hz, ^4J 2.2 Hz, 2-H') 7.06 (1H, dt, ^3J 10.4 Hz, ^3J 8.2 Hz. 5-H').

δc (400 MHz, $CDCl_3$): 17.22 (3-C), 25.65 (d, ^4J 18 Hz, 2-C), 26.6 (1-C), 114.8 (d, ^2J 18 Hz, 2-C'), 117.1 (d, ^2J 17 Hz, 5-C'), 122.2 (dd, ^3J 6.2 Hz, ^4J 3.5 Hz, 6-C'), 137.5 (dd, ^3J 6.0 Hz, ^4J 3.6 Hz, 1- C'), 149.2 (dd, ^1J 246 Hz, ^2J 13 Hz, 4-C') 150.32 (dd, ^1J 249 Hz, ^2J 13 Hz, 3-C') 173.8 (carboxamide).

$[\alpha]_D^{20}$ = -321.4 (*c* 1.0 in $CHCl_3$)

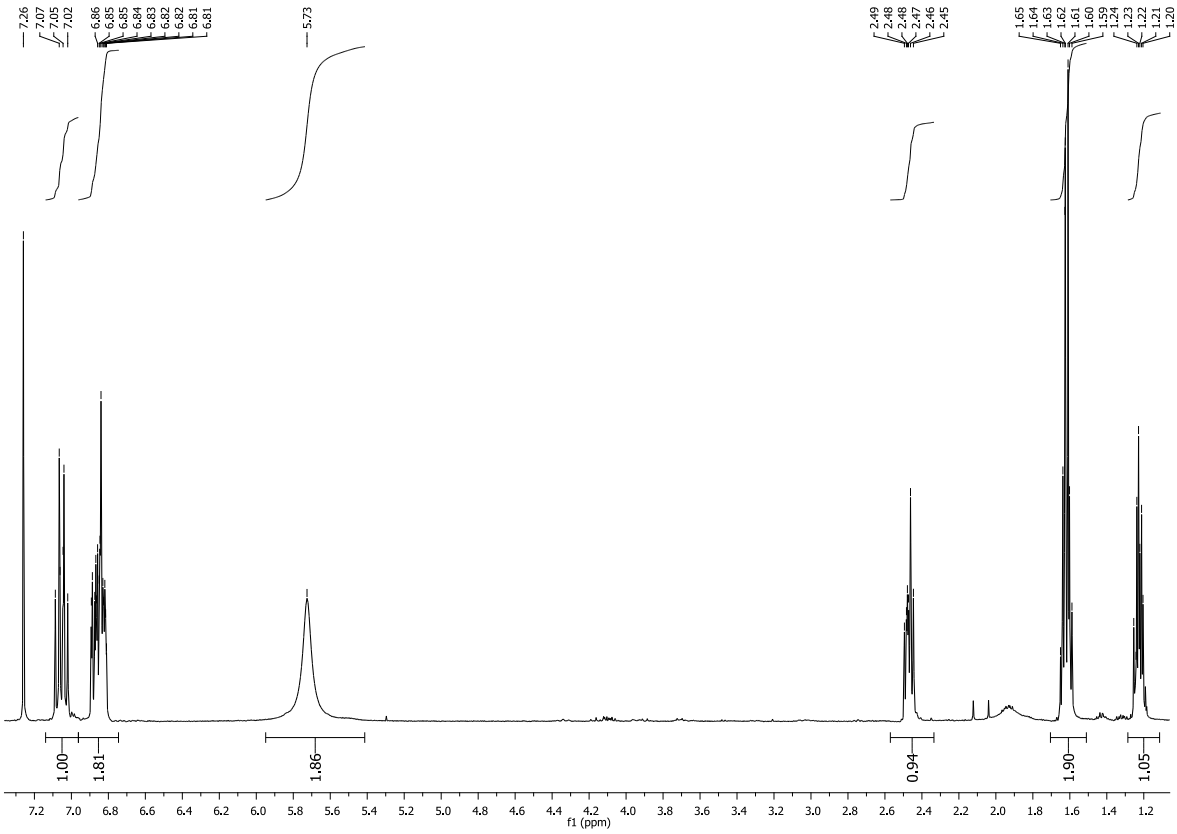
7.26
7.07
7.05
7.02
6.86
6.85
6.85
6.84
6.83
6.82
6.82
6.81
6.81
5.73
2.49
2.48
2.48
2.47
2.46
2.45
1.65
1.64
1.63
1.62
1.61
1.60
1.59
1.24
1.23
1.22
1.21
1.20
1.00
1.81
1.86
0.94
1.90
1.05
f1 (ppm)

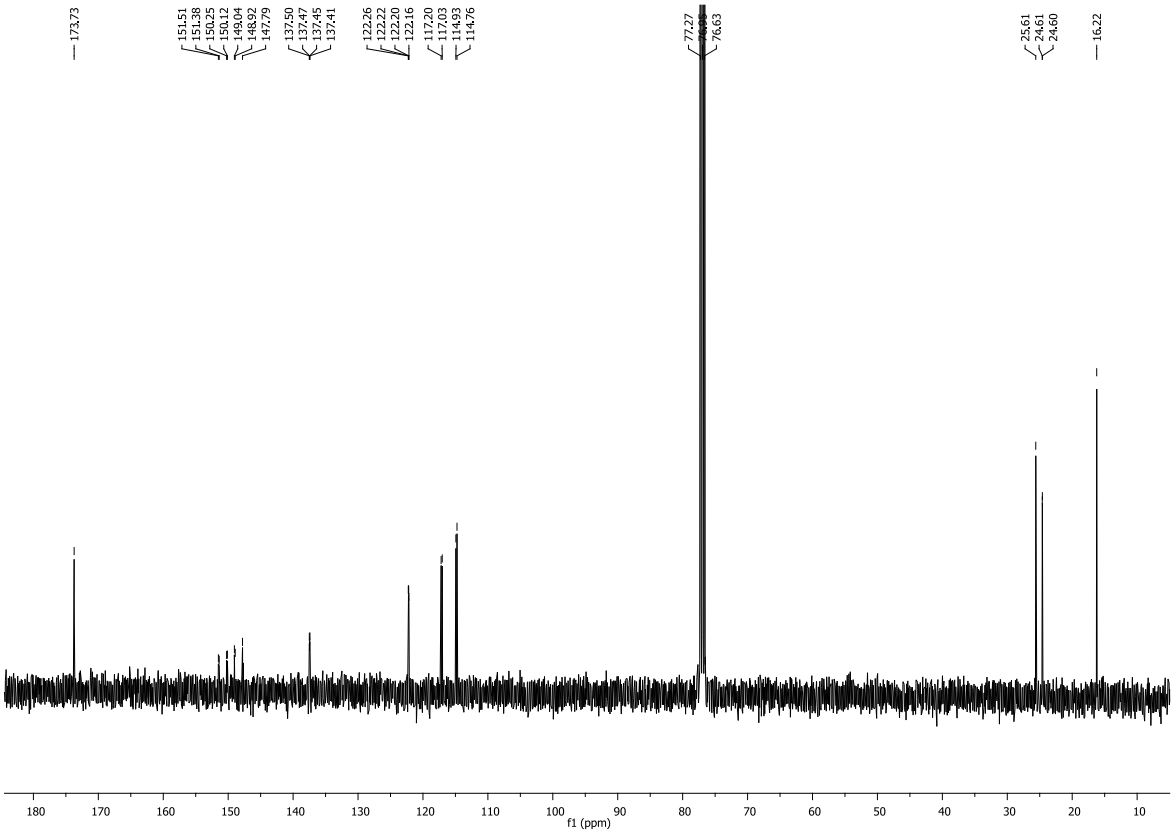
173.73
151.51
151.38
150.25
150.12
149.04
148.92
147.79
137.50
137.47
137.45
137.41
122.26
122.22
122.20
122.16
117.20
117.03
114.93
114.76
77.27
76.63
25.61
24.61
24.60
16.22
f1 (ppm)

(±)-trans-ethyl 2-(3,4-difluorophenyl)Cyclopropanecarboxylate **48** $C_{12}H_{12}F_2O_2$

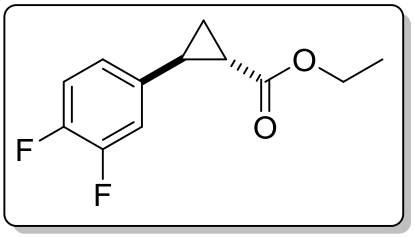

Kindly provided by CHEMO

GC-MS (EI) *m/z*: (sample submitted, instrument busy)

δ_H (400 MHz, $CDCl_3$): 1.25 (1H, ddd, ^3J 8.4 Hz, ^3J 6.4 Hz, ^2J 4.5 Hz , 3-H); 1.28 (3H, t ^3J 6.4 Hz CH_{3Ethyl}) 1.57-1.62 (2H, m, ^3J 9.2 Hz, ^3J 5.2 Hz, ^2J 4.5 Hz, 3-H + H_2O), 1.84 (1H, ddd, ^3J 8.5 Hz, ^3J 5.3 Hz, ^3J 4.3 Hz , 2-H), 2.47 (1H, ddd, ^3J 9.5 Hz, ^3J 6.4 Hz, ^3J 4.2 Hz , 1-H), 4.17 (2H, q, ^3J 6.3 Hz, CH_{2Ethyl}) 6.81-6.87 (1H, m, ^3J 8.5 Hz, ^4J 7.6 Hz, ^4J 2.4 Hz, 6-H'), 6.88 (1H, ddd, ^3J 11.5 Hz, ^4J 7.6 Hz, ^4J 2.2 Hz, 2-H') 7.06 (1H, dt, ^3J 10.3 Hz, ^3J 8.2 Hz. 5-H').

δc (400 MHz, $CDCl_3$): 14.27 (CH_{3Ethyl}), 16.84 (3-C) 24.04 (1-C), 25.14 (d, ^4J 1.4, 2-C), 60.71 (CH_{2Ethyl}), 114.74 (d, ^2J 19 Hz, 2-C'), 117.09 (d, ^2J 18 Hz, 5-C'), 122.25 (dd, ^3J 6.1 Hz, ^4J 3.4 Hz, 6-C'), 137.06 (dd, ^3J 6.1 Hz, ^4J 3.4 Hz, 1- C'), 149.2 (dd, ^1J 248 Hz, ^2J 13 Hz, 4-C') 151.32 (dd, ^1J 249 Hz, ^2J 12.5 Hz, 3-C') 172.87 ($C_{carbonyl}$).

$[\alpha]_D^{20}$ = -381.9 (*c* 1.0 in EtOH)

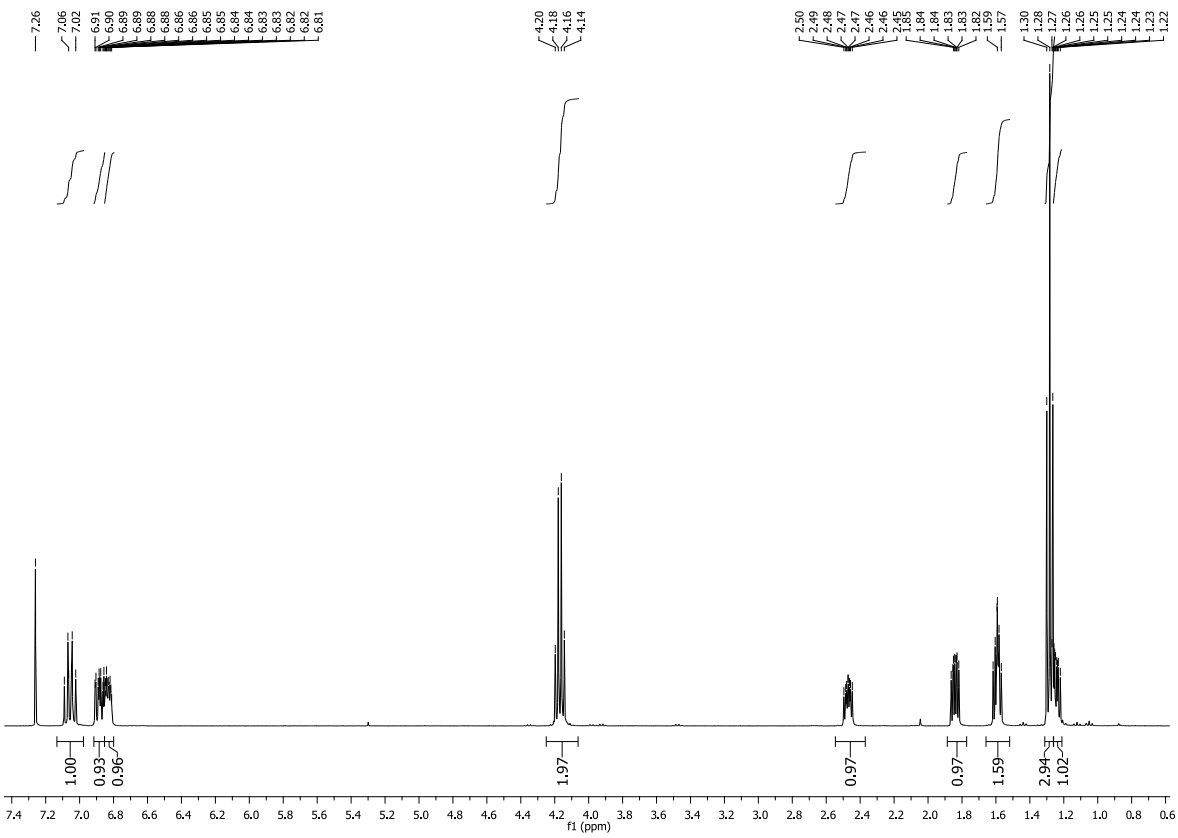
7.26
7.06
7.02
6.91
6.90
6.89
6.89
6.88
6.88
6.86
6.86
6.85
6.85
6.84
6.84
6.83
6.83
6.82
6.82
6.81
4.20
4.18
4.16
4.14
2.50
2.49
2.48
2.47
2.47
2.46
2.46
1.85
1.84
1.84
1.83
1.83
1.82
1.59
1.57
1.30
1.28
1.27
1.26
1.26
1.25
1.25
1.24
1.24
1.23
1.22
1.00
0.93
0.96
1.97
0.97
0.97
1.59
2.94
1.02
f1 (ppm)

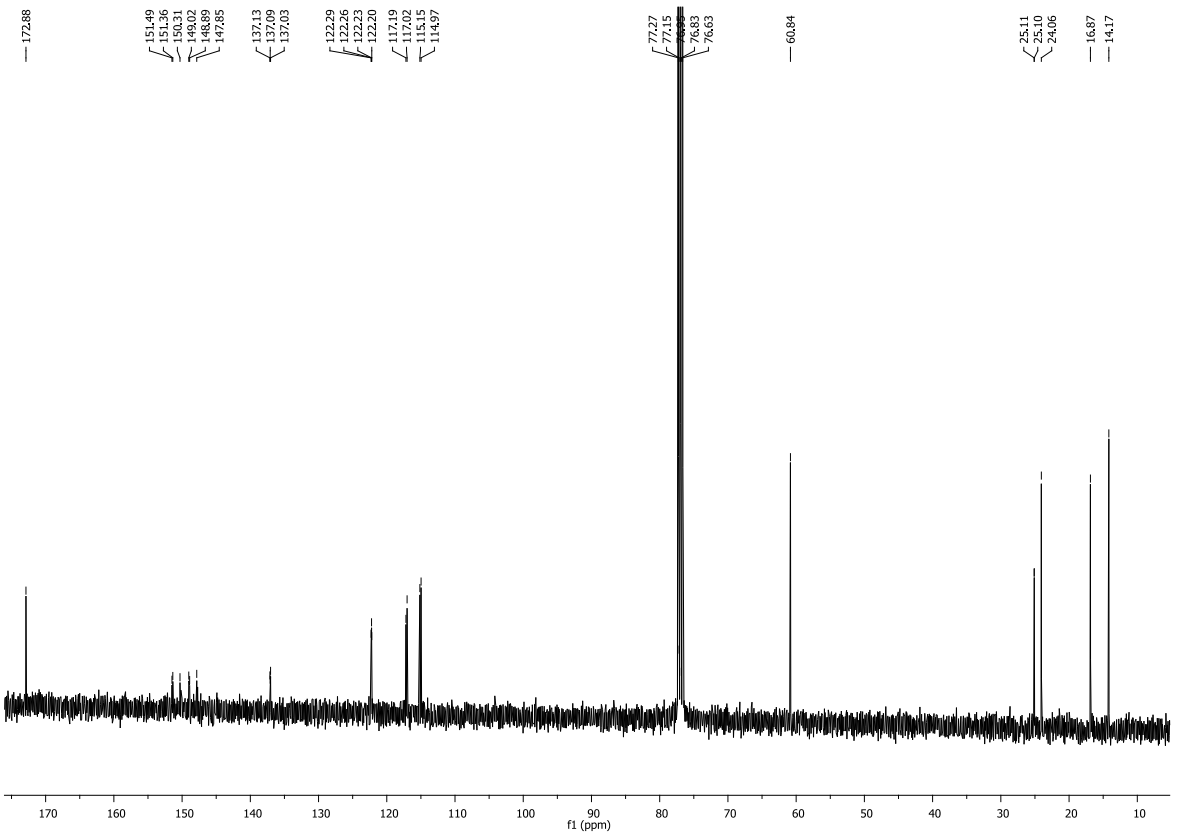
172.88
151.49
151.36
150.31
149.02
148.89
147.85
137.13
137.09
137.03
122.29
122.26
122.23
122.20
117.19
117.02
115.15
114.97
77.27
77.15
76.83
76.63
60.84
25.11
25.10
24.06
16.87
14.17
f1 (ppm)

1-(3,4-difluorophenyl)-3-nitropropan-1-one **52** C9H7F2NO3

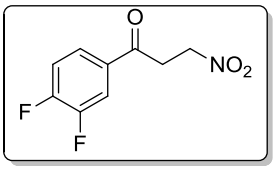

Kindly provided by CHEMO

GC-MS (EI) *m/z*: (sample submitted, instrument busy)

MS (ES+, m/z) 215 [M^+], 238 [M + Na]

δ_H (400 MHz, $CDCl_3$): 3.61 (2H, t, ^3J 6 Hz, 2-H); 4.83 (2H, t, ^3J 6 Hz, 3-H), 7.31 (1H, ddd, ^3J 9.6 Hz, ^4J 7.6 Hz, ^4J 2 Hz, 2-H'), 7.78 (1H, ddd, ^3J 7.8 Hz, ^4J 4.2 Hz, ^4J 1.4 Hz, 6-H') 7.83 (1H, ddd, ^3J 10.2 Hz, ^3J 7.6 Hz. 5-H').

δc (400 MHz, $CDCl_3$): 34.65 (3-C), 68.9 (2-H), 117.5 (dd, ^2J 18 Hz, ^4J 2 Hz, 2-C'), 117.83 (d, ^2J 18 Hz, 5- C'), 125.24 (dd, ^3J 7.6 Hz, ^4J 2.5 Hz, 6- C'), 132.76 (dd, ^3J 4.4 Hz, ^4J 3.7 Hz, 1- C'), 150.62 (dd, 1J 252 Hz, ^2J 12 Hz, 4- C'), 154.32 (dd, 1J 258 Hz, ^2J 12.8 Hz, 3- C') 197.4 (1-C).

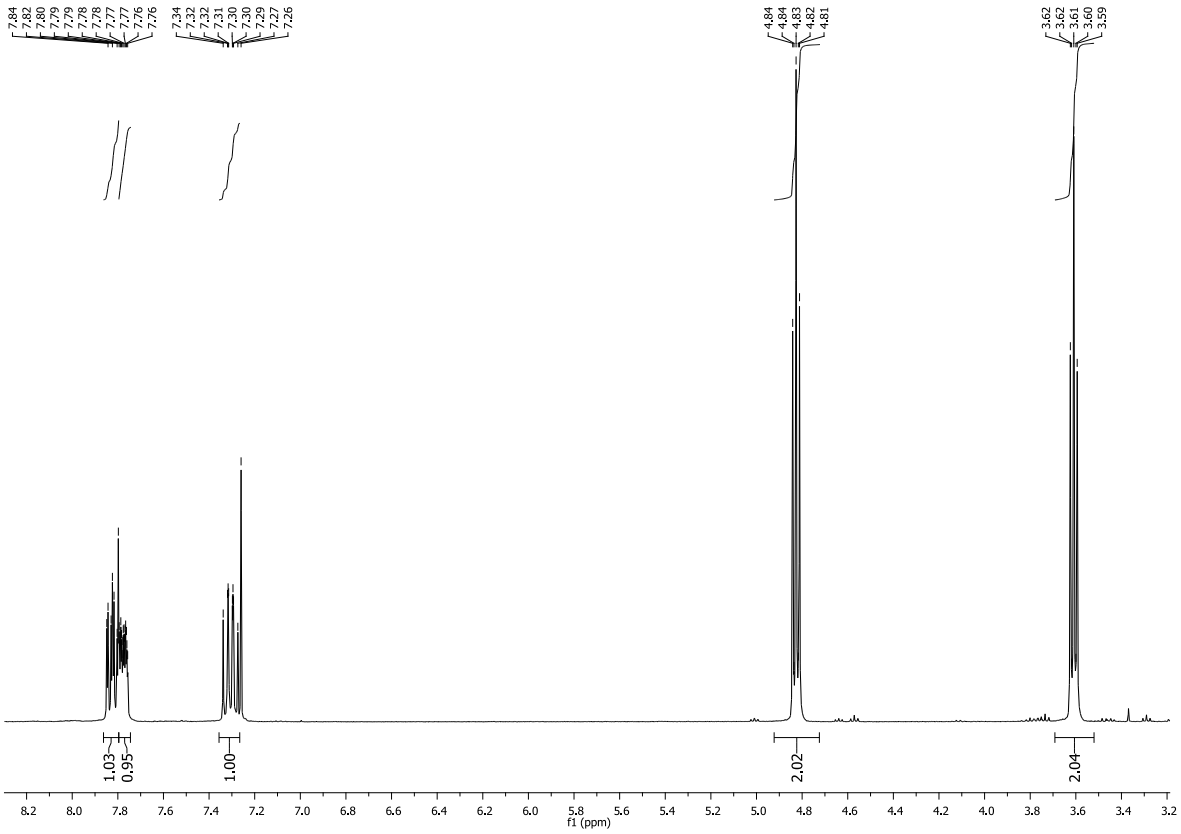
7.84
7.82
7.80
7.79
7.79
7.78
7.78
7.77
7.76
7.76
7.34
7.32
7.32
7.31
7.30
7.30
7.29
7.27
7.26
4.84
4.84
4.83
4.82
4.81
3.62
3.62
3.61
3.60
3.59
1.03
0.95
1.00
2.02
2.04
f1 (ppm)

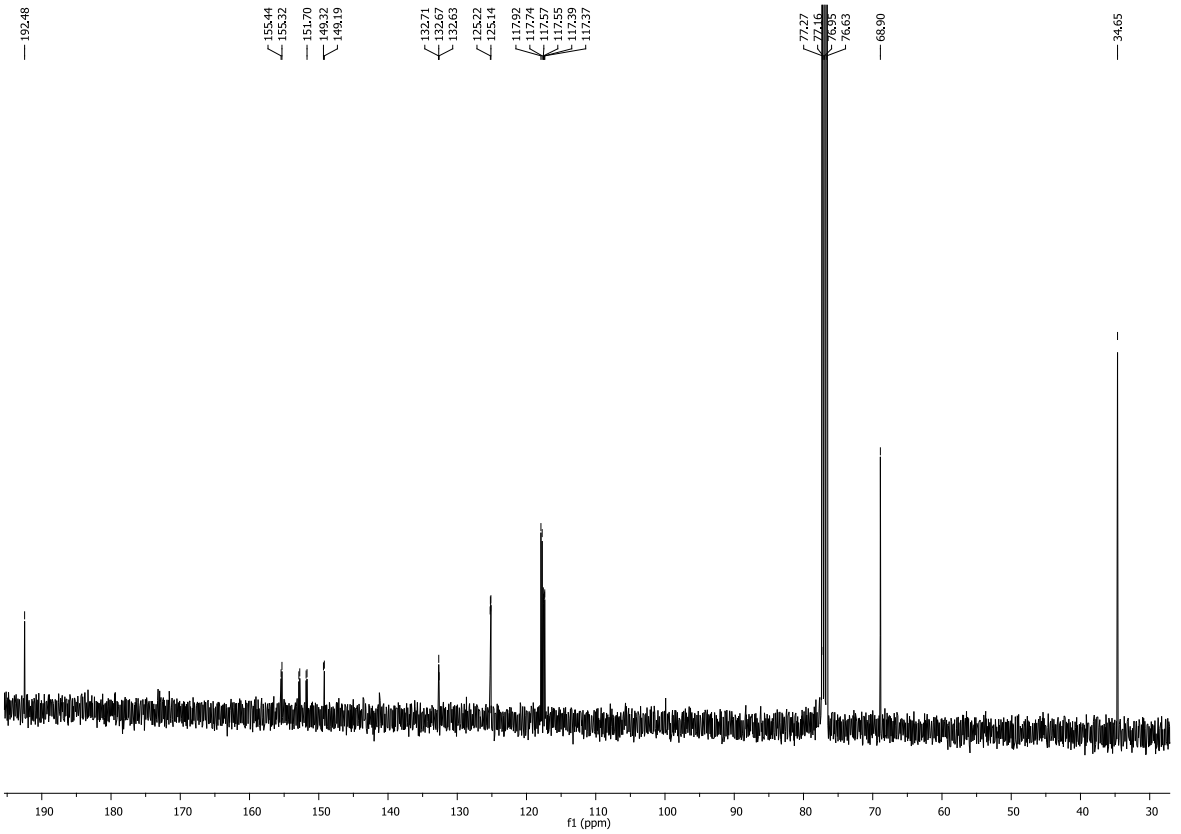
192.48
155.44
155.32
151.70
149.32
149.19
132.71
132.67
132.63
125.22
125.14
117.92
117.74
117.57
117.55
117.39
117.37
77.27
77.16
76.95
76.63
68.90
34.65
f1 (ppm)

rac-1-(3,4-difluorophenyl)-3-nitropropan-1-ol **53** $C_9H_9F_2NO_3$

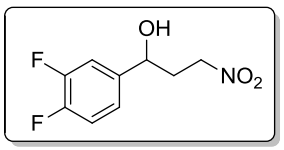

9 (60 mg, 0.3 mmol) were dissolved in THF (4 mL) and $NaBH_4$ (1.25 equivalents 11 mg, 0.4 mmol) and water (0.5 ml) were added. The reaction was stirred at RT for 40 min. The organic layer was then washed with sodium hydrogen carbonate solution and dried over $MgSO_4$. The solvent was removed *in vacuo* to yield a clear oil. >10 % starting material can still be observed in the crude NMR. The compound was used for HPLC analysis only.

GC-MS (EI) *m/z*: (sample submitted, instrument busy)

MS (ES+, m/z) 217 [M^+], 240 [M + Na]

δ_H (400 MHz, $CDCl_3$): 2.30 (1H, dt, ^2J 9 Hz, ^3J 6 Hz 3-H); 2.37 – 2.45 (1H, m, 3-H), 4.47 (1 H dt, ^2J 13.8 Hz, ^3J 6.3 Hz 2-H), 4.61-4.68 (1H, , ^2J 14.2 Hz, ^3J 8.4, ^3J 6.2, 2-H), 4.84 (1H, dd, ^3J 8.7, ^3J 4.4, 1-H), 7.06-7.10 (1H, m, 6-H'), 7.78 (1H, dt, ^3J 10.2 Hz, ^3J 8.1 Hz, 5-H') 7.83 (1H, m, 2-H').

δc (400 MHz, $CDCl_3$): 35.73 (2-C), 69.99 (d, ^4J 1.5 Hz, 1-C), 71.86 (3-C), 114.54 (d, ^2J 17.8), 117.51 (d, ^2J 16.8 Hz, 5- C'), 121.46 (dd, ^3J 6.4 Hz, ^4J 3.7 Hz, 6- C'). 140 (t, ^3J 4.7 Hz, ^4J 4.0 Hz, 1-C'), 149.97 (dd, ^1J 248.77 Hz, ^2J 12.7 Hz, 4- C'), 150.34 (dd, ^1J 250 Hz, ^2J 13 Hz, 3- C').

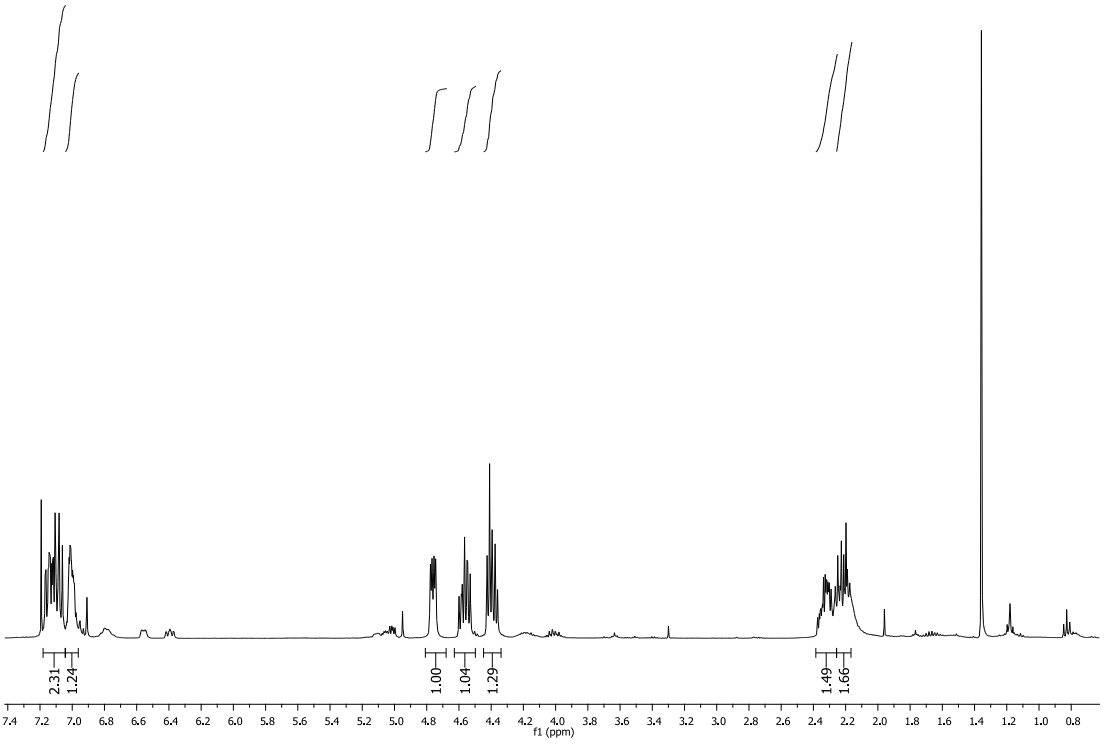
2.31
1.24
1.00
1.04
1.29
1.49
1.66
f1 (ppm)

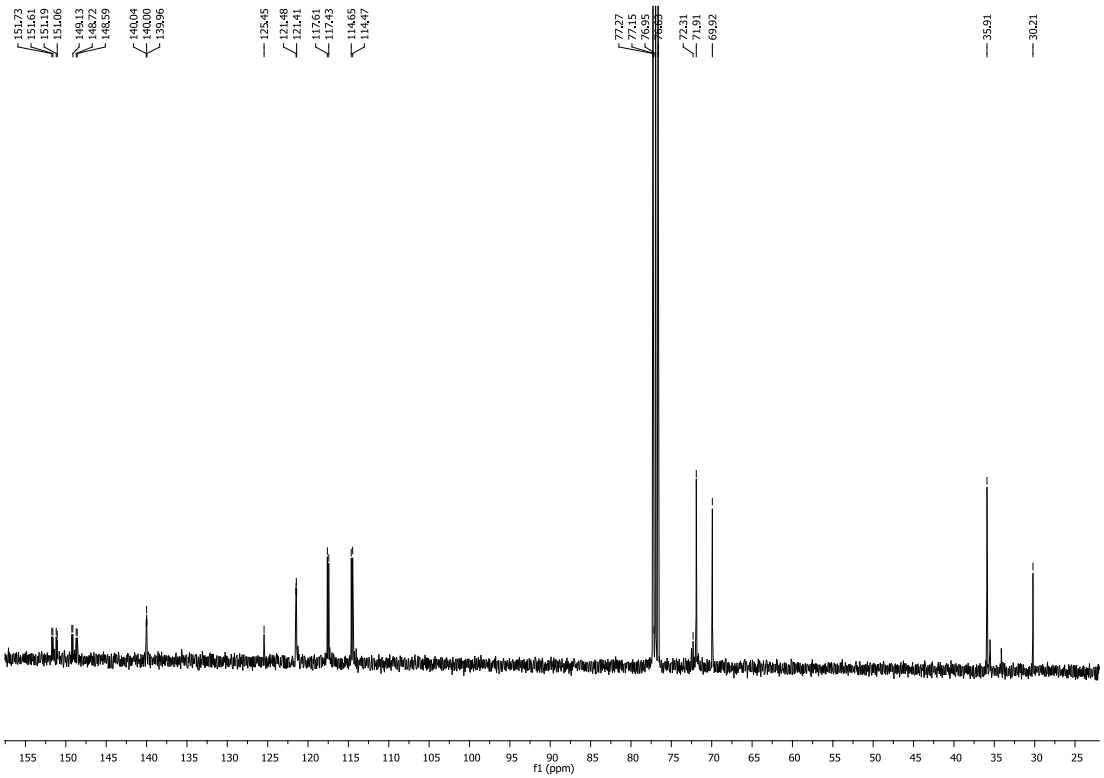
151.73
151.61
151.19
151.06
149.13
148.72
148.59
140.04
140.00
139.96
125.45
121.48
121.41
117.61
117.43
114.65
114.47
77.27
77.15
76.95
76.63
72.31
71.91
69.92
35.91
30.21
f1 (ppm)

5 Literature

R. Akada, T. Murakane, Y. Nishizawa, DNA extraction method for screening yeast clones by PCR, *BioTechniques* **2000**, *28*, 668-670, 672, 674.

P. T. Anastas, *Green chemistry : theory and practice*, Oxford University Press, Oxford, **1998**.

J. L. Anderson, C. D. Adams, E. M. Antman, C. R. Bridges, R. M. Califf, D. E. Casey, Jr., W. E. Chavey, 2nd, F. M. Fesmire, J. S. Hochman, T. N. Levin, A. M. Lincoff, E. D. Peterson, P. Theroux, N. K. Wenger, R. S. Wright, S. C. Smith, Jr., A. K. Jacobs, J. L. Halperin, S. A. Hunt, H. M. Krumholz, F. G. Kushner, B. W. Lytle, R. Nishimura, J. P. Ornato, R. L. Page, B. Riegel, ACC/AHA 2007 guidelines for the management of patients with unstable angina/non ST-elevation myocardial infarction: a report of the American College of Cardiology/American Heart Association Task Force on Practice Guidelines (Writing Committee to Revise the 2002 Guidelines for the Management of Patients With Unstable Angina/Non ST-Elevation Myocardial Infarction): developed in collaboration with the American College of Emergency Physicians, the Society for Cardiovascular Angiography and Interventions, and the Society of Thoracic Surgeons: endorsed by the American Association of Cardiovascular and Pulmonary Rehabilitation and the Society for Academic Emergency Medicine, *Circulation* **2007**, *116*, e148-304.

N. G. Anderson, *Practical Process Research & Development*, Academic Press, Jacksonville, Oregon, USA, **2000**.

M. B. Ansorge-Schumacher, O. Thum, Immobilised lipases in the cosmetics industry, *Chem Soc Rev* **2013**, *42*, 6475-6490.

C. Aouf, E. Durand, J. Lecomte, M.-C. Figueroa-Espinoza, E. Dubreucq, H. Fulcrand, P. Villeneuve, The use of lipases as biocatalysts for the epoxidation of fatty acids and phenolic compounds, *Green Chemistry* **2014**, *16*, 1740-1754.

A. Babtie, N. Tokuriki, F. Hollfelder, What makes an enzyme promiscuous?, *Current Opinion in Chemical Biology* **2010**, *14*, 200-207.

T. Barcellos, K. Tauber, W. Kroutil, L. H. Andrade, Stereocomplementary asymmetric bioreduction of boron-containing ketones mediated by alcohol dehydrogenases, *Tetrahedron: Asymmetry* **2011**, *22*, 1772-1777.

I. R. Baxendale, S. V. Ley, A. C. Mansfield, C. D. Smith, Multistep Synthesis Using Modular Flow Reactors: Bestmann–Ohira Reagent for the Formation of Alkynes and Triazoles, *Angewandte Chemie International Edition* **2009**, *48*, 4017-4021.

S. Baxter, S. Royer, G. Grogan, F. Brown, K. E. Holt-Tiffin, I. N. Taylor, I. G. Fotheringham, D. J. Campopiano, An improved racemase/acylase biotransformation for the preparation of enantiomerically pure amino acids, *J Am Chem Soc* **2012**, *134*, 19310-19313.

C. L. Bennett, C. Angelotta, P. R. Yarnold, et al., THalidomide- and lenalidomide-associated thromboembolism among patients with cancer, *JAMA* **2006**, *296*, 2555-2560.

J. M. Berg, J. L. Tymoczko, L. Stryer, *Biochemistry*, W.H. Freeman, Basingstoke, **2012**.

G. Bertani, Studies on lysogenesis I. The mode of phage liberation by lysogenic Escherichia coli, *Journal of bacteriology* **1951**, *62*, 293-300.

F. R. Bisogno, I. n. Lavandera, W. Kroutil, V. Gotor, Tandem Concurrent Processes: One-Pot Single-Catalyst Biohydrogen Transfer for the Simultaneous Preparation of Enantiopure Secondary Alcohols, *The Journal of Organic Chemistry* **2009**, *74*, 1730-1732.

G. Blaschke, H. P. Kraft, K. Fickentscher, F. Kohler, [Chromatographic separation of racemic thalidomide and teratogenic activity of its enantiomers (author's transl)], *Arzneimittel-Forschung* **1979**, *29*, 1640-1642.

E. Boel, I. B. Huge-Jensen, Recombinant Humicola lipase and process for the production of recombinant humicola lipase, *EP305216B1* **1995**.

L. Bora, D. Gohain, R. Das, Recent advances in production and biotechnological applications of thermostable and alkaline bacterial lipases, *Journal of Chemical Technology & Biotechnology* **2013**, *88*, 1959-1970.

R. F. Borne, M. L. Forrester, I. W. Waters, Conformational analogs of antihypertensive agents related to guanethidine, *Journal of Medicinal Chemistry* **1977**, *20*, 771-776.

U. T. Bornscheuer, G. W. Huisman, R. J. Kazlauskas, S. Lutz, J. C. Moore, K. Robins, Engineering the third wave of biocatalysis, *Nature* **2012**, *485*, 185-194.

U. T. Bornscheuer, R. J. Kazlauskas, in *Enzyme Catalysis in Organic Synthesis, Enzymatic Catalytic Promiscuity and the Design of New Enzyme Catalyzed Reactions*, Wiley-VCH Verlag GmbH & Co. KGaA, **2012**, pp. 1693-1733.

G. N. Bowers, Jr., R. B. McComb, R. G. Christensen, R. Schaffer, High-purity 4-nitrophenol: purification, characterization, and specifications for use as a spectrophotometric reference material, *Clinical chemistry* **1980**, *26*, 724-729.

C. Branneby, P. Carlqvist, A. Magnusson, K. Hult, T. Brinck, P. Berglund, Carbon−Carbon Bonds by Hydrolytic Enzymes, *Journal of the American Chemical Society* **2002**, *125*, 874-875.

R. K. Bretthauer, F. J. Castellino, Glycosylation of Pichia pastoris-derived proteins, **1999**, *30 (Pt 3)*, 193-200.

A. M. Brzozowski, H. Savage, C. S. Verma, J. P. Turkenburg, D. M. Lawson, A. Svendsen, S. Patkar, Structural Origins of the Interfacial Activation in Thermomyces (Humicola) lanuginosa Lipase†, *Biochemistry* **2000**, *39*, 15071-15082.

K. Buchholz, V. Kasche, U. T. Bornscheuer, *Biocatalysts and enzyme technology*, Wiley-VCH, Weinheim ; [Germany], **2005**.

K. Buchholz, V. Kasche, U. T. Bornscheuer, *Biocatalysts and Enzyme Technology*, 2nd edition ed., Wiley VCH, Weinheim, **2012**.

O. Buddrick, O. A. H. Jones, P. D. Morrison, D. M. Small, Heptane as a less toxic option than hexane for the separation of vitamin E from food products using normal phase HPLC, *RSC Advances* **2013**, *3*, 24063-24068.

D. Capodanno, K. Dharmashankar, D. J. Angiolillo, Mechanism of action and clinical development of ticagrelor, a novel platelet ADP P2Y12 receptor antagonist, *Expert Review of Cardiovascular Therapy* **2010**, *8*, 151-158.

G. Carrea, Biocatalysis in water-organic solvent two-phase systems, *Trends in Biotechnology* **1984**, *2*, 102-106.

B. Castillo, V. Bansal, A. Ganesan, P. Halling, F. Secundo, A. Ferrer, K. Griebenow, G. Barletta, On the activity loss of hydrolases in organic solvents: II. a mechanistic study of subtilisin Carlsberg, *BMC Biotechnology* **2006**, *6*, 51.

G. P. L. Cereghino, J. L. Cereghino, C. Ilgen, J. M. Cregg, Production of recombinant proteins in fermenter cultures of the yeast Pichia pastoris, *Current Opinion in Biotechnology* **2002**, *13*, 329-332.

J. L. Cereghino, J. M. Cregg, Heterologous protein expression in the methylotrophic yeast Pichia pastoris, *FEMS Microbiology Reviews* **2000**, *24*, 45-66.

H. Chahinian, L. Sarda, Distinction between esterases and lipases: comparative biochemical properties of sequence-related carboxylesterases, *Protein and peptide letters* **2009**, *16*, 1149-1161.

C. S. Chen, Y. Fujimoto, G. Girdaukas, C. J. Sih, Quantitative analyses of biochemical kinetic resolutions of enantiomers, *Journal of the American Chemical Society* **1982**, *104*, 7294-7299.

H. K. Chenault, E. S. Simon, G. M. Whitesides, Cofactor regeneration for enzyme-catalysed synthesis, *Biotechnology & genetic engineering reviews* **1988**, *6*, 221-270.

A. Clark, E. Jones, U. Larsson, A. Mindis, *Process for the Preparation of Cyclopropyl Carboxylic Acid Esters and Derivates*, WO2001092200, **2001**.

K. A. Clarkson, A. J. Morgan, Z. C. Wang, Google Patents, **1999**.

J. M. Cregg, T. S. Vedvick, W. C. Raschke, Recent Advances in the Expression of Foreign Genes in Pichia pastoris, *Nat Biotech* **1993**, *11*, 905-910.

R. Csuk, M. J. Schabel, Y. v. Scholz, Synthesis of the enantiomer of the antidepressant tranylcypromine, *Tetrahedron: Asymmetry* **1996**, *7*, 3505-3512.

A. Cuetos, A. Rioz-Martínez, F. R. Bisogno, B. Grischek, I. Lavandera, G. de Gonzalo, W. Kroutil, V. Gotor, Access to Enantiopure α-Alkyl-β-hydroxy Esters through Dynamic Kinetic Resolutions Employing Purified/Overexpressed Alcohol Dehydrogenases, *Advanced Synthesis & Catalysis* **2012**, *354*, 1743-1749.

R. J. D'Amato, M. S. Loughnan, E. Flynn, J. Folkman, Thalidomide is an inhibitor of angiogenesis, *Proceedings of the National Academy of Sciences* **1994**, *91*, 4082-4085.

J.-P. Dejonghe, K. Peeters, M. Renard, *Chemical Process for Preparation of Aromatic Cyclopropane Esters and Amides*, WO2008018822, **2008**.

J.-P. P. Dejonghe, Koen; Renard, Marc, WO2008/018822 **2006**.

M. Delgado-García, B. Valdivia-Urdiales, C. N. Aguilar-González, J. C. Contreras-Esquivel, R. Rodríguez-Herrera, Halophilic hydrolases as a new tool for the biotechnological industries, *Journal of the Science of Food and Agriculture* **2012**, *92*, 2575-2580.

N. Demaurex, pH Homeostasis of Cellular Organelles, *Physiology* **2002**, *17*, 1-5.

U. Derewenda, L. Swenson, Y. Y. Wei, R. Green, P. M. Kobos, R. Joerger, M. J. Haas, Z. S. Derewenda, Conformational Lability of Lipases Observed in the Absence of an Oil-Water Interface - Crystallographic Studies of Enzymes from the Fungi Humicola-Lanuginosa and Rhizopus-Delemar, *J Lipid Res* **1994**, *35*, 524-534.

G. DeSantis, K. Wong, B. Farwell, K. Chatman, Z. Zhu, G. Tomlinson, H. Huang, X. Tan, L. Bibbs, P. Chen, K. Kretz, M. J. Burk, Creation of a Productive, Highly Enantioselective Nitrilase through Gene Site Saturation Mutagenesis (GSSM), *Journal of the American Chemical Society* **2003**, *125*, 11476-11477.

S. Dhawan, J. Kaur, Microbial Mannanases: An Overview of Production and Applications, *Critical Reviews in Biotechnology* **2007**, *27*, 197-216.

K. Edegger, H. Mang, K. Faber, J. Gross, W. Kroutil, Biocatalytic oxidation of sec-alcohols via hydrogen transfer, *Journal of Molecular Catalysis A: Chemical* **2006**, *251*, 66-70.

G. M. Ehrenfeld, J. B. Shipley, D. C. Heimbrook, H. Sugiyama, E. C. Long, J. H. Van Boom, G. A. Van der Marel, N. J. Oppenheimer, S. M. Hecht, Copper-dependent cleavage of DNA by bleomycin, *Biochemistry* **1987**, *26*, 931-942.

T. Eriksson, S. Bjöurkman, B. Roth, Å. Fyge, P. Höuglund, Stereospecific determination, chiral inversion in vitro and pharmacokinetics in humans of the enantiomers of thalidomide, *Chirality* **1995**, *7*, 44-52.

M. E. Franks, G. R. Macpherson, W. D. Figg, Thalidomide, *The Lancet* **2004**, *363*, 1802-1811.

E. García-Urdiales, F. Rebolledo, V. Gotor, Enzymatic one-pot resolution of two nucleophiles: Alcohol and amine, *Tetrahedron Asymmetry* **2000**, *11*, 1459-1463.

M. Gawlitzek, U. Valley, M. Nimtz, R. Wagner, H. S. Conradt, Characterization of changes in the glycosylation pattern of recombinant proteins from BHK-21 cells due to different culture conditions, *Journal of Biotechnology* **1995**, *42*, 117-131.

J. George, I. Morrissey, The bactericidal activity of levofloxacin compared with ofloxacin, D-ofloxacin, ciprofloxacin, sparfloxacin and cefotaxime against Streptococcus pneumoniae, *Journal of Antimicrobial Chemotherapy* **1997**, *39*, 719-723.

H. Griengl, H. Schwab, M. Fechter, The synthesis of chiral cyanohydrins by oxynitrilases, *Trends in Biotechnology* **2000**, *18*, 252-256.

S. Guile, D. Hardern, B. Springthorpe, P. Willis, *Novel Ttriazolo-(4,5-D)-Pyrimidine Compounds*, WO2000034283, **2000**.

A. F. Hartog, T. van Herk, R. Wever, Efficient Regeneration of NADPH in a 3-Enzyme Cascade Reaction by in situ Generation of Glucose 6-Phosphate from Glucose and Pyrophosphate, *Advanced Synthesis & Catalysis* **2011**, *353*, 2339-2344.

E. M. K. Hedin, P. Høyrup, S. A. Patkar, J. Vind, A. Svendsen, K. Hult, Implications of Surface Charge and Curvature for the Binding Orientation of Thermomyces lanuginosus Lipase on Negatively Charged or Zwitterionic Phospholipid Vesicles As Studied by ESR Spectroscopy†, *Biochemistry* **2005**, *44*, 16658-16671.

B. Hernández-Rodríguez, J. Córdova, E. Bárzana, E. Favela-Torres, Effects of organic solvents on activity and stability of lipases produced by thermotolerant fungi in solid-state fermentation, *Journal of Molecular Catalysis B: Enzymatic* **2009**, *61*, 136-142.

F. Hollmann, I. W. C. E. Arends, K. Buehler, A. Schallmey, B. Buhler, Enzyme-mediated oxidations for the chemist, *Green Chemistry* **2011a**, *13*, 226-265.

F. Hollmann, I. W. C. E. Arends, D. Holtmann, Enzymatic reductions for the chemist, *Green Chemistry* **2011b**, *13*, 2285-2314.

M. Holmquist, Alpha/Beta-hydrolase fold enzymes: structures, functions and mechanisms, *Current protein & peptide science* **2000**, *1*, 209-235.

M. Holmquist, M. Martinelle, P. Berglund, I. G. Clausen, S. Patkar, A. Svendsen, K. Hult, Lipases from Rhizomucor-Miehei and Humicola Lanuginosa - Modification of the Lid Covering the Active-Site Alters Enantioselectivity, *J Protein Chem* **1993a**, *12*, 749-757.

M. Holmquist, M. Martinelle, I. G. Clausen, S. Patkar, A. Svendsen, K. Hult, Trp89 in the Lid of Humicola-Lanuginosa Lipase Is Important for Efficient Hydrolysis of Tributyrin, *Lipids* **1994**, *29*, 599-603.

M. Holmquist, M. Norin, K. Hult, The role of arginines in stabilizing the active open-lid conformation ofRhizomucor miehei lipase, *Lipids* **1993b**, *28*, 721-726.

J. Hora, G. A. A. Kivits, Google Patents, **1981**.

A. Houde, A. Kademi, D. Leblanc, Lipases and their industrial applications: an overview, *Applied biochemistry and biotechnology* **2004**, *118*, 155-170.

W. Hu, Z. Guan, X. Deng, Y. H. He, Enzyme catalytic promiscuity: The papain-catalyzed Knoevenagel reaction, *Biochimie* **2012**, *94*, 656-661.

K. Huber, B. Hamad, P. Kirkpatrick, Ticagrelor, *Nat Rev Drug Discov* **2011**, *10*, 255-256.

K. G. Hugentobler, Thesis, Kinetic Resolution of (±)-trans-Cyclopropane-1,2-dicarboxylic Acid Derivatives Using Microorganisms, University of Greifswald, **2011**,

K. G. Hugentobler, F. Rebolledo, Enantioselective bacterial hydrolysis of amido esters and diamides derived from (+/-)-trans-cyclopropane-1,2-dicarboxylic acid, *Organic & Biomolecular Chemistry* **2014**, *12*, 615-623.

K. Hult, P. Berglund, Enzyme promiscuity: mechanism and applications, *Trends in Biotechnology* **2007**, *25*, 231-238.

W. Hummel, K. Abokitse, K. Drauz, C. Rollmann, H. Groeger, Towards a Large-Scale Asymmetric Reduction Process with Isolated Enzymes: Expression of an (S)-Alcohol Dehydrogenase in E. coli and Studies on the Synthetic Potential of this Biocatalyst, *ChemInform* **2003**, *34*, no-no.

Invitrogen.

Invitrogen, Pichia EasyComp^{TM} Kit.

H. Jochens, D. Aerts, U. T. Bornscheuer, Thermostabilization of an esterase by alignment-guided focussed directed evolution, *Protein Engineering Design and Selection* **2010**, *23*, 903-909.

V. Juturu, J. C. Wu, Microbial xylanases: Engineering, production and industrial applications, *Biotechnology Advances* **2012**, *30*, 1219-1227.

H. Kakeya, N. Sakai, T. Sugai, H. Ohta, Microbial hydrolysis as a potent method for the preparation of optically active nitriles, amides and carboxylic acids, *Tetrahedron Letters* **1991**, *32*, 1343-1346.

R. Karan, M. D. Capes, S. DasSarma, Function and biotechnology of extremophilic enzymes in low water activity, *Aquatic Biosystems* **2012**, *8*.

M. Kashiwagi, K.-I. Fuhshuku, T. Sugai, Control of the nitrile-hydrolyzing enzyme activity in Rhodococcus rhodochrous IFO 15564: preferential action of nitrile hydratase and amidase depending on the reaction condition factors and its application to the one-pot preparation of amides from aldehydes, *Journal of Molecular Catalysis B: Enzymatic* **2004**, *29*, 249-258.

B. Kasprzyk-Hordern, Pharmacologically active compounds in the environment and their chirality, *Chemical Society reviews* **2010**, *39*, 4466-4503.

R. J. Kazlauskas, U. T. Bornscheuer, Finding better protein engineering strategies, *Nat Chem Biol* **2009**, *5*, 526-529.

R. J. Kazlauskas, A. N. E. Weissfloch, A. T. Rappaport, L. A. Cuccia, A rule to predict which enantiomer of a secondary alcohol reacts faster in reactions catalyzed by cholesterol esterase, lipase from Pseudomonas cepacia, and lipase from Candida rugosa, *The Journal of Organic Chemistry* **1991**, *56*, 2656-2665.

V. Khalameyzer, I. Fischer, U. T. Bornscheuer, J. Altenbuchner, Screening, nucleotide sequence, and biochemical characterization of an esterase from Pseudomonas fluorescens with high activity towards lactones, *Applied and Environmental Microbiology* **1999**, *65*, 477-482.

S. A. Khile, J. Patel, N. Trivedi, S. N. Pradhan, *Novel Process for Preparing Phenylcyclopropylamine Derivatives Using Novel Intermediates*, WO2011132083, **2011**.

T. Kitazume, T. Ikeya, K. Murata, J. Chem. Soc., Chem. Commun, **1986**, 1331-1333.

S. Kobayashi, The new world of organic reactions in water, *Pure and Applied Chemistry* **2013**, *85*, 1089-1101.

C. Laane, S. Boeren, K. Vos, C. Veeger, Rules for optimization of biocatalysis in organic solvents, *Biotechnology and Bioengineering* **1987**, *30*, 81-87.

I. Lavandera, G. Oberdorfer, J. Gross, S. de Wildeman, W. Kroutil, Stereocomplementary Asymmetric Reduction of Bulky–Bulky Ketones by Biocatalytic Hydrogen Transfer, *European Journal of Organic Chemistry* **2008a**, *2008*, 2539-2543.

I. n. Lavandera, A. Kern, B. Ferreira-Silva, A. Glieder, S. de Wildeman, W. Kroutil, Stereoselective Bioreduction of Bulky-Bulky Ketones by a Novel ADH from Ralstonia sp, *The Journal of Organic Chemistry* **2008b**, *73*, 6003-6005.

J. Liang, J. Lalonde, B. Borup, V. Mitchell, E. Mundorff, N. Trinh, D. A. Kochrekar, R. Nair Cherat, G. G. Pai, Development of a Biocatalytic Process as an Alternative to the (−)-DIP-Cl-Mediated Asymmetric Reduction of a Key Intermediate of Montelukast, *Organic Process Research & Development* **2009**, *14*, 193-198.

P. Licence, J. Ke, M. Sokolova, S. K. Ross, M. Poliakoff, Chemical reactions in supercritical carbon dioxide: from laboratory to commercial plant, *Green Chemistry* **2003**, *5*, 99-104.

J. Lovric, Wiley-Blackwell, **2011**.

S. Macauley-Patrick, M. L. Fazenda, B. McNeil, L. M. Harvey, Heterologous protein production using the Pichia pastoris expression system, *Yeast* **2005**, *22*, 249-270.

H. Mallin, J. Muschiol, E. Byström, U. T. Bornscheuer, Efficient Biocatalysis with Immobilized Enzymes or Encapsulated Whole Cell Microorganism by Using the SpinChem Reactor System, *ChemCatChem* **2013**, *5*, 3529-3532.

M. Martinelle, M. Holmquist, I. G. Clausen, S. Patkar, A. Svendsen, K. Hult, The role of Glu87 and Trp89 in the lid of Humicola lanuginosa lipase, *Protein Eng* **1996**, *9*, 519-524.

C. A. Martinez, S. Hu, Y. Dumond, J. Tao, P. Kelleher, L. Tully, Development of a Chemoenzymatic Manufacturing Process for Pregabalin, *Organic Process Research & Development* **2008**, *12*, 392-398.

G. W. Mellin, M. Katzenstein, The saga of thalidomide. Neuropathy to embryopathy, with case reports of congenital anomalies, *The New England journal of medicine* **1962**, *267*, 1184-1192 contd.

A. T. F. Members, F. Van de Werf, J. Bax, A. Betriu, C. Blomstrom-Lundqvist, F. Crea, V. Falk, G. Filippatos, K. Fox, K. Huber, A. Kastrati, A. Rosengren, P. G. Steg, M. Tubaro, F. Verheugt, F. Weidinger, M. Weis, E. C. f. P. Guidelines, A. Vahanian, J. Camm, R. De Caterina, V. Dean, K. Dickstein, G. Filippatos, C. Funck-Brentano, I. Hellemans, S. D. Kristensen, K. McGregor, U. Sechtem, S. Silber, M. Tendera, P. Widimsky, J. L. Zamorano, D. Reviewers, S. Silber, F. V. Aguirre, N. Al-Attar, E. Alegria, F. Andreotti, W. Benzer, O. Breithardt, N. Danchin, C. D. Mario, D. Dudek, D. Gulba, S. Halvorsen, P. Kaufmann, R. Kornowski, G. Y. H. Lip, F. Rutten, Management of acute myocardial infarction in patients presenting with persistent ST-segment elevation: The Task Force on the management of ST-segment elevation acute myocardial infarction of the European Society of Cardiology, *European Heart Journal* **2008**, *29*, 2909-2945.

M. Mitsuda, T. Moroshima, K. Tsukuya, K. Watabe, M. Yamada, *A Process for the Preparation of Optically Active Cycloporpylamines*, WO2008018823 **2008**.

R. Montesino, M. Nimtz, O. Quintero, R. García, V. Falcón, J. A. Cremata, Characterization of the oligosaccharides assembled on the Pichia pastoris—expressed recombinant aspartic protease, *Glycobiology* **1999**, *9*, 1037-1043.

R. Morán-Ramallal, R. Liz, V. Gotor, Bacterial Preparation of Enantiopure Unactivated Aziridine-2-carboxamides and Their Transformation into Enantiopure Nonnatural Amino Acids and vic-Diamines, *Organic Letters* **2007**, *9*, 521-524.

R. Morán-Ramallal, R. Liz, V. Gotor, Enantiopure trans-3-Arylaziridine-2-carboxamides: Preparation by Bacterial Hydrolysis and Ring-Openings toward Enantiopure, Unnatural d-α-Amino Acids†, *The Journal of Organic Chemistry* **2010**, *75*, 6614-6624.

T. Nagasawa, T. Nakamura, H. Yamada, Production of acrylic acid and methacrylic acid using Rhodococcus rhodochrous J1 nitrilase, *Appl Microbiol Biotechnol* **1990**, *34*, 322-324.

S. Naik, A. Basu, R. Saikia, B. Madan, P. Paul, R. Chaterjee, J. Brask, A. Svendsen, Lipases for use in industrial biocatalysis: Specificity of selected structural groups of lipases, *Journal of Molecular Catalysis B: Enzymatic* **2010**, *65*, 18-23.

M. Nardini, B. W. Dijkstra, Alpha/beta hydrolase fold enzymes: the family keeps growing, *Current opinion in structural biology* **1999**, *9*, 732-737.

J. J. Nawarskas, S. M. Clark, Ticagrelor: a novel reversible oral antiplatelet agent, *Cardiology in review* **2011**, *19*, 95-100.

M. T. Neves Petersen, P. Fojan, S. B. Petersen, How do lipases and esterases work: the electrostatic contribution, *Journal of Biotechnology* **2001**, *85*, 115-147.

H. Nishiyama, Y. Itoh, Y. Sugawara, H. Matsumoto, K. Aoki, K. Itoh, Chiral Ruthenium(II)–Bis(2-oxazolin-2-yl)pyridine Complexes. Asymmetric Catalytic Cyclopropanation of Olefins and Diazoacetates, *Bulletin of the Chemical Society of Japan* **1995**, *68*, 1247-1262.

S. Noinville, M. Revault, M.-H. Baron, A. Tiss, S. Yapoudjian, M. Ivanova, R. Verger, Conformational Changes and Orientation of Humicola lanuginosa Lipase on a Solid Hydrophobic Surface: An in Situ Interface Fourier Transform Infrared-Attenuated Total Reflection Study, *Biophysical journal* **2002**, *82*, 2709-2719.

M. O'Neill, D. Beecher, D. Mangan, A. S. Rowan, A. Monte, S. Sroka, J. Modregger, B. Hundle, T. S. Moody, A novel lipase enzyme panel exhibiting superior activity and selectivity over lipase B from Candida antarctica for the kinetic resolution of secondary alcohols, *Tetrahedron: Asymmetry* **2012**, *23*, 583-586.

M. Osset, M. Pinol, M. J. Fallon, R. de Llorens, C. M. Cuchillo, Interference of the carbohydrate moiety in coomassie brilliant blue R-250 protein staining, *Electrophoresis* **1989**, *10*, 271-273.

A. Palmieri, S. V. Ley, A. Polyzos, M. Ladlow, I. R. Baxendale, Continuous flow based catch and release protocol for the synthesis of α-ketoesters, *Beilstein Journal of Organic Chemistry* **2009**, *5*, 23.

V. I. Pârvulescu, C. Hardacre, Catalysis in Ionic Liquids, *Chem Rev* **2007**, *107*, 2615-2665.

P. Pollet, E. A. Davey, E. E. Urena-Benavides, C. A. Eckert, C. L. Liotta, Solvents for sustainable chemical processes, *Green Chemistry* **2014**, *16*, 1034-1055.

D. Prat, O. Pardigon, H.-W. Flemming, S. Letestu, V. Ducandas, P. Isnard, E. Guntrum, T. Senac, S. Ruisseau, P. Cruciani, P. Hosek, Sanofi's Solvent Selection Guide: A Step Toward More Sustainable Processes, *Organic Process Research & Development* **2013**, *17*, 1517-1525.

P. Rathi, R. K. Saxena, R. Gupta, A novel alkaline lipase from Burkholderia cepacia for detergent formulation, *Process Biochemistry* **2001**, *37*, 187-192.

M. T. Reetz, J. D. Carballeira, J. Peyralans, H. Höbenreich, A. Maichele, A. Vogel, Expanding the Substrate Scope of Enzymes: Combining Mutations Obtained by CASTing, *Chemistry – A European Journal* **2006**, *12*, 6031-6038.

S. Rehm, P. Trodler, J. Pleiss, Solvent-induced lid opening in lipases: A molecular dynamics study, *Protein Science* **2010**, *19*, 2122-2130.

J. Ricard, A. Cornish-Bowden, Co-operative and allosteric enzymes: 20 years on, *European Journal of Biochemistry* **1987**, *166*, 255-272.

R. J. Roberts, M. Belfort, T. Bestor, A. S. Bhagwat, T. A. Bickle, J. Bitinaite, R. M. Blumenthal, S. K. Degtyarev, D. T. F. Dryden, K. Dybvig, K. Firman, E. S. Gromova, R. I. Gumport, S. E. Halford, S. Hattman, J. Heitman, D. P. Hornby, A. Janulaitis, A. Jeltsch, J. Josephsen, A. Kiss, T. R. Klaenhammer, I. Kobayashi, H. Kong, D. H. Krüger, S. Lacks, M. G. Marinus, M. Miyahara, R. D. Morgan, N. E. Murray, V. Nagaraja, A. Piekarowicz, A. Pingoud, E. Raleigh, D. N. Rao, N. Reich, V. E. Repin, E. U. Selker, P. C. Shaw, D. C. Stein, B. L. Stoddard, W. Szybalski, T. A. Trautner, J. L. Van Etten, J. M. B. Vitor, G. G. Wilson, S. y. Xu, A nomenclature for restriction enzymes, DNA methyltransferases, homing endonucleases and their genes, *Nucleic Acids Research* **2003**, *31*, 1805-1812.

S. Sanchez, A. L. Demain, Enzymes and bioconversions of industrial, pharmaceutical, and biotechnological significance, *Organic Process Research and Development* **2011**, *15*, 224-230.

R. D. Schmid, R. Verger, Lipases: Interfacial Enzymes with Attractive Applications, *Angewandte Chemie International Edition* **1998**, *37*, 1608-1633.

H. Sharif, Thesis, Novel and environmentally sustainable routes towards API, University of Manchester, **2013**,

R. A. Sheldon, Fundamentals of green chemistry: efficiency in reaction design, *Chem Soc Rev* **2012**, *41*, 1437-1451.

B. Springthorpe, A. Bailey, P. Barton, T. N. Birkinshaw, R. V. Bonnert, R. C. Brown, D. Chapman, J. Dixon, S. D. Guile, R. G. Humphries, S. F. Hunt, F. Ince, A. H. Ingall, I. P. Kirk, P. D. Leeson, P. Leff, R. J. Lewis, B. P. Martin, D. F. McGinnity, M. P. Mortimore, S. W. Paine, G. Pairaudeau, A. Patel, A. J. Rigby, R. J. Riley, B. J. Teobald, W. Tomlinson, P. J. H. Webborn, P. A. Willis, From ATP to AZD6140: The discovery of an orally active reversible P2Y12 receptor antagonist for the prevention of thrombosis, *Bioorganic & Medicinal Chemistry Letters* **2007**, *17*, 6013-6018.

A. J. J. Straathof, S. Panke, A. Schmid, The production of fine chemicals by biotransformations, *Current opinion in biotechnology* **2002**, *13*, 548-556.

G. A. Strohmeier, H. Pichler, O. May, M. Gruber-Khadjawi, Application of Designed Enzymes in Organic Synthesis, *Chem Rev* **2011**, *111*, 4141-4164.

M. Svedendahl, C. Branneby, L. Lindberg, P. Berglund, Reversed Enantiopreference of an ω-Transaminase by a Single-Point Mutation, *ChemCatChem* **2010**, *2*, 976-980.

M. Svedendahl, K. Hult, P. Berglund, Fast Carbon−Carbon Bond Formation by a Promiscuous Lipase, *Journal of the American Chemical Society* **2005**, *127*, 17988-17989.

P.-O. Syrén, P. Hendil-Forssell, L. Aumailley, W. Besenmatter, F. Gounine, A. Svendsen, M. Martinelle, K. Hult, Esterases with an Introduced Amidase-Like Hydrogen Bond in the Transition State Have Increased Amidase Specificity, *ChemBioChem* **2012**, *13*, 645-648.

P.-O. Syrén, K. Hult, Amidases Have a Hydrogen Bond that Facilitates Nitrogen Inversion, but Esterases Have Not, *ChemCatChem* **2011**, *3*, 853-860.

G. P. Taber, D. M. Pfisterer, J. C. Colberg, A New and Simplified Process for Preparing N-[4-(3,4-Dichlorophenyl)-3,4-dihydro-1(2H)-naphthalenylidene]methanamine and a Telescoped Process for the Synthesis of (1S-cis)-4-(3,4-Dichlorophenol)-1,2,3,4-tetrahydro-N-methyl-1-naphthalenamine Mandelate: Key Intermediates in the Synthesis of Sertraline Hydrochloride, *Organic Process Research & Development* **2004**, *8*, 385-388.

R. Teng, Pharmacokinetic, pharmacodynamic and pharmacogenetic profile of the oral antiplatelet agent ticagrelor, *Clin Pharmacokinet* **2012**, *51*, 305-318.

S. Teo, W. Colburn, W. Tracewell, K. Kook, D. Stirling, M. Jaworsky, M. Scheffler, S. Thomas, O. Laskin, Clinical Pharmacokinetics of Thalidomide, *Clin Pharmacokinet* **2004**, *43*, 311-327.

N. J. Turner, Directed evolution drives the next generation of biocatalysts, *Nat Chem Biol* **2009**, *5*, 567-573.

N. J. Turner, E. O'Reilly, Biocatalytic retrosynthesis, *Nature Chemical Biology* **2013**, *9*, 285-288.

F. E. Valera, M. Quaranta, A. Moran, J. Blacker, A. Armstrong, J. T. Cabral, D. G. Blackmond, The Flow's the Thing… Or Is It? Assessing the Merits of Homogeneous Reactions in Flask and Flow, *Angewandte Chemie International Edition* **2010**, *49*, 2478-2485.

R. H. Valivety, P. J. Halling, A. D. Peilow, A. R. Macrae, Relationship between water activity and catalytic activity of lipases in organic media, *European Journal of Biochemistry* **1994**, *222*, 461-466.

T. W. J. M. van Herpen, K. Cankar, M. Nogueira, D. Bosch, H. J. Bouwmeester, J. Beekwilder, Nicotiana benthamiana as a production platform for artemisinin precursors, *PLoS ONE* **2010**, *5*.

N. Vargesson, Thalidomide-induced limb defects: resolving a 50-year-old puzzle, *BioEssays* **2009**, *31*, 1327-1336.

L. G. Villahermosa, T. T. Fajardo, Jr., R. M. Abalos, M. V. Balagon, E. V. Tan, R. V. Cellona, J. P. Palmer, J. Wittes, S. D. Thomas, K. A. Kook, G. P. Walsh, D. S. Walsh, A randomized, double-blind, double-dummy, controlled dose comparison of thalidomide for treatment of erythema nodosum leprosum, *The American journal of tropical medicine and hygiene* **2005**, *72*, 518-526.

L. Wallentin, R. C. Becker, A. Budaj, C. P. Cannon, H. Emanuelsson, C. Held, J. Horrow, S. Husted, S. James, H. Katus, K. W. Mahaffey, B. M. Scirica, A. Skene, P. G. Steg, R. F. Storey, R. A. Harrington, Ticagrelor versus Clopidogrel in Patients with Acute Coronary Syndromes, *New England Journal of Medicine* **2009**, *361*, 1045-1057.

M.-X. Wang, G.-Q. Feng, Enzymatic synthesis of optically active 2-methyl- and 2,2-dimethylcyclopropanecarboxylic acids and their derivatives, *Journal of Molecular Catalysis B: Enzymatic* **2002a**, *18*, 267-272.

M.-X. Wang, G.-Q. Feng, Nitrile Biotransformation for Highly Enantioselective Synthesis of 3-Substituted 2,2-Dimethylcyclopropanecarboxylic Acids and Amides, *The Journal of Organic Chemistry* **2002b**, *68*, 621-624.

M.-X. Wang, G.-Q. Feng, A novel approach to enantiopure cyclopropane compounds from biotransformation of nitriles, *New Journal of Chemistry* **2002c**, *26*, 1575-1583.

E. Watson, B. Shah, L. Leiderman, Y.-R. Hsu, S. Karkare, H. S. Lu, F.-K. Lin, Comparison of N-Linked Oligosaccharides of Recombinant Human Tissue Kallikrein Produced by Chinese Hamster Ovary Cells on Microcarrier Beads and in Serum-Free Suspension Culture, *Biotechnology Progress* **1994**, *10*, 39-44.

W. Winter, E. Frankus, Thalidomide enantiomers, *The Lancet* **1992**, *339*, 365.

F. Wöhler, Ueber künstliche Bildung des Harnstoffs, *Annalen der Physik* **1828**, *88*, 253-256.

W. B. Wu, N. Wang, J. M. Xu, Q. Wu, X. F. Lin, Penicillin G acylase catalyzed Markovnikov addition of allopurinol to vinyl ester, *Chemical Communications* **2005a**, 2348-2350.

W. B. Wu, J. M. Xu, Q. Wu, D. S. Lv, X. F. Lin, D-aminoacylase-catalyzed Markovnikov addition of azoles to vinyl esters in organic solvents, *Synlett* **2005b**, 2433-2436.

W. B. Wu, J. M. Xu, Q. Wu, D. S. Lv, X. F. Lin, Promiscuous acylases-catalyzed Markovnikov addition of N-heterocycles to vinyl esters in organic media, *Advanced Synthesis and Catalysis* **2006**, *348*, 487-492.

Y. Xue, L.-P. Li, Y.-H. He, Z. Guan, Protease-catalysed Direct Asymmetric Mannich Reaction in Organic Solvent, *Sci. Rep.* **2012**, *2*.

G. Yang, Z. Ou, S. Yao, J. Xu, Asymmetric reduction of 3-chloropropiophenone to (S)-3-chloro-1-phenylpropanol using immobilized Saccharomyces cerevisiae CGMCC 2266 cells, *Journal of Molecular Catalysis B: Enzymatic* **2009**, *57*, 83-88.

M. Yokoyama, N. Imai, T. Sugai, H. Ohta, Preparation of both enantiomers of methyl 3-benzoyloxypentanoate by enzyme-catalysed hydrolysis of corresponding racemic nitrile and amide, *Journal of Molecular Catalysis B: Enzymatic* **1996**, *1*, 135-141.

J. Yu, J. R. Falck, C. Mioskowski, Intramolecular Mitsunobu displacement with carbon nucleophiles: preparation of .alpha.-nitrocyclopropanes, *The Journal of Organic Chemistry* **1992**, *57*, 3757-3759.

R. Yuryev, A. Liese, Biocatalysis: The Outcast, *ChemCatChem* **2010**, *2*, 103-107.

A. Zaks, A. M. Klibanov, Enzyme-catalyzed processes in organic solvents, *Proceedings of the National Academy of Sciences* **1985**, *82*, 3192-3196.

J. Zindel, A. de Meijere, Synthesis of 3-(trans-2'-Nitrocyclopropyl)alanine, a Constituent of the Natural Peptide-Lactone Hormaomycin, *The Journal of Organic Chemistry* **1995**, *60*, 2968-2973.